Integrated Ocean Drilling Program Expedition 329 Preliminary Report

South Pacific Gyre subseafloor life

9 October–13 December 2010

Expedition 329 Scientists

Published by
Integrated Ocean Drilling Program Management International, Inc.,
for the Integrated Ocean Drilling Program

Publisher's notes

Citation:

Expedition 329 Scientists, 2011. South Pacific Gyre subseafloor life. *IODP Prel. Rept.,* 329. doi:10.2204/iodp.pr.329.2011

Distribution:
Electronic copies of this series may be obtained from the Integrated Ocean Drilling Program (IODP) Scientific Publications homepage on the World Wide Web at **www.iodp.org/scientific-publications/.**

This publication was prepared by the Integrated Ocean Drilling Program U.S. Implementing Organization (IODP-USIO): Consortium for Ocean Leadership, Lamont Doherty Earth Observatory of Columbia University, and Texas A&M University, as an account of work performed under the international Integrated Ocean Drilling Program, which is managed by IODP Management International (IODP-MI), Inc. Funding for the program is provided by the following agencies:

National Science Foundation (NSF), United States

Ministry of Education, Culture, Sports, Science and Technology (MEXT), Japan

European Consortium for Ocean Research Drilling (ECORD)

Ministry of Science and Technology (MOST), People's Republic of China

Korea Institute of Geoscience and Mineral Resources (KIGAM)

Australian Research Council (ARC) and GNS Science (New Zealand), Australian/New Zealand Consortium

Ministry of Earth Sciences (MoES), India

Disclaimer

August 2011

Expedition 329 participants

Expedition 329 scientists

Steven D'Hondt
Co-chief Scientist
Graduate School of Oceanography
University of Rhode Island
100A Horn Building
215 South Ferry Road
Narragansett RI 02882
USA
dhondt@gso.uri.edu

Fumio Inagaki
Co-chief Scientist
Kochi Institute for Core Sample Research
Japan Agency for Marine-Earth Science and Technology
200 Manobe Otsu
Nankoku City
Kochi 783-8502
Japan
inagaki@jamstec.go.jp

Carlos Alvarez Zarikian
Expedition Project Manager/Staff Scientist
Integrated Ocean Drilling Program
Texas A&M University
1000 Discovery Drive
College Station TX 77845-9547
USA
zarikian@iodp.tamu.edu

Helen Evans
Logging Staff Scientist
Borehole Research Group
Lamont-Doherty Earth Observatory
PO Box 1000, Route 9W
Palisades NY 10964
USA
helen@ldeo.columbia.edu

Nathalie Dubois
Organic Geochemist
Department of Oceanography
Dalhousie University
1355 Oxford Street
Halifax NS B3H 4J1
Canada
nathalie.dubois@dal.ca

Tim Engelhardt
Microbiologist
Institut für Chemie und Biologie Des Meeres (ICBM)
Carl von Ossietzky Universität Oldenburg
Oldenburg 26129
Germany
tim.engelhardt@icbm.de

Timothy Ferdelman
Inorganic Geochemist
Department of Biogeochemistry
Max-Planck-Institute of Marine Microbiology
Celsiusstrasse 1
28359 Bremen
Germany
tferdelm@mpi-bremen.de

Britta Gribsholt
Microbiologist
Center for Geomicrobiology
Aarhus Universitet
Ny Munkegade 114, Building 1540
8000 Aarhus
Denmark
britta.gribsholt@biology.au.dk

Robert N. Harris
Downhole Tools/Physical Properties Specialist
College of Oceanic and Atmospheric Sciences
Oregon State University
104 COAS Admin Building
Corvallis OR 97331-5503
USA
rharris@coas.oregonstate.edu

Bryce W. Hoppie
Sedimentologist
Minnesota State University, Mankato
Department of Chemistry and Geology
Ford Hall 241
Mankato, MN 56001
USA
bryce.hoppie@mnsu.edu

Jung-Ho Hyun
Inorganic Geochemist
Department of Environmental Marine Sciences
Hanyang University
1271 Sa-3dong
Ansan Gyeonggi-do 426-791
Korea
hyunjh@hanyang.ac.kr

Jens Kallmeyer
Microbiologist
Institut for Geowissenschaften
University of Potsdam
Kari-Liebknecht Strasse 24, Haus 27
14476 Potsdam
Germany
kallm@geo.uni-potsdam.de

Jinwook Kim
Physical Properties Specialist
Earth Systems Sciences
Yonsei University
134 Shinchon dong
Seoul
Korea
jinwook@yonsei.ac.kr

Jill E. Lynch
Microbiologist
School of Earth Sciences
University of Melbourne
McCoy Building, Room 312
Melbourne VIC 3010
Australia
j.lynch3@pgrad.unimelb.edu.au

Satoshi Mitsunobu
Inorganic Geochemist
Institute for Environmental Sciences
Shizuoka University
52-1 Yada, Suruuga-ku
Shizuoka 422-8526
Japan
mitunobu@u-shizuoka-ken.ac.jp

Yuki Morono
Microbiologist
Kochi Institute for Core Sample Research
Japan Agency for Marine-Earth Science and Technology
Monobe B200, Naankoku
Kochi 783-8502
Japan
morono@jamstec.go.jp

Richard W. Murray
Inorganic Geochemist
Department of Earth Sciences
Boston University
675 Commonwealth Avenue
Boston MA 02215
USA
rickm@bu.edu

Brandi K. Reese (shore based)
Microbiologist
Department of Oceanography
Texas A&M University
Mail Stop 3146
College Station TX 77843-3146
USA
brandi@ocean.tamu.edu

Takaya Shimono
Paleomagnetist
Graduate School of Life and Environmental Sciences
University of Tsukuba
1-1-1 Tennoudai, Tsukuba
Ibaraki 305-8572
Japan
t-shimono@aist.go.jp

Fumito Shiraishi
Sedimentologist
Department of Evolution of Earth Environments
Kyushu University
744 Motooka, Nishi-ku
Fukuoka 819-0395
Japan
Fshirai@scs.kyushu-u.ac.jp

David C. Smith
Microbiologist
Graduate School of Oceanography
University of Rhode Island
Bay Campus, South Ferry Road
Narragansett RI 02882
USA
dcsmith@gso.uri.edu

Christopher E. Smith-Duque
Petrologist
National Oceanography Centre
University of Southampton
European Way
Southampton SO14 3ZH
United Kingdom
csd2@noc.soton.ac.uk

Arthur J. Spivack
Inorganic Geochemist
Graduate School of Oceanography
University of Rhode Island
Bay Campus, South Ferry Road
Narragansett RI 02882
USA
spivack@gso.uri.edu

Bjorn Olav Steinsbu
Microbiologist
Department of Earth Science
University of Bergen
Allegaten 41
5007 Bergen
Norway
bjorn.steinsbu@geo.uib.no

Yohey Suzuki
Microbiologist
Institute for Geo-Resources and Environment
National Insitute of Advanced Industrial Science and Technology (Geological Survey of Japan, AIST)
1-1-1 Higashi, TsukubaI
Ibaraki 305-8567
Japan
Yohey-suzuki@aist.go.jp

Michal Szpak
Inorganic Geochemist
School of Chemical Sciences
Dublin City University
Collins Avenue
Glasnevin, Dublin 9
Ireland
szpaqlec@gmail.com

Laurent Toffin
Microbiologist
Centre de Brest
Institut Francais de Recherche pour l'Expoitation de la Mer
BP 70
29280 Plouzane
France
laurent.toffin@ifremer.fr

Goichiro Uramoto
Sedimentologist
Department of Earth Sciences
Chiba University
Chiba 263-8522
Japan
uramoto_go-ichiro@graduate.chiba-u.jp

Yasuhiko Yamaguchi
Organic Geochemist
Atmosphere and Ocean Research Institute
University of Tokyo
5-1-5 Kashiwa-no-ha, Kashiwa
Chiba 275-8564
Japan
y-t-yamaguchi@ori.u-tokyo.ac.jp

Guo-liang Zhang
Petrologist
South China Sea Institute of Oceanology
Chinese Academy of Sciences
7 Nanhai Road, Shinan Region
Qingdao
People's Republic of China
tswc_zgl@163.com

Xiao-Hua Zhang
Microbiologist
Department of Marine Biology
Ocean University of China
5 Yushan Road
Qingdao 266003
People's Republic of China
xhzhang@ouc.edu.cn

Wiebke Ziebis
Microbiologist
Department of Biological Sciences
University of Southern California
3616 Trousdale Boulevard
AHF 335
Los Angeles CA 90089
USA
wziebis@usc.edu

Education and outreach

Joe Monaco
Teacher at Sea
Redlands East Valley High School
31000 East Colton Avenue
Redlands CA 92374
USA
joe_monaco@redlands.k12.ca.us

Operational and technical staff

John Beck
Imaging Specialist

Michael Bertoli
Chemistry Laboratory

Lisa Brandt
Chemistry Laboratory

Timothy Bronk
Assistant Laboratory Officer

Chad Broyles
Curator

Lisa Crowder
Assistant Laboratory Officer

Roy Davis
Laboratory Officer

Clayton Furman
Logging Engineer

Randy Gjesvold
Marine Instrumentation Specialist

Dennis Graham
Chemistry Laboratory (temporary)

Margaret Hastedt
Paleomagnetism Laboratory

Kristin Hillis
Underway Geophysics Laboratory

Michael Hodge
Marine Computer Specialist

Eric Jackson
XRD Laboratory

Zenon Mateo
Core Laboratory

Matt Mefferd
Marine Computer Specialist

Stephen Midgley
Operations Superintendent

Algie Morgan
Applications Developer

Jamie Smidt
Publications Specialist

Garrick Van Rensburg
Marine Instrumentation Specialist

Maxim Vasilyev
Physical Properties Laboratory

Jacob Virtue
Core Laboratory (temporary)

Stephanie Zeliadt
Applications Developer

Nicholette Zeliadt
Chemistry Laboratory (temporary)

Abstract

Integrated Ocean Drilling Program Expedition 329 made major strides toward fulfilling its objectives. Shipboard studies (1) documented many fundamental aspects of subseafloor sedimentary habitats, metabolic activities, and biomass in this very low-activity sedimentary ecosystem; (2) significantly improved understanding of how oceanographic factors control variation in subseafloor sedimentary habitats, activities, and biomass from gyre center to gyre margin; (3) quantified the availability of dissolved hydrogen throughout the sediment column; and (4) document first-order patterns of basement habitability and potential microbial activities. A broad range of postexpedition studies will complete the expedition objectives.

Expedition 329 sites are located along two transects, hinged in the center of the South Pacific Gyre. The first transect progresses from the western edge of the gyre (Site U1365) to the gyre center (Site U1368). The second transect goes from the gyre center (Site U1368) through the southern gyre edge (Site U1370) to the northern edge of the upwelling region south of the gyre (Site U1371).

Subseafloor sedimentary habitability and life

The dominant lithology is zeolitic metalliferous clay at the deeper water sites on older basement (58 to ≤120 Ma) within the gyre (Sites U1365, U1366, U1369, and U1370). Manganese nodules occur at the seafloor and intermittently within the upper sediment column at these sites. Chert and porcellanite layers are pronounced in the lower half of the sediment column at Sites U1365 and U1366. The dominant lithology is carbonate ooze at Site U1368, the site on youngest basement (13.5 Ma) and, consequently, in the shallowest water. At Site U1371, which lies on relatively old basaltic basement (71.5–73 Ma) just south of the gyre, the dominant lithology is siliceous ooze, with metalliferous zeolitic clay at the base of the sediment column.

Throughout the South Pacific Gyre (Sites U1365–U1370), dissolved oxygen and dissolved nitrate are present throughout the entire sediment column. Concentration profiles of oxygen and nitrate demonstrate subseafloor O_2 loss and NO_3^- production and indicate that the subseafloor rate of microbial respiration is generally extremely low. In contrast, at Site U1371 in the upwelling zone just south of the gyre, detectable dissolved oxygen and dissolved nitrate are limited to just below the sediment/water interface and just above the sediment/basalt interface. Manganese reduction is a prominent electron-accepting process throughout most of this sediment column.

Geographic variation in subseafloor profiles of dissolved oxygen, dissolved nitrate, dissolved phosphate, dissolved inorganic carbon (DIC), solid-phase total organic carbon (TOC), and solid-phase total nitrogen (TN) are consistent with the magnitude of organic-fueled subseafloor respiration declining from outside the gyre to the gyre center.

At all sites located within the gyre, microbial cell counts are three or more orders of magnitude lower than at the same sediment depths at all sites previously cored by scientific ocean drilling. Microbial cell counts are generally higher at the site outside the gyre (Site U1371) than at the sites within the gyre but are lower than at all other sites previously drilled. Countable cells disappear within the upper sediment column at every site in the gyre (Sites U1365–U1370). Dissolved oxygen content, dissolved nitrate concentration, TOC, and TN also decrease with depth and then stabilize as countable cells disappear. The downhole disappearance of countable cells and measurable organic oxidation appears to result from the disappearance of organic electron donors.

Dissolved electron acceptors (oxygen at Sites U1365–U1370 and sulfate at Site U1371), dissolved nitrate, dissolved phosphate, and DIC are present throughout the entire sediment column at all sites in the gyre, indicating that microbial life is not limited by availability of electron acceptors or major nutrients (carbon, nitrogen, and phosphorus) in these sedimentary environments.

Dissolved hydrogen concentration is below detection in the upper sediment column of all sites within the gyre. At most sites, it rises above detection with increasing depth. Because dissolved H_2 is continually produced by in situ water radiolysis, the presence of dissolved H_2 in many samples suggests that hydrogen-utilizing microbial activity is impaired or absent at sample depths where H_2 concentration is detectable and oxygen is present. At Site U1371, which is anoxic throughout most of the sediment column, dissolved hydrogen concentration is low but above detection through much of the column, with slightly higher values at the base of the column.

Paleoceanography

High-resolution measurements of dissolved chloride and nitrate concentrations, as well as formation factor, provide the opportunity for reconstruction of glacial seawater characteristics through the South Pacific Gyre. Given the importance of this region in terms of ocean circulation, such reconstruction will greatly contribute to understanding of the global ocean-climate system.

Basalt alteration and habitability

At the sites with oldest basement, alteration of the basement basalt continues on the timescale of formation fluid replacement. At all sites, the presence of dissolved oxygen in the lowermost sediment at below-deepwater concentrations suggests that either (1) basement oxidation has occurred since seawater migrated into the formation or (2) oxygen has been lost to the overlying sediment along the flow path. At the sites with deepest sediment (Sites U1365, U1370, and U1371), dissolved potassium profiles indicate that (1) dissolved potassium fluxes into the underlying basalt and (2) basalt alteration continues despite the great age of basement at all three sites (84–120, 74–79.5, and 71.5–73 Ma, respectively). Profiles of dissolved oxygen, DIC, dissolved nitrate, and dissolved phosphate in the lowermost sediment at each site indicate that if microbial life is present in the uppermost basalt, it is not limited by access to electron acceptors (oxygen and nitrate) or major nutrients (carbon, nitrogen, and phosphorus).

Introduction

The nature of life in the sediment beneath mid-ocean gyres is very poorly known. Almost all sites where subseafloor sedimentary life has been studied are on ocean margins (Ocean Drilling Program [ODP] Legs 112, 180, 201, and 204 and Integrated Ocean Drilling Program [IODP] Expeditions 301, 307, and 323) or in the equatorial ocean (ODP Legs 138 and 201). Despite those advances, the extent and character of subsurface life throughout most of the ocean remains unknown (Ocean Studies Board, 2003). This absence of knowledge is largely due to ignorance of subseafloor life in the major ocean gyres, which collectively cover most of the area of the open ocean.

The South Pacific Gyre is the ideal region for exploring the nature of subseafloor sedimentary communities and habitats in the low-activity heart of an open-ocean gyre. It is the largest of the ocean gyres and its center is farther from continents than the center of any other gyre. Surface chlorophyll concentrations and primary productivity are lower in this gyre than in other regions of the world ocean (Behrenfeld and Falkowski, 1997) (Fig. **F1**). Its surface water is the clearest in the world (Morel et al., 2007). The sediment of this region has some of the lowest organic burial rates in the ocean (Jahnke, 1996). Our recent survey cruise demonstrates that shallow sediment of this region contains the lowest cell concentrations and lowest rates of microbial activity ever encountered in shallow marine sediment (D'Hondt et al., 2009).

The region is also ideal for testing hypotheses of the factors that limit hydrothermal circulation and chemical habitability in aging oceanic crust (sedimentary overburden, basement permeability, and decreasing basal heat flux). It contains a continuous sweep of oceanic crust with thin (1–100 m) sedimentary cover spanning thousands of kilometers and >100 m.y. of seafloor age.

The South Pacific Gyre contains the largest portion of the seafloor that has never been explored with scientific ocean drilling. Consequently, IODP Expedition 329 will advance scientific understanding across a broad front, will help to constrain the nature of crustal inputs to the subduction factory, and will constrain the origin of the Cretaceous Normal Superchron and tectonic history of a region as large as Australia. Recovery of sedimentary interstitial waters at several of the proposed sites will provide novel constraint on glacial–interglacial pCO_2 models.

Background

Expedition history

Expedition 329 is based on IODP drilling Proposal 662-Full3, "Life beneath the seafloor of the South Pacific Gyre" (available at **iodp.tamu.edu/scienceops/precruise/spacificgyre/662-Full3_DHondt.pdf**). Following ranking by the IODP Scientific Advisory Structure, the expedition was scheduled for the R/V *JOIDES Resolution*, operating under contract with the U.S. Implementing Organization (USIO). The expedition started in Papeete, Tahiti, on 8 October 2010 and ended in Auckland, New Zealand, on 13 December. Further details about USIO and the facilities aboard the *JOIDES Resolution* can be found at **www.iodp-usio.org/.** Supporting site survey data for Expedition 329 are archived at the IODP Management International, Inc., Site Survey Data Bank (**ssdb.iodp.org/**).

Geological setting

Expedition 329 sites span nearly the entire width of the Pacific plate in the Southern Hemisphere between 20° and 45°S (Fig. **F2**). This ocean crust was accreted along at least four different plate boundaries (e.g., Pacific/Phoenix, Pacific/Antarctic, Pacific/Farallon, and Pacific/Nazca). Crustal ages range from ~100 Ma (Chron 34n) at Site U1365 to ~6 Ma (Chron 3An.1n) at alternate Proposed Site SPG-7A. Calculated spreading rates range from slow–intermediate (<20 km/m.y., half-rate) to ultrafast (>80 km/m.y., half-rate).

The site locations cover a relatively wide range of crustal ages, spreading rates, and tectonic/volcanic environments. The depth and crustal age of each coring site correlates well with the predicted depth versus age curve (Stein and Stein, 1994), which suggests the sites are located on representative crust. Calculated spreading rates at each site are somewhat biased toward fast and ultrafast spreading rates (28–95 km/m.y., half-rate). Surprisingly, the 95 km/m.y. value is one of the fastest spreading half-rates measured globally. The abyssal hill fabric is relatively well defined for most coring sites. However, off-axis volcanism at alternate Site SPG-5A and Site U1368 masked the original seafloor fabric. Sediment thickness ranges from <3 to 122–130 m and generally increases west and south of our survey area. This sediment thickness trend is consistent with greater sediment cover on older crust and on crust located farther away from the center of the gyre. The notable exception to this trend is along the northern transect on crust accreted along the Pacific-Farallon spreading system and older than ~30 m.y. Sediment at each of the sites generally appears as pelagic drape, with some localized mass wasting deposits. Seismic images also reveal areas of bottom current activity occasionally resulting in localized scouring of all sediment above volcanic basement (e.g., alternate Site SPG-5A).

Microbiological setting

The sedimentary communities and activities of shallow (0–8 mbsf) South Pacific Gyre sediment are unlike those in any sediment of equal depth previously explored by IODP or ODP (D'Hondt et al., 2009). The survey expedition, KNOX-02RR, demonstrated that cell concentrations and organic fueled respiration in the shallow sediment (0–8 meters below seafloor [mbsf]) of Sites U1365–U1370 are orders of magnitude lower than concentrations in previously examined sediment of equivalent depth (Fig. **F3**) (D'Hondt et al., 2009). Dissolved oxygen (O_2) penetrates extremely deeply (Fig. **F4**) (Fischer et al., 2009).

These results demonstrated that at least in the shallow sediment (1) net metabolic activities are low and oxygen is the principal net terminal electron acceptor and (2) biomass is substantially different than in any previously examined deep-sea sediment. In contrast, on the southern edge of the gyre, where sea-surface chlorophyll content is much higher, cell concentrations and dissolved chemical concentrations in the shallow (0–4 mbsf) sediment (D'Hondt et al., 2009) resemble those of ODP Site 1231 (on the northeastern edge of the gyre) (Figs. **F3, F4**), where most of the subseafloor pore water is anoxic and the community may be principally supported by oxidation of organic matter coupled to reduction of Mn(IV), Fe(II), and NO_3^- migrating up from the

underlying basaltic aquifer (Shipboard Scientific Party, 2003; D'Hondt et al., 2004). These results suggest that biomass and microbial activity in subseafloor sediment may vary predictably with sea-surface chlorophyll content.

Seismic studies/Site survey data

From 18 December 2006 to 27 January 2007, Expedition KNOX-02RR, aboard the R/V *Revelle*, surveyed all 11 drilling sites (Fig. **F1**). Sediment was geophysically imaged and cored at all 11 sites. Sites U1365–U1370 are in the central portion of the South Pacific Gyre. Site U1371 is below higher productivity water at the gyre's southern edge. All of the sites are at a crossing point of two track lines or on a single track line immediately adjacent to a crossing point. The multibeam and seismic results are provided in figure form for each site (see D'Hondt et al., 2010).

Geophysical data collected at each site include SIMRAD EM120 swath map bathymetry and Knudsen digitally recorded 3.5 kHz seismic reflection and multichannel seismic reflection. Data were collected at 4.5–6 kt with continuous Global Positioning System (GPS) navigation, including at least one set of intersecting track lines. Following each geophysical survey, shallow sediment (0–8 mbsf) was recovered using gravity, piston, and multicores. At sites with water depths deeper than 4 km, this shallow sediment is principally abyssal clay capped by manganese nodules. At sites in shallower water (proposed Sites SPG-6A and SPG-7A), the shallow sediment is clayey nannofossil ooze.

All Expedition 329 drill sites are supported by seismic, navigation, and bathymetric data and classified as "1Aa" by the Site Survey Panel (SSP). The 1Aa classification indicates that all required data are in the data bank and have been reviewed by the SSP and that they image the target adequately and there are no scientific concerns of drill site location and penetration.

Scientific objectives

Our study has the following fundamental objectives:

1. To document the habitats, metabolic activities, genetic composition and biomass of microbial communities in subseafloor sediment with very low total activity.

2. To test how oceanographic factors (such as surface ocean productivity) control variation in sedimentary habitats, activities and communities from gyre center to gyre margin.
3. To quantify the extent to which subseafloor microbial communities of this region may be supplied with electron donors (food) by water radiolysis, a process independent of the surface photosynthetic world.
4. To determine how basaltic basement habitats, potential activities and, if measurable, microbial communities vary with crust age and hydrologic regime (from ridge crest to abyssal plain).

We proposed to meet these objectives by (1) coring the entire sediment column at several sites along two transects in the region of the South Pacific Gyre (Figs. **F1, F2**); (2) coring and logging the upper 100 m of the basaltic basement at three key sites; and (3) undertaking extensive microbiological, biogeochemical, geological, and geophysical analyses of the cores and drill holes.

The project results address several significant questions. Are the communities in mid-gyre subseafloor sediment uniquely structured? Do they contain previously unknown organisms? What are their principal sources of metabolic energy? Do their principal metabolic activities, and composition vary with properties of the surface world, such as sea-surface chlorophyll concentrations or organic flux to the seafloor? Is microbial activity is sustainable in subseafloor basalt by mineral oxidation (e.g., oxidation of iron and sulfur species in the basaltic minerals) for tens of millions of years after basalt formation? Are microbial communities recognizably present in subseafloor basalt older than 13 Ma?

These questions can be framed as hypotheses to be tested. For example, we hypothesized that:

1. A living community persists in the most organic poor sediment of the world ocean.
2. Organic-fueled metabolic activity is extremely low and oxygen is the principal net terminal electron acceptor in this sediment. Consequently, the degree of anaerobic activities is far lower here than in previously examined subseafloor sediments.
3. The biomass and composition of this subseafloor sedimentary community is distinctly different from the communities observed in organic-rich anaerobic subseafloor ecosystems on the continental margins.

4. H_2 from water radiolysis is a significant electron donor for microbial respiration in the most organic-poor subseafloor sediment.
5. Open flow continues in the very old basalt of the western gyre.
6. Basalt oxidation may support chemolithotrophic microbial activity for 100 m.y. here.
7. Biomass and activity decrease with basement age as electron donor accessibility decreases.

Even if none of the above hypotheses are found to be valid, the results of Expedition 329 will significantly advance understanding of the subsurface world. Scientists will test the extent to which distinct oceanographic and geologic provinces contain distinct subseafloor habitats and distinct subseafloor communities. They will document the extent to which life in the low-activity gyre sediment depends on the surface photosynthetic world—and the extent, if any, to which it is metabolically independent of the surface world. They will place firm constraints on the potential for microbial redox activity in ancient subseafloor basalt and how that potential varies with crustal age over 100 m.y. or more. They will place firm constraints on estimates of total subseafloor biomass and habitable space on our planet.

The results of Expedition 329 and subsequent shore-based studies will also test

1. The factors that control evolution of geothermal circulation and chemical alteration in oceanic crust,
2. Models of regional tectonic history,
3. Geodynamo models, and
4. Models of glacial–interglacial ocean-climate change.

Explanation of primary objectives

1. *To document the habitats, metabolic activities, genetic composition, and biomass of microbial communities in subseafloor sediment with very low total activity.*

Key questions: What are the principal microbial activities in mid-gyre subseafloor sediment? What are the rates of those activities? How dense are the populations in this sediment? What are the communities active here? How do these communities and activities compare to those in subseafloor sediment with much higher levels of activity? How unique are their organisms?

Expedition 329 provides a crucial opportunity to document microbial habitats, activities, and community composition in a subseafloor sedimentary ecosystem that has never been explored by scientific ocean drilling.

Metabolic activities

The penetration of high concentrations of O_2 and NO_3^- meters into the sediment at KNOX-02RR survey sites suggested that the net rate of electron-accepting activity is even lower in the South Pacific Gyre than at Site 1231 (in the Peru Basin) (D'Hondt et al., 2009). Along with chemical data from Deep Sea Drilling Project (DSDP) Leg 92, these O_2 and NO_3^- profiles also suggested that the principal electron-accepting activity in the deep subseafloor sediment of this region may be different than at any of the sites where subseafloor sedimentary communities have been previously explored. A sequence of sites was drilled during Leg 92 at ~20°S in the northern portion of the gyre (Leinen, Rea, et al., 1986). At all Leg 92 sites where pore water chemistry was analyzed, dissolved NO_3^- is present throughout the entire sediment column, which is as thick as 50 m (Gieskes and Boulègue, 1986). Because NO_3^- concentrations do not significantly change with depth in the KNOX-02RR survey cores (except at Site U1371) or the Leg 92 cores, O_2 was predicted to be the principal net electron acceptor in subseafloor sediment throughout the South Pacific Gyre (D'Hondt et al., 2009).

Biomass

Quantification of subseafloor biomass in the South Pacific Gyre will place strong constraints on the size of Earth's subseafloor biomass and total biomass.

On the basis of acridine orange direct counts in subseafloor sediment of relatively high activity sites, subseafloor sedimentary biomass has been estimated to comprise one-tenth to one-third of total carbon of living biomass on Earth (Parkes et al., 2000; Whitman et al., 1999). A subsequent study of intact polar lipids estimated living archaeal biomass in subseafloor sediment to be 90 Pg (Lipp and Hinrichs, 2009), equal to ~15% of Earth's living biomass. These estimates make a key assumption that needs to be tested by Expedition 329; they assume that the sites where cells were counted are representative of biomass content in the subseafloor sediment of all regions. However, most sites used for these biomass estimates are in relatively organic-rich high-biomass sedimentary environments and therefore may not accurately represent much of the world ocean. As described earlier, cell concentrations in the KNOX-02RR cores are orders of magnitude lower than concentrations at the same depths in all previous IODP/ODP sediment (D'Hondt et al., 2009) (Fig. **F3**). Therefore, living subseafloor

biomass may be far lower than 10%–30% of Earth's total biomass. This fundamental issue will be addressed by Expedition 329.

Community composition

Genetic analyses of bulk sediment samples and cultured bacterial isolates from deep beneath the seafloor have demonstrated that similar subseafloor sedimentary environments separated by thousands of kilometers contain similar phylogenetic types of microbial communities. For example, hydrate-bearing sediment of the Peru margin and the northwestern U.S. margin (Hydrate Ridge) resulted in statistically similar compositions of 16S ribosomal ribonucleic acid (rRNA) gene clone libraries (Inagaki et al., 2006). In contrast, nearby sites with different sedimentary environments contain very different populations, suggesting that environmental factors on energetic constraints and availability may significantly affect the geographic distribution of microbial communities and their metabolic processes (Inagaki et al., 2006).

Other studies demonstrated the presence of previously undiscovered and therefore uncharacterized phylogenetic lineages in subseafloor sediment, even within a few meters of the seafloor (Sørensen et al., 2004). For example, archaeal 16S rRNA gene clone libraries from shallow sediment (≤2.1 mbsf) collected during the KNOX-02RR cruise show that the diversity of predominant archaeal components shift from *Nitrosopmilus*-related ammonia oxidizers (a-subgroup) to physiologically unknown members of η- and υ-subgroups within the Marine Crenarchaeota Group I (MG-I) (Durbin and Teske, 2010).

In combination with the metabolic points described above, these genetic discoveries underscore three important points about potential community composition in subseafloor sediment of the South Pacific Gyre. First, the gyre's subseafloor microbial communities may greatly differ from those of any subseafloor environments explored to date. Second, the very low activity and potentially aerobic communities of the deepest sediment in the South Pacific Gyre are likely to contain unique and previously undiscovered microorganisms. Third, exploration of the gyre sediment may provide deep insight into community composition and structure throughout much of the open ocean, because the genetic communities of subseafloor sediment in the other major ocean gyres may resemble those of the South Pacific Gyre.

2. *To test how oceanographic factors (such as surface ocean productivity) control variation in sedimentary habitats, activities and communities from gyre center to gyre margin.*

Key question: How are subseafloor sedimentary activities and communities affected by oceanographic properties that vary predictably from gyre center to gyre margin?

Expedition 329 provides a unique opportunity to document how the nature of subseafloor sedimentary life varies with oceanographic properties in the least biologically active region of the world ocean.

Pore water surveys of regions with higher organic fluxes to the seafloor, such as the equatorial Pacific and continental margins, suggest that the principal electron-accepting activity and the net rates of electron-accepting activities vary predictably with sea-surface chlorophyll content and organic flux to the seafloor (D'Hondt et al., 2002, 2004). These relationships appear principally due to reliance of subseafloor sedimentary communities on burial of photosynthesized organic matter for electron donors. Other sedimentary properties that vary with measures of oceanic productivity include sediment composition, which depends on the rate of microfossil production in the overlying water column as well as on the position of the carbonate compensation depth (CCD), and sediment thickness, which largely depends on the rate of calcium carbonate and biosilica production in the overlying water column.

The KNOX-02RR results (D'Hondt et al., 2009) suggest that the principal electron-accepting activity, net rates of activities, and cell concentrations in the shallow subseafloor sediment of the South Pacific Gyre vary with sea-surface chlorophyll content from within the gyre to outside the gyre and perhaps from site to site within it. Expedition 329 will test these predictions.

3. *To quantify the extent to which these sedimentary communities may be supplied with electron donors (food) by water radiolysis.*

Key question: To what extent does the ecosystem of organic-poor sediment depend on *in situ* radiolysis of pore water?

Expedition 329 will provide an unprecedented opportunity to determine if subseafloor life in very low activity sediment is nourished to a significant extent by H_2 from in situ radiolysis of water.

Buried organic matter appears to be the principal source of electron donors in subseafloor sediment of ocean margins and the equatorial Pacific (D'Hondt et al., 2004).

However, the burial flux of organic carbon is so low in the South Pacific Gyre that in situ radiolysis of water may be the principal source of electron donors there (D'Hondt et al., 2009) (Fig. **F5**).

Water radiolysis has been described as a possible source of energy for ecosystems in hard rock far beneath continental surfaces (Pedersen, 1996; Lin et al., 2005a). The longest-lived products of water radiolysis are the electron donor H_2 and the electron acceptor O_2 (Debierne, 1909). H_2 can be supplied by in situ radiolysis or, in theory, by transport of radiolytic H_2 from a much deeper biologically dead environment (e.g., the mantle and oceanic basement deep beneath sediment).

The potential importance of water radiolysis to subseafloor sedimentary communities can be assessed by comparing radiolytic H_2 production to organic-fueled respiration. For this comparison, in situ H_2 production by water radiolysis must be quantified from (1) logging estimates of uranium, thorium, and potassium concentrations (D'Hondt, Jørgensen, Miller, et al., 2003) or inductively coupled plasma–mass spectrometry data (Blair et al., 2007), (2) shipboard physical property measurements (porosity and density) (D'Hondt, Jørgensen, Miller, et al., 2003), and (3) a numerical model of water radiolysis (Blair et al., 2007).

Water radiolysis may provide a higher flux of electron donors than buried organic matter in gyre sediment. Organic-fueled respiration rates are much lower in this sediment than in any previously drilled regions of the world ocean. Clay-rich sediment contains much higher concentrations of radioactive elements than other deep-sea sediment. Furthermore, in fine-grained porous sediment, most alpha and beta production occurs within striking range of pore water. Consequently, clay-rich sediment will yield much higher rates of water radiolysis than other geological environments.

Quantification of rates of microbial uptake of radiolytic H_2 requires measurement of dissolved H_2 concentrations in the cored sediment (Fig. **F6**). The expected rate of radiolytic H_2 production is so high (D'Hondt et al., 2009) that in situ H_2 concentrations are measurable onboard if the H_2 is not biologically utilized. If H_2 is biologically utilized, its in situ concentrations will be below detection; because of its high activation enthalpy, the recombination of O_2 and H_2 does not occur at measurable rates at temperatures below 400°C. Bacterial catalysis allows this reaction on a timescale of minutes.

A number of postexpedition studies will help to further constrain the role of radiolysis in the subseafloor sediment and basalt of the South Pacific Gyre. Measurement and

transport modeling of He^{-4} concentration profiles will constrain estimates of radiolysis rates independently of estimates based on abundances of radioactive elements. Postcruise experiments with sterilized samples of cored sediment and basalt plus tritium-labeled water may be used to verify rates of H_2 production by water radiolysis Similar (unlabeled) experiments with artificial radiation sources were done by Lin et al. (2005b). Radiolysis rates may be compared to measured hydrogen turnover in sediment incubations with known numbers of microbial cells using an array of relevant electron acceptors (O_2, NO_3^-, and oxidized metals). In this way, possible rates of microbial hydrogen oxidation in the subsurface ecosystem can be constrained.

4. *To determine how basement habitats, potential activities and, if measurable, communities vary with crust age and hydrologic regime (from ridge crest to abyssal plain).*

Key questions: How does the habitability of subseafloor basalt change with crust age? How does this change depend on basement hydrologic evolution and mineral alteration? Do fractures remain open for flow in basalt as old as 100 Ma? What is the role of sediment cover in controlling hydrologic flow, alteration, and habitability in subseafloor basalt? Are dissolved oxidants (oxygen and nitrate) available in thinly sedimented subseafloor basalt as old as 100 Ma? Are reduced elements (e.g., iron and sulfur) available for oxidation in basalt as old as 100 Ma? Does mineral oxidation support measurable microbial activity in this basalt?

Expedition 329 provides a unique opportunity to determine how basement habitability and microbial communities vary with crust age, sediment cover, and hydrologic conditions over 100 m.y. or more of basement history in the most thinly sedimented region of the world ocean.

Subseafloor basalt has been described as the largest potential microbial habitat on Earth (Fisk et al., 1998). Glass alteration textures have been interpreted as evidence of microbial colonization in subseafloor basalt as old as 145 Ma (Fisk et al., 1998; Furnes and Staudigel, 1999). Laboratory experiments indicate that microbial communities may play an important role in basalt weathering (Staudigel et al., 1998). Other experiments with cultured isolates and biomineralogical studies using seafloor basalts suggest that microbes can derive their energy from rock weathering (e.g., oxidation of reduced iron and sulfur in minerals) (Edwards et al., 2003). A study of fluid samples from a cased borehole in 3.5 Ma basalt on the eastern flank of the Juan de Fuca ridge showed that microbes exist in the borehole (Cowen et al., 2003).

Despite this evidence, the nature and extent of subseafloor basaltic communities remain largely unknown and the factors that control the "metabolic habitability" of the basalt (the ability of the basalt to fuel microbial reactions) are largely unexplored. The biological significance of the textural features and the factors that control alteration and its timing in crust are not well constrained.

Metabolic habitability of subseafloor basalt ultimately depends on the supply of electron donors (including reduced Fe and S) in the basalt and hydrogen from in situ radiolysis and the supply of electron acceptors (e.g., O_2 and NO_3^-) from seawater flowing into and through the basalt. Processes that change these supplies over the basalt's lifetime include mineral alteration, which changes the supply of electron donors, and the evolution of hydrologic flow through the basalt, which changes the supply of electron acceptors.

Evolution of crust alteration and metabolic habitability

Compilation of DSDP/ODP geochemical data, mostly from the North Atlantic, suggests that oxidation of Fe and S in the upper few hundred meters of subseafloor basalt occurs principally during the first 10 m.y. after basalt formation (Bach and Edwards, 2003). During this interval, the Fe(III)/ΣFe ratio of the bulk basalt in the database increases from ~0.15 to 0.35 and most of the sulfur is oxidized (Bach and Edwards, 2003). Whether this alteration is microbially mediated or not, it changes the redox habitability of the basalt. Alteration patterns are heterogeneous within and between cores, with greatest alteration in permeable zones, such as brecciated pillows (Bach and Edwards, 2003).

Recent studies of altered basalt at ODP Site 801 (~170 Ma) showed that alteration characteristics of this ancient oceanic basement are generally similar to those observed in much younger crust (e.g., ODP Hole 504B at ~6 Ma), suggesting that most alteration takes place when oceanic crust is young (Alt et al., 1992). If oxidative alteration ceases 10–15 m.y. after basalt formation, then the oceanic crust inhabitable by mineral-oxidizing microbes is limited to basalt younger than 10–15 Ma.

Other evidence suggests that oxidative alteration need not be limited to basalt younger than 10–15 Ma. Older basalt has potential for continued redox alteration, and it probably occurs in some geochemical/hydrological regimes. Geophysical measures of matrix density suggest that about half of all intergrain-scale crustal alteration in the uppermost basalt occurs in basement older than 10–15 Ma (Jarrard et al., 2003). In the equatorial Pacific, dissolved O_2 and NO_3^- are present in basement as old as 35

Ma (D'Hondt et al., 2004). As much as 65% of the Fe remains as Fe(II) in shallow oceanic basalt older than 10 Ma (Bach and Edwards, 2003). Whether this Fe(II) continues to be oxidized at very slow rates where exposed to dissolved O_2 and NO_3^- or is physically inaccessible to oxidation remains to be determined.

Sediment thickness provides one explanation for the average change in redox alteration at 10–15 Ma. Once sedimentary cover is thick enough and anoxic enough to seal basement from contact with oxidized seawater, redox disequilibria (habitability) may disappear and oxidative alteration cease. Drilling basement of different ages beneath the unusually thin sediment cover in this region of the Pacific presents a unique test of this hypothesis. If a critical sediment thickness is necessary to curtail oxidative alteration, then the young (13.5 Ma), moderate (33.5 Ma), and old (84–125 Ma) basement sites drilled during Expedition 329 will exhibit more intense or differing styles of alteration relative to other fast-spreading sites of comparable age and greater sediment cover (e.g., Site 801, ~400 m of sediment at ~170 Ma; ODP Site 1256, ~200 m of sediment at 15 Ma; and Hole 504B, ~250 m of sediment at ~6 Ma). If this is the case, the basaltic environment of the South Pacific Gyre is redox habitable for many tens of millions of years after basalt formation.

Evolution of crustal hydrology and chemical habitability

The timing and distribution of shallow basement alteration is intriguingly linked to evidence of the hydrologic evolution of subseafloor basalt. Seismic velocity and macroporosity data suggest that porosity and bulk permeability of subseafloor basalt decrease rapidly during the first 10–15 m.y. after basalt formation (Jarrard et al., 2003). These decreases are thought to derive from secondary mineralization in the basalt. This mineralization reduces surface area within the basalt and may limit electron donor and nutrient availability in the basaltic aquifer.

Global compilations of heat flow data indicate that advective heat loss is high in young seafloor and decreases with increasing age until ~65 Ma, where, on average, advective heat loss ceases (Stein and Stein, 1994) (Fig. **F7**). Fisher and Becker (2000) explain these observations by invoking closure of small-scale permeability in basement within 10–15 m.y. but ongoing flow for 65 m.y. in large fractures and faults that fill a relatively small volume of the rock. Three mechanisms are thought responsible for limiting hydrothermal circulation in old crust:

1. Buildup of low-permeability sediment cover, which reduces basement relief and isolates the oceanic crust from overlying seawater;

2. Ongoing mineralization, which decreases basement permeability with age; and
3. Decreasing basal heat flux with age, which reduces the driving force for buoyant fluid flow.

Basement permeability is commonly thought to ultimately control the cessation of hydrothermal circulation (Stein and Stein, 1994; Jarrard et al., 2003).

However, a growing body of evidence suggests that oceanic basalt remains permeable enough to sustain advective heat loss through its life. This evidence includes the significant variance in age-dependent heat flow averages (Stein and Stein, 1994) (Fig. **F7**), large variations in heat flow survey data of Cretaceous-aged basement (Von Herzen, 2004; Fisher and Von Herzen, 2005) velocity logs, macroporosity data, matrix data (Jarrard et al., 2003), present-day fluid flow within ~132 Ma basement at ODP Site 1149 (Shipboard Scientific Party, 2000), and celadonite precipitation ages that indicate low-temperature fluid circulation at the Trodos ophiolite (Gallahan and Duncan, 1994). Given these lines of evidence, the termination of the average heat flow deficit at ~65 Ma probably signifies that much of the open circulation between basaltic basement and ocean has largely stopped by then, rather than that hydrothermal flow has ended (Anderson and Skilbeck, 1981; Jacobson, 1992; Stein and Stein, 1994).

We hypothesize that advective fluid flow paths remain open even on old seafloor. If this is true, the apparent waning of hydrothermal circulation at ~65 Ma is controlled by sediment thickness or declining heat flow, rather than by basement permeability. The South Pacific Gyre offers a unique opportunity to test this hypothesis because its sediment is thin and its basement relief is relatively variable. If the hypothesis is true, large-scale permeability will be high regardless of basement age and heat flow data at the drill sites may deviate significantly from conductive values. Surface heat flow data from our recent survey (Fig. **F7**) and from scattered older measurements within 200 km of Sites U1365 and U1367 suggest that an active flow system may be present in the basement throughout the region of proposed drilling.

If this hypothesis is correct, the supply of the dissolved electron acceptors O_2 and NO_3^- to the upper basement of the South Pacific Gyre may remain high long past the first 10–15 m.y. after basalt formation. If drilling of the lowermost sediment and the basalt shows the occurrence of these electron acceptors in the upper basement at the sites, either (1) the metabolic habitability of South Pacific Gyre basalt remains sufficient to support life for as long as 100 m.y. or (2) the metabolic habitability of this basalt is ultimately controlled by the inaccessibility of electron donors in the basalt

rather than by access to electron acceptors. If the first case applies, increased oxidative alteration may be evident in crust of increasingly greater age (e.g., alteration at Site U1365 will be greater than alteration at Site U1367, which will be greater than alteration at Site U1368). If the second case applies, oxidative alteration will be similar at all three sites.

Assessment of the extent and relative importance of secondary alteration to the basaltic basement will require an integrated program of petrographic, geochemical, and borehole analyses. At hand-sample and thin section scales, we will carefully describe general alteration textures and characteristics (e.g., veins, halos, vesicle filling, mineral/matrix replacement, and glass palagonitization), principal secondary mineralogy (e.g., saponite, celadonite, calcite, Fe oxyhydroxide, etc.), and the size, distribution, and orientation of veins and other structural features in the crust. Discrete samples of the core, representing "fresh" (e.g., pristine glass, if recovered), average, and end-member altered domains, will be powdered and analyzed for bulk major, trace, and volatile element chemistry, as a means of characterizing the bulk crustal composition and geochemical effects of alteration. Borehole logging and core-log integration are invaluable for reconstructing recovery gaps and estimating bulk geochemical and structural characteristics of deep basement drill sites (Barr et al., 2002; Révillon et al., 2002; Kelley et al., 2003; Pockalny and Larson, 2003). Post-expedition radiogenic isotope measurements will place important constraints on the timing of alteration at each site. For example, calcite formed during crust alteration often contains high concentrations of uranium but little to no lead, making the lead isotopic system a potentially useful calcite precipitation geochronometer, especially in old oceanic crust (Hauff et al., 2003).

Basement community composition

Drilling of the basalt sites during Expedition 329 provides a direct opportunity to test the existence and composition of microbial communities in oceanic basement of three very different ages (13.5, 33.5, and 80–125 Ma). Molecular microscopic analyses of uncontaminated basalt from the site with youngest basement will test whether or not microbes take full advantage of the redox habitability of relatively young basalt in open exchange with the overlying ocean while analyses of samples from the sites with older basement will test whether or not ongoing oxidation of the subseafloor basalt (by occurrence of reduced Fe and supply of dissolved O_2 and NO_3^- by ongoing advection and diffusion through the sediment) sustains similar (or different) communities, albeit at slower rates of redox activity. Collectively, the study of these

sites will track the compositional and functional evolution of basement microbial communities >100 m.y. in a thinly sedimented region of fast-spreading crust, where we hypothesize supply of dissolved oxidants to continue for as long as 100 m.y. (or more).

Explanation of secondary objectives

Oceanic crust inputs to the subduction factory

The altered oceanic crust at our oldest basement sites (U1365 and U1366) is outboard of the Tonga-Kermadec subduction zone. Characterizing the style and extent of alteration in this subducting plate will provide an important reference for assessing the role of altered oceanic crust in the subduction process. Of global arcs, the Tonga arc has perhaps the smallest sediment flux (Plank and Langmuir, 1998) and the altered oceanic crust in this system is proportionally more influential in the subduction process than at most other arcs. If the low sedimentation rate at this site has resulted in unusual alteration characteristics in the subducting oceanic crust, these differences may translate into geochemically distinct signatures in the magmas produced at the Tonga arc.

Regional tectonics

Sites U1365 and U1366 are centrally located in ocean crust accreted during the Cretaceous Normal Superchron (CNS). The tectonic history of this Australia-sized area is poorly constrained because correlatable magnetic seafloor anomalies are not present. Although limited bathymetry data suggest a general north–south spreading direction, the actual direction(s) and the presence of a failed rift within the region are poorly constrained. Drilling and logging ocean crust at these sites would address these questions. Radiometric dating of plagioclase within the recovered basalt would provide important age constraints (Koppers et al., 2003) and structural analysis of dipping flow units with core logging data would provide a spreading direction (Pockalny and Larson, 2003). Resolving the tectonic history of this region is critical to understanding the effect of large igneous provinces on tectonic processes and whether the Ontong Java, Manihiki, and Hikurangi plateaus were created by one or multiple mantle plumes (Taylor, 2006).

Geodynamo

The causal mechanisms for the Cocos-Nazca spreading center are still debated. Some authors have proposed the presence of a strong magnetic field during superchrons

(Larson and Olson, 1991; Tarduno et al., 2001), which would argue for an efficient geodynamo (i.e., large intensities during low reversal frequency). Others argue for a weak field (Loper and McCartney, 1986; Pick and Tauxe, 1993), suggesting that increased convective vigor in the core would increase the reversal rate by generating frequent instabilities. If the latter model applies, the Cocos-Nazca spreading center record is low in paleointensity but may contain frequent reversals. To add further controversy, the limited number of paleointensity measurements from the Cocos-Nazca spreading center yield very different results for different methods (Pick and Tauxe, 1993; Tarduno et al., 2001). Drilling basement at Site U1365 will provide important data and samples to test these models and methods. The paleointensity methods could be compared and the measurements would provide important data (in conjunction with the radiometric age) for the origin of the Cocos-Nazca spreading center and its relationship to the geodynamo.

Paleoceanography

Interstitial waters of the South Pacific Gyre represent a unique archive of glacial-aged water from which relict NO_3^- can be used to test hypotheses of glacial–interglacial ocean-climate change with significantly lower uncertainty than through proxy measurements.

It has been hypothesized that changes in strength of the biological carbon pump caused the dominant variation in Earth's climate and atmospheric CO_2 over the last 1 m.y. (Broecker, 1982). We will test the two principal models of this variation by reconstructing the preformed NO_3^- content and deep ocean $\delta^{15}NO_3^-$ of the last glacial maximum (LGM) through measurement of O_2, NO_3^-, and $\delta^{15}NO_3^-$ in the interstitial fluid of gyre sediment. Our tests utilize the fact that pore fluids from depths greater than ~30–50 mbsf (e.g., at Sites U1365 and U1370) are samples of paleo–bottom water that have effectively been out of diffusive contact with the ocean since the LGM.

Relationship to previous drilling

Site U1365 is located in the western portion of the gyre, near DSDP Sites 595 and 596 (Menard, Natland, Jordan, Orcutt, et al., 1987). There are no DSDP/ODP/IODP sites near any of the other Expedition 329 sites. The closest sites were cored during Leg 92, which recovered Oligocene and younger sediment from a series of sites at 20°S (Leinen, Rea, et al., 1986). The Leg 92 sites are located beneath higher productivity waters than the central gyre (Fig. **F1**). The entire sediment column was cored at the

Leg 92 sites; basement was encountered between 1 and 50 mbsf (with sediment depth increasing westward).

Coring-drilling strategy

Our general strategy during Expedition 329 was to core the entire sediment column multiple times at seven sites and to core the upper basement at three sites. The sites collectively underlie the full range of surface-ocean productivity conditions present in the South Pacific Gyre, ranging from the extremely low productivity conditions of the gyre center (Site U1368) to the moderately high (for open ocean) productivity at the southern edge of the gyre (Site U1371, at the northern edge of the Antarctic Convergence) (Figs. **F1, F2**). This series of sites is composed of two transects (Fig. **F1**), with the first transect centered at ~26°S, beneath the heart of the South Pacific Gyre, and the second transect centered at ~42°S in the southern portion of the gyre.

The sites in the northern sequence have been continuously far from shore and beneath the low-productivity gyre waters for many tens of millions of years (Figs. **F1, F2**). They provide an ideal opportunity to meet our first objective (to document the nature of life in subseafloor sediment with very low biomass and very low rates of activity). In combination with the southern transect, the northern transect is also necessary to meet our second objective (to determine how subseafloor sedimentary activities and communities vary from gyre center to gyre margin).

Sites U1365 to U1371 are necessary for our third objective (to quantify the extent to which subseafloor communities in organic-poor sediment are sustained by H_2 from radiolysis of water). Sites U1365, U1370, and U1371 are particularly crucial for this objective because their sediment columns are thick enough that their dissolved He^{-4} (alpha particle) concentrations and fluxes will be measurable.

The sites in the second transect have been in the southern portion of the present gyre (Sites U1369 and U1370) or south of the gyre (Site U1371) for tens of millions of years. Particularly at Site U1371, chlorophyll-a concentrations and primary productivity are much higher than at all of the sites in the northern transect (Figs. **F1, F2**). This transect is necessary to meet our second objective (to document how subseafloor sedimentary activities and communities vary from gyre center to gyre margin). Because Site U1371 provides an anoxic standard of comparison for the other sites, it is also crucial for documenting the potential uniqueness (or ubiquity) of the communities

and activities that persist in the low-activity, low-biomass sediment beneath the gyre center.

The northern sequence of sites (U1365–U1368) is placed on basaltic basement of steadily increasing age from east to west (Fig. F2). Basaltic basement ranges in age from 7 to as much as 125 Ma (Site U1365). Basement age of the southern sites ranges from 39 to 73 Ma. Their water depths generally follow the classic curve (Parsons and Sclater, 1977) of increasing water depth with increasing basement age (Fig. F2). These sites are necessary to meet our fourth objective (to document the evolution of basalt hydrology and its implications for metabolic habitability and microbial communities in ocean crust under very thin sediment cover).

Expedition synthesis

Sediment

Expedition 329 sites are located along two transects, hinged in the center of the South Pacific Gyre (Figs. F1, F2). The first transect progresses from the western edge of the gyre (Site U1365) to the gyre center (Site U1368). The second transect goes from the gyre center (Site U1368) through the southern gyre edge (Site U1370) to the northern edge of the upwelling region south of the gyre (Site U1371).

The dominant lithology is zeolitic metalliferous clay at the deeper water sites on older basement (58 to ≤120 Ma) within the gyre (Sites U1365, U1366, U1369, and U1370) (Figs. F2, F8). Manganese nodules occur at the seafloor and intermittently within the upper sediment column at these sites. Chert and porcellanite layers are pronounced in the lower half of the sediment column at Sites U1365 and U1366. The dominant lithology is carbonate ooze at Site U1368, the site on youngest basement (13.5 Ma) and, consequently, in the shallowest water. At Site U1371, which lies on relatively old basaltic basement (71.5–73 Ma) just south of the gyre, the dominant lithology is siliceous ooze, although metalliferous zeolitic clay dominates the lowest portion of this sediment column.

The dominant lithology shifts from clay to carbonate ooze at depth in two of the sites (Fig. F8). At Site U1367, the transition from clay to carbonate at 6–7 mbsf marks the time that the site subsided beneath the CCD as the underlying basement cooled with age. At Site U1370, carbonate ooze is the dominant lithology for a short interval de-

posited during planktonic foraminiferal Zone P1. This foraminifer-bearing interval is most simply interpreted as resulting from the CCD diving to greater water depth than the water depth of this site during the early Paleocene interval of low planktonic carbonate production.

Sediment thickness is generally very low throughout the gyre (Fig. **F8**). When sites of broadly similar age are compared (Site U1366, 84–120 Ma; Site U1369, 58 Ma; Site U1370; 74–80 Ma; and Site U1371, 71.5–73 Ma), thickness of the sediment column generally increases with increasing distance from the gyre center (Figs. **F1, F2, F8**).

Sedimentary microbial communities and habitability

Throughout the South Pacific Gyre (Sites U1365–U1370), dissolved oxygen and dissolved nitrate are present throughout the entire sediment column (Fig. **F9**), indicating that microbial respiration is oxic throughout the column, as predicted by D'Hondt et al. (2009) and Fischer et al. (2009). The concentration profiles of oxygen and nitrate demonstrate subseafloor O_2 loss and NO_3^- production and indicate that the subseafloor rate of microbial respiration is generally extremely low.

In contrast, at Site U1371 in the upwelling zone just south of the gyre (Fig. **F1**), detectable dissolved oxygen and dissolved nitrate are limited to just below the sediment/water interface and just above the sediment/basalt interface. Between these interfaces, the sediment is anoxic. Very high concentrations of dissolved (presumably reduced) manganese indicate that manganese reduction is a prominent electron-accepting process throughout most of this sediment column, with perhaps very short intervals of iron reduction suggested by minor peaks in dissolved iron concentration associated with local minima in dissolved manganese concentration. The rapid drop of dissolved oxygen and nitrate below their detection limits at the upper and lower edges of this sediment column and the relatively high concentrations of dissolved phosphate within this column suggest that the subseafloor rate of microbial respiration is much higher at this site than at the sites located in the gyre.

Geographic variation in subseafloor profiles of dissolved oxygen, dissolved nitrate, dissolved phosphate, dissolved inorganic carbon (DIC), total solid-phase organic carbon (TOC), and total solid-phase nitrogen (TN) are consistent with the magnitude of organic-fueled subseafloor respiration declining from outside the gyre (Site U1371) to gyre margins (Sites U1365 and U1370) to gyre center (Site U1368) (Figs. **F1, F9, F10**).

At all sites located within the gyre (Sites U1365–U1370), microbial cell counts are three or more orders of magnitude lower than at the same sediment depths in all sites previously cored by scientific ocean drilling (Fig. **F11**). Microbial cell counts are generally higher at Site U1371 than at the sites within the gyre (Sites U1365–U1370) but are lower than at all other sites previously drilled.

At all of the sites in the gyre, TOC and TN decline rapidly with depth in the upper sediment column and are generally constant at greater depth (Fig. **F10**). In contrast, at Site U1371 TOC and TN are generally much higher than at the other sites at all depths.

Countable cells disappear within the upper sediment column at every site in the gyre. Dissolved oxygen content, dissolved nitrate concentration, TOC, and TN stabilize as countable cells disappear. The downhole disappearance of countable cells and measurable oxygen reduction appears to result from the disappearance of organic electron donors.

Dissolved oxygen, dissolved nitrate, dissolved phosphate and DIC are present throughout the entire sediment column at all sites in the gyre (Sites U1365–U1370) (Fig. **F9**), indicating that microbial life is not limited by availability of electron acceptors or major nutrients (carbon, nitrogen, and phosphorus) in this sedimentary environment. At Site U1371, dissolved oxygen is absent from most of the sediment column, but the dissolved manganese concentration profile suggests that manganese reduction occurs through most of the sequence. Dissolved sulfate, dissolved nitrate, dissolved phosphate, and DIC are present throughout the entire sediment column at Site U1371, indicating that microbial life is not limited by availability of electron acceptors or major nutrients in this sedimentary environment either.

Dissolved hydrogen concentration is below detection in the upper sediment column of all sites within the gyre (Fig. **F10**). At most sites, it rises above detection with increasing depth. Because dissolved H_2 is continually produced by in situ water radiolysis, the presence of dissolved H_2 in many samples suggests that hydrogen-utilizing microbial activity is impaired or absent at sample depths where H_2 concentration is detectable and oxygen is present. At Site U1371, which is anoxic throughout most of the sediment column, dissolved hydrogen concentration is low, but above detection through much of the column, with slightly higher values at the base of the column. In the deepest sediment at that site, the apparent coexistence of dissolved oxygen, dissolved manganese, and dissolved hydrogen suggests that microbial activity at that

depth is insufficient to fully remove either oxygen or the electron donors, manganese and hydrogen.

The sulfate anomaly profile and the occurrence of disseminated pyrite in the upper 10 m of sediment at Site U1371 suggest that sulfate and manganese reduction co-occur within the column.

Paleoceanography

High-resolution measurements of dissolved chloride and nitrate concentrations, as well as formation factor, provide the opportunity for reconstruction of glacial seawater characteristics through the South Pacific Gyre. Given the importance of this region in terms of ocean circulation, such reconstruction will greatly contribute to understanding of the global ocean-climate system.

Basalt

The uppermost basaltic basement at Site U1365 is composed of lava flows, whereas the uppermost basement at Sites U1367 and U1368 is primarily composed of pillow basalt.

Basalt alteration

Alteration in lava flow units, as evident at Site U1365, appears to be strongly controlled by lithologic structure, with most alteration focused at the flow boundaries (Fig. **F14**). In contrast, alteration in pillow lava units (the dominant lithologies at Sites U1367 and U1368) appears to be more evenly distributed.

At all sites, the presence of dissolved oxygen in the lowermost sediment at below–deep water concentrations (Fig. **F9**) suggests that either (1) basement oxidation has occurred since seawater migrated into the formation or (2) oxygen has been lost to the overlying sediment along the flow path.

At the sites with oldest basement, alteration of the basement basalt continues on the timescale of formation fluid replacement. Natural gamma radiation (NGR) core logs, downhole NGR logs (Site U1368), and chemical analyses of the rock demonstrate that potassium has been consistently taken up during basalt alteration at all three sites where the basaltic basement was drilled (Sites U1365, U1367, and U1368) (Fig. **F13**). At the sites with deepest sediment (Site U1365, where basalt was drilled, plus Sites U1370 and U1371, where basalt was not drilled), dissolved potassium concentrations

are noticeably lower in the deepest sediment than in the shallow sediment (Fig. F14), indicating that (1) dissolved potassium fluxes into the underlying basalt and (2) basalt alteration continues despite the great age of basement at all three sites (84–120, 74–79.5, and 71.5–73, respectively).

At all three sites where basement was rotary cored (Sites U1365, U1367, and U1368), secondary minerals provide evidence of both oxidative alteration (iron oxyhydroxide and celadonite) and oxygen-poor alteration (saponite and secondary sulfides). Some samples have undergone multiple stages of alteration. Late vein infills suggest that alteration may be continuous or at least occur intermittently throughout the life of the ocean crust. At Site U1365, the presence in the lowermost sediment of dissolved Mg at below–deep water concentrations and dissolved Ca at above–deep water concentrations indicates that basalt-water interaction in the form of Mg exchange for Ca has occurred since seawater migrated into the formation. This exchange may continue to drive late-stage calcite precipitation, despite the great age of basement at this site (80–120 Ma).

Habitability of basaltic basement

Profiles of dissolved oxygen, DIC, dissolved nitrate, and dissolved phosphate in the lowermost sediment at each site indicate that if microbial life is present in the uppermost basalt (Fig. F9), it is not limited by access to electron acceptors (oxygen and nitrate) or major nutrients (carbon, nitrogen, and phosphorus).

Past microbial activity?

Tubelike micro-scale weathering features occur in altered glass from Site U1365 (Fig. F12). They are arranged in discrete clusters or in masses adjacent to or near fractures and iron oxyhydroxide within the glass. Similar features have been observed in marine basaltic glass elsewhere and attributed to microbial origin (e.g., Fisk et al, 1998).

Technical advances

Expedition 329 used a wide range of instruments and techniques that have not often been used on scientific ocean drilling expeditions. Details of their Expedition 329 application are provided in the "Methods" chapter of the *Expedition Report,* particularly in the "Biogeochemistry," "Microbiology," and "Physical properties" sections.

Two technical approaches were used by the Expedition 329 Scientific Party on an experimental basis, with the intention of refining them heavily for future application.

The first of these techniques was flow cytometric cell counting. The second was use of NGR core logging for shipboard quantification of absolute concentrations of ^{238}U-series elements, ^{232}Th-series elements, and potassium. Because these techniques were used on an experimental basis, they are described in dedicated chapters of the *Expedition Report.*

Preliminary scientific assessment

Expedition 329 had the following four fundamental objectives:

1. To document the habitats, metabolic activities, genetic composition and biomass of microbial communities in subseafloor sediment with very low total activity.
2. To test how oceanographic factors (such as surface ocean productivity, sedimentation rate, and distance from shore) control variation in sedimentary habitats, activities and communities from gyre center to gyre margin.
3. To quantify the extent to which subseafloor microbial communities of this region may be supplied with electron donors (food) by water radiolysis, a process independent of the surface photosynthetic world.
4. To determine how basement habitats, potential activities and, if measurable, microbial communities vary with crust age and hydrologic regime (from ridge crest to abyssal plain).

The expedition made major strides toward fulfilling all of these objectives.

Shipboard biogeochemistry, lithostratigraphy, microbiology, and physical property studies documented many fundamental aspects of subseafloor sedimentary habitats, metabolic activities, and biomass in this very low activity sedimentary ecosystem. Documentation of genetic composition and additional aspects of sedimentary habitability and biomass must await shore-based study.

Shipboard biogeochemical and cell-enumeration results have also significantly improved understanding of how oceanographic factors control variation in subseafloor sedimentary habitats, activities, and biomass from gyre center to gyre margin. Postexpedition studies are necessary to improve understanding of the underlying mechanisms and to test how oceanographic factors control variation in community composition.

Shipboard studies have quantified the availability of dissolved hydrogen throughout the sediment column and taken the samples necessary to quantify in situ rates of radiolytic hydrogen production. Postexpedition analyses of these samples are required to quantify these rates and their distribution throughout the sediment column of each site.

Shipboard biogeochemical, petrological, and physical property data document first-order patterns of basement habitability and potential microbial activities. A broad range of postexpedition studies will be necessary to further constrain habitability and to test how microbial community structure varies with basement age, water-rock interactions, and hydrologic regime.

Operations

During Expedition 329 we conducted operations in 42 holes at 7 sites ranging from 3749 to 5707 meters below sea level (mbsl). We cored 1321.8 m of sediment and basalt and recovered 1168.8 m of core (Table **T1**). Downhole logs were collected in one hole. Here we describe the coring and logging operations at each of these sites. The overall time distribution included 5.1 days in port, 27.26 days in transit, and 33.7 days on site. We covered 6655 nmi, of which 4503 nmi was transit between the first and the last site. All times in the operations section are given in local ship time unless otherwise noted. For most of the expedition, local time was Universal Time Coordinated – 10 h.

Papeete port call

Expedition 329 began with the first line ashore on Papeete, Tahiti (French Polynesia), at 0734 h on 7 October 2010. The first Tahiti port call for the *JOIDES Resolution* included refueling after the long journey from Victoria, British Columbia. After refueling, the ship was secured by tugboats and moved to the EPI North Pier, across from the town center, on 8 October. USIO staff, the expedition Co-Chiefs, and some members of the Scientific Party boarded the ship on 9 October to start setting up third-party instrumentation in the ship's laboratories in preparation for the expedition. The rest of the Science Party moved onboard on 10 October. Port call lasted 5.1 days.

Transit to Site U1365

The *JOIDES Resolution* departed Papeete for the 982 nmi journey to Site U1365 in the morning of 12 October 2010. The vessel sailed at full speed, averaging 11.5 kt, and arrived at Site U1365 at 0030 h on 16 October. The position reference was a combination of GPS signals. Although an acoustic beacon was deployed, it was not used for positioning at this site because of an electronic malfunction in the dynamic positioning system. The positioning beacon was deployed at 0805 h on 17 October and recovered at 2044 h on 21 October.

Site U1365

Five holes were cored at Site U1365. The first four holes were cored with the advanced piston coring (APC) system. The fifth and final hole was drilled with a 9⅞ inch rotary core bit. Downhole logging was originally scheduled for this site but was canceled when the overall depth of the hole was reduced because of the low penetration rates with the rotary core barrel (RCB) bit. As a proxy for microbial contamination, perfluorocarbon tracer (PFT) was continuously injected into the drilling fluid for all coring of Holes U1365B–U1365E. The advanced piston corer temperature tool (APCT-3) was deployed 8 times on the APC system, and usable data was recovered 7 times. On one of the tool runs, the data was lost while trying to recover it from the tool. For this site, APC system recovery was 95.2% and RCB system recovery was 74.5%. Overall core recovery for this site was 90.8%. A total of 55 cores were recovered after coring 251.1 m. The total length of core recovered was 228.07 m.

Hole U1365A

Rig floor operations started at 0030 h on 16 October 2010. The trip to the seafloor was without incident while measuring and drifting the tubulars and assembling the bottom-hole assembly (BHA). The top drive was picked up, the drill string was spaced out, and a washdown hole was drilled to determine depth of basement. The center bit was pulled by wireline, the vessel was offset 20 m west, and the top drive was spaced out to spud Hole U1365A. After making up the first APC core, the core barrel was run to bottom on the wireline and Hole U1365A was spudded at 0530 h on 17 October. Seafloor depth was established with a mudline core at 5706.3 meters below rig floor (mbrf). Nonmagnetic core barrels and the Flexit tool were used for the first 4 cores and APCT-3 temperature measurements were taken on Cores 329-U1365A-1H, 3H, and 4H. APC continued until basement was reached at 75.5 mbsf. A total of 26 cores were taken in Hole U1365A, with a total recovery of 74.06 m (98.1%). All cores after Core

4H were incomplete strokes, and the recovery was slowed by a very thick layer of chert formation from ~42 to 63.5 mbsf. After reaching basement on Core 26H, the bit was tripped back to just above the seafloor, ending Hole U1365A at 0845 h on 19 October.

Hole U1365B

Hole U1365B was offset 20 m north of Hole U1365A and was spudded at 1010 h. The mudline core established seafloor depth at 5705.4 mbrf. APC continued until 42.5 mbsf. Temperature measurements were taken with the APCT-3 on Cores 329-U1365B-3H, 4H, and 5H, although the data on Core 3H was lost trying to download the data from the tool. The center bit was then deployed and the formation was drilled from 42.5 to 63.5 mbsf. The center bit was pulled and APC continued until basement was reached at 75.6 mbsf. A total of 8 cores were taken with a total recovery of 55.79 m (102.2%). All cores after Core 5H were incomplete strokes and a 21 m section of hole was drilled to avoid coring a very thick layer of chert formation from ~42 to 63.5 mbsf. The drill string was tripped to just above the mudline, clearing the sea floor at 0640 h on 20 October and ending Hole U1365B.

Hole U1365C

After offsetting the vessel 20 m north, Hole U1365C was spudded at 0940 h on 20 October and advanced with the APC system to 37.5 mbsf before encountering the first hard chert layer. Temperature measurements were taken with the APCT-3 on Cores 329-U1365C-3H and 4H. The center bit was then dropped and the subsequent drilled interval ended again at 63.5 mbsf after advancing 26 m. The center bit was pulled and the APC system was redeployed and advanced by recovery until basement was encountered at 74.8 mbsf. A total of 8 cores were taken with a total recovery of 39.67 m (81.3%). All cores after Core 4H were incomplete strokes. The drill string was then tripped to just above the mudline, clearing the seafloor at 0435 h on 21 October and ending Hole U1365C.

Hole U1365D

After offsetting the vessel 20 m east, Hole U1365D was spudded at 0540 h on 21 October. The hole was advanced with the APC system for 2 cores to 19 mbsf and 18.89 m of sediment was recovered, for an overall recovery of 99.4%. After the second core, the drill string was tripped to surface and the bit cleared the rotary table at 2030 h, ending Hole U1365D.

Hole U1365E

The objective at Hole U1365E was to drill and core through the sediment/basalt interface and ~100 m into the basaltic basement. However, we cored ~50 m of basement with good recovery, did not capture the sediment/basement interface, and ran out of allocated time because of slow coring rates (<1 m/h). After a 20 m offset to the south, Hole U1365E began at 2030 h on 21 October. The BHA was set back, the APC bit was removed, and the rotary core bit and RCB coring system were assembled in preparation for running the new RCB BHA. The BHA was being assembled when a worrisome noise was noticed on the rig floor. Subsequent investigation revealed a failed crown block sheave bearing on the Number 2 sheave. After discussions with onboard staff, Transocean management, Transocean engineering, and the original equipment manufacturer, a decision was reached to restring the blocks to a 10-part configuration, isolating the damaged sheave from the system. Work was completed on the field modification and repair at 0600 h on 23 October. The BHA was then run into the hole, followed by the drill pipe, and the top drive was picked up and the drill string was spaced out to spud Hole U1365E. Water depth was recorded at 5705 mbrf using the offset from the previous hole. The center bit was deployed and Hole U1365E was spudded at 2210 h on 23 October. At 71 mbsf, the center bit was pulled and the RCB was dropped and coring began. RCB coring continued from 71 to 124.2 mbsf with good recovery. Because of extremely slow penetration rates, after the first core, half cores were cut and retrieved. A total of 53.2 m was cored and 39.66 m was recovered (74.6% recovery). Contamination testing was done with fluorescent microspheres (as well as PFT) on all cores after the sediment/basement interface core. The drill string was then tripped back to the rig floor and secured for the 494 nmi transit to the next site, ending Hole U1365E and Site U1365 at 2115 h on 27 October.

Transit to Site U1366

After a 48.85 h transit from Site U1365, covering 494 nmi and averaging 10.1 kt, the speed was reduced and thrusters and hydrophones were lowered. Speed was less than expected because two of the propulsion motors on the starboard shaft were offline with failed field coils. Dynamic positioning was initiated over Site U1366 at 2215 h on 29 October 2010. The position reference was a combination of GPS signals. No acoustic beacon was deployed, but a beacon remained on standby in the event of loss of GPS satellite coverage. Whereas automatic input into the dynamic positioning system was not possible, it was possible to manually hold the vessel in position to clear the seafloor with the BHA, if necessary.

Site U1366

Six holes were drilled or cored at this site. The first hole was a washdown hole drilled with the center bit in order to establish the sediment depth. The next five holes were cored and drilled with the APC system. PFT was continuously injected into the drilling fluid for all coring of Holes U1366B–U1366F. The APCT-3 was not deployed because the sediment thickness was only ~20 m. APC system recovery for Site U1366, was 100.6%. Extended core barrel (XCB) recovery was 0%. A total of 14 cores were attempted after coring 97.9 m. The total length of core recovered from this site was 96.45 m for a recovery of 98.5%.

Hole U1366A

Rig floor operations commenced at 2215 h on 29 October 2010. The trip to the seafloor was uneventful. The top drive was picked up, and the drill string was spaced out and spudded at 0815 h. The PFT pump was turned on to distribute PFT evenly throughout the fluid in the drill string. The washdown hole was drilled to determine depth of basement. Mud line was established at 5146.0 mbrf by tagging with the bit. After drilling down, basement was established at 17.8 mbsf. The bit was pulled back, clearing the seafloor at 0845 h and ending Hole U1366A.

Hole U1366B

After clearing the seafloor, the center bit was pulled by wireline, the vessel was offset 20 m west, and the drill string was spaced out to spud Hole U1366B. After making up the first APC core barrel, the core barrel was run to bottom on the wireline and Hole U1366B was spudded at 1045 h on 30 October. Seafloor depth was established with a mudline core at 5141.8 mbrf. APC coring continued to 17.2 mbsf. Two cores were taken with a total recovery of 17.31 m (100.6% recovery). After Core 329-U1366A-2H, the bit was tripped back to just above the seafloor, ending Hole U1366B at 1300 h on 30 October.

Hole U1366C

Hole U1366C began at 1300 h when the APC assembly cleared the seafloor after completing Hole U1366B. After offsetting the vessel 20 m north, Hole U1366C was spudded at 1345 h on 30 October and advanced with the APC system to 25 mbsf before encountering basement. Seafloor was established at 5140.5 mbrf. Three cores were taken with a total recovery of 25.42 m (101.7% recovery). The drill string was then

tripped to just above the mudline, clearing the seafloor at 1715 h on 30 October and ending Hole U1366C.

Hole U1366D

Hole U1366D began at 1715 h when the APC assembly cleared the seafloor after completing Hole U1366C. After offsetting the vessel 20 m east, Hole U1366D was spudded at 1800 h on 30 October and advanced with the APC system for three cores to 18.9 mbsf with an 18.86 m recovery (99.8% recovery). Seafloor was established at 5137.1 mbrf. After APC refusal, an XCB core barrel was deployed and advanced 2 m into the formation without any recovery. After the last core, the drill string was tripped to just above the mudline, clearing the seafloor at 2330 h on 30 October and ending Hole U1366D.

Hole U1366E

After clearing the seafloor, the vessel was offset 40 m west and the drill string was spaced out to spud Hole U1366E. After making up the first APC core barrel, the core barrel was run to bottom on the wireline and Hole U1366E was spudded at 0015 h on 31 October. Seafloor depth was established with a mudline core at 5138.8 mbrf. APC coring consisted of a single mudline core to 4.7 mbsf. One core was taken with a total recovery of 4.71 m (100.2% recovery). Core 329-U1366E-1H was recovered with a shattered liner and was not acceptable for microbiology. Hole U1366E ended with the first APC core at 0015 h on 31 October.

Hole U1366F

Hole U1366F began at 0015 h after the mudline core of Hole U1366E was completed. After offsetting the vessel 20 m west, Hole U1366F was spudded at 0130 h on 31 October and advanced with the APC coring system for four cores to 30.1 mbsf with a 30.15 m recovery. Overall recovery in Hole U1366F was 100.2%. After the last core, the drill string was tripped to surface and all drilling equipment was secured at 1815 h on 31 October, ending Hole U1366F and beginning the 1019 nmi transit to the next site.

Transit to Site U1367

After a 100.75 h transit from Site U1366, covering 1019 nmi and averaging 10.1 kt, the speed was reduced and thrusters were lowered. Speed was less than expected because two of the propulsion motors were offline, one on the starboard shaft and one

on the port shaft, both with failed field coils. Dynamic positioning was initiated over Site U1367 at 2304 h on 4 November 2010. The position reference was a combination of GPS signals. No acoustic beacon was deployed, but a beacon remained on standby in the event of loss of GPS satellite coverage. Whereas automatic input into the dynamic positioning system was not possible because of a system malfunction, it was possible to manually hold the vessel in position to clear the seafloor with the BHA if necessary.

Site U1367

Six holes were drilled or cored at this site. The first hole was a washdown hole drilled with the center bit in order to establish the sediment depth of 21.2 mbsf. The next four holes were cored with the APC system. The last remaining hole was drilled and cored with the RCB system ~33.5 m into basement. The APCT-3 was not deployed because of the sediment depths. PFT was pumped in for the entire drilling/coring interval until the last core was on deck. APC system recovery for Site U1367 was 98.1%. RCB system recovery was 11.2%. A total of 20 cores were attempted while coring 137.4 m. The total length of core recovered at this site was 101.34 m (73.8% recovery).

Hole U1367A

Rig floor operations commenced at 2300 h on 4 November 2010. The trip to the seafloor was uneventful. The top drive was picked up and the drill string was spaced out and spudded at 0740 h on 5 November. The PFT pump was turned on to displace the drill string with the contamination testing fluid. The washdown hole was drilled to determine depth of basement. Mud line was established at 4302.0 mbrf by tagging with the bit. After drilling down, basement was established at 21.2 mbsf. The bit was pulled back above the seafloor, clearing the seafloor at 0810 h on 5 November and ending Hole U1367A.

Hole U1367B

After clearing the seafloor, the center bit was pulled by wireline, the vessel was offset 20 m west, and the drill string was spaced out to spud Hole U1367B. After making up the first APC core barrel, the core barrel was run to bottom on the wireline and Hole U1367B was spudded at 1000 h on 5 November. Seafloor depth was established with a mudline core at 4300 mbrf. APC coring continued to 22.3 mbsf. Four cores were taken with a total recovery of 22.31 m (100.0% recovery). After Core 329-U1367B-4H, the bit was tripped back to just above the seafloor, ending Hole U1367B at 1440 h.

PFT was mixed with the drilling fluid (sea water) and pumped on all cores for contamination testing.

Hole U1367C

Hole U1367C began at 1440 h when the APC assembly cleared the seafloor after completing Hole U1367B. After offsetting the vessel 20 m north, Hole U1367C was spudded at 1520 h on 5 November and advanced with the APC system to 26.7 mbsf before encountering basement. Seafloor was established at 4299.3 mbrf. PFT was mixed with the drilling fluid (sea water) and pumped on all cores for contamination testing. Four cores were taken with a total recovery of 27.01 m (101.2% recovery). The drill string was then tripped to just above the mudline, clearing the seafloor at 2005 h and ending Hole U1367C.

Hole U1367D

Hole U1367D began at 2005 h on 5 November when the APC assembly cleared the seafloor after completing Hole U1367C. After offsetting the vessel 20 m east, Hole U1367D was spudded at 2205 h and advanced with the APC system for four cores to 25.5 mbsf with a 24.54 m recovery (96.2%). Seafloor was established at 4299.1 mbrf. PFT was mixed with the drilling fluid (sea water) and pumped on all cores for contamination testing. The drill string was tripped to just above the mudline, clearing the seafloor at 0255 h on 6 November and ending Hole U1367D.

Hole U1367E

Hole U1367E began at 0255 h on 6 November when the APC assembly cleared the seafloor after completing Hole U1367D. After making up the first APC core barrel, the core barrel was run to bottom on the wireline and Hole U1367E was spudded at 0340 h. Seafloor depth was established with a mudline core at 4298.7 mbrf. The APC system was used to take three cores to 24.4 mbsf with a 23.15 m recovery (94.9%). PFT was mixed with the drilling fluid (sea water) and pumped on all cores for contamination testing. The drill string was tripped to the surface, clearing the rotary table at 1400 h and ending Hole U1367E.

Hole U1367F

After a 20 m offset to the south, Hole U1367F began on 6 November at 1400 h when the bit cleared the rotary table after tripping out of Hole U1367E. The BHA was set back, the APC bit was removed, and the rotary core bit and rotary coring system were assembled in preparation for running the new RCB BHA. The BHA was run into the

hole followed by the drill pipe. The top drive was picked up and the drill string was spaced out to spud Hole U1367F. Water depth was recorded at 4300 mbrf using the BHA tag depth. The center bit was deployed and Hole U1367F was spudded at 2345 h. At 17 mbsf, the center bit was pulled and the RCB was dropped and coring began. RCB coring continued from 17 to 55.5 mbsf with poor recovery. A total of 38.5 m was cored with a recovery of 4.33 m of core. RCB system recovery in Hole U1367F was 11.2%. PFT was mixed with the drilling fluid (sea water) and pumped on all cores for contamination testing. Microspheres were also deployed on all RCB cores in Hole U1367E. The drill string was tripped back to the rig floor and secured for the 793 nmi transit to the next site, ending Hole U1367F and Site U1367 at 0545 h on 9 November.

Transit to Site U1368

After an 80.75 h transit from Site U1367, covering 793 nmi and averaging 9.8 kt, a sonar survey was initiated over Site U1368. The survey essentially replicated the lines of the original site survey in order to confirm depths of bottom and hard returns under the seafloor. After the survey was completed at 1515 h, the speed was reduced and thrusters were lowered. Speed was less than expected because one of the propulsion motors was offline and the vessel sailed most of the voyage into head winds and seas. Dynamic positioning was initiated over Site U1368 at 1545 h on 12 November 2010. The reference position was a combination of GPS signals. No acoustic beacon was deployed, but a beacon remained on standby in the event of a loss of GPS satellite coverage. Whereas automatic input into the dynamic positioning system was not possible because of a system malfunction, it was possible to manually hold the vessel in position to clear the seafloor with the BHA if necessary.

Site U1368

Six holes were drilled or cored at this site. The first hole was a washdown hole drilled with the center bit in order to establish the sediment depth of 13.6 mbsf. The next four holes were cored with the APC system. The last hole was drilled and cored with the RCB system 115.1 m below seafloor and into basement. The APCT-3 was not deployed because of the shallow sediment depth. PFT was pumped for the entire drilling/coring interval until the last core was on deck. APC system recovery for Site U1368 was 99.8%. RCB system recovery was 27.6%. A total of 23 cores were attempted while coring 173 m. The total length of core recovered at this site was 89.52 m (51.7% recovery).

Hole U1368A

Rig floor operations commenced at 1545 h on 12 November 2010. The trip to the sea floor was uneventful. The top drive was picked up and the drill string was spaced out and spudded at 0130 h on 13 November. The PFT pump was turned on to displace the drill string with the contamination testing fluid. The washdown hole was drilled to determine depth of basement. Mud line was established as 4302.0 mbrf by tagging with the bit. After drilling down, basement was established at 13.6 mbsf. The bit was pulled back above the seafloor, clearing the seafloor at 0200 hours and ending Hole U1368A.

Hole U1368B

After clearing the seafloor, the center bit was pulled by wireline, the vessel was offset 20 m west, and the drill string was spaced out to spud Hole U1368B. After making up the first APC core barrel, the core barrel was run to bottom on the wireline and Hole U1368B was spudded at 0330 h on 13 November. Seafloor depth was established at 3750 mbrf with a mudline core. APC coring continued to 16.0 mbsf. Three cores were taken with a total recovery of 15.84 m for an overall recovery in Hole U1368B of 99.0%. After Core 329-U1368B-3H, the bit was tripped back to just above the seafloor, ending Hole U1368B at 0655 h on 13 November. PFT was mixed with the drilling fluid (sea water) and pumped on all cores for contamination testing.

Hole U1368C

Hole U1368C began at 0655 h when the APC assembly cleared the seafloor after completing Hole U1368B. After offsetting the vessel 20 m north, Hole U1368C was spudded at 0730 h on 13 November and advanced with the APC system to 16.3 mbsf before encountering basement. Seafloor was established at 3749.5 mbrf. PFT was mixed with the drilling fluid (sea water) and pumped on all cores for contamination testing. Two cores were taken with a total recovery of 16.34 m for an overall recovery in Hole U1368C of 100.2%. The drill string was tripped to just above the mudline, clearing the seafloor at 0915 h and ending Hole U1368C.

Hole U1368D

Hole U1368D began at 0915 h on 13 November when the APC assembly cleared the seafloor after completing Hole U1368C. After offsetting the vessel 20 m east, Hole U1368D was spudded at 1000 h and advanced with the APC system for two cores to 15.0 mbsf with a 15.04 m recovery (100.3%). Seafloor was established at 3750 mbrf. PFT was mixed with the drilling fluid (sea water) and pumped on all cores for contam-

ination testing. The drill string was tripped to just above the mudline, clearing the seafloor at 1135 h and ending Hole U1368D.

Hole U1368E

Hole U1368E began at 1135 h on 13 November when the APC assembly cleared the seafloor after completing Hole U1368D. The vessel was offset 20 m east of Hole U1368D. After making up the first APC core barrel, the core barrel was run to bottom on the wireline and Hole U1368E was spudded at 1210 h. Seafloor depth was established with a mudline core at 3751.9 mbrf. The APC system was used to take two cores to 10.6 mbsf with a 10.58 m recovery (99.8%). PFT was mixed with the drilling fluid (sea water) and pumped on all cores for contamination testing. The drill string was tripped to the surface, clearing the rotary table at 2000 h on 13 November and ending Hole U1368E.

Hole U1368F

After a 20 m offset to the south, Hole U1368F began on 13 November at 2000 h when the bit cleared the rotary table after tripping out of Hole U1368E. The BHA was set back, the APC bit was removed, and the rotary core bit and rotary coring system were assembled in preparation for running the new RCB BHA. The BHA was run into the hole, followed by the drill pipe. After reaching 3741 mbrf, the top drive was picked up and the drill string was spaced out to spud Hole U1368F. Water depth was recorded at 3751.9 mbrf using an offset depth from Hole U1368E. Rotary coring began at the seafloor when Hole U1368F was spudded at 0520 h on 14 November. Core 329-U1368F-2R crossed the sediment/basalt interface at 11.8 mbsf. RCB coring continued from 11.8 to 115.1 mbsf with average recovery. A total of 14 cores were taken. A total of 115.1 m were cored with a recovery of 31.74 m of core. RCB system recovery for Hole U1368F was 27.6%. PFT was mixed with the drilling fluid (sea water) and pumped on all cores for contamination testing. Microspheres were also deployed on all RCB cores after Core 2R. After reaching a total depth of 115.1 mbsf, the center bit was deployed and the hole was conditioned for logging. The mechanical bit release was activated, dropping the RCB bit at the bottom of the hole. The drill string, minus the bottom half of the mechanical bit release and RCB bit, was tripped to ~30 mbsf and the logging tools were rigged up and deployed. Four logging runs, two with the triple combination (triple combo) and two with the Formation MicroScanner (FMS) tool string (no sonic) were performed successfully. At the end of logging activities, the tools were rigged down and the drill string was tripped back to the rig floor and se-

cured for the 1073 nmi transit to the next site, ending Hole U1368F and Site U1368 at 1233 h on 18 November.

Transit to Site U1369

After an 98.1 h transit from Site U1368, covering 1073 nmi and averaging 10.9 kt, the speed was reduced and thrusters were lowered. Dynamic positioning was initiated over Site U1369 at 1454 h on 22 November 2010. The position reference was a combination of GPS signals. No acoustic beacon was deployed, but a beacon remained on standby in the event of a loss of GPS satellite coverage. Whereas automatic input into the dynamic positioning system was not possible because of a system malfunction, it was possible to manually hold the vessel in position to clear the seafloor with the BHA if necessary.

Site U1369

Five holes were drilled or cored at Site U1369. The first hole was a washdown hole drilled with the center bit in order to establish the sediment depth of 12.2 mbsf. The next four holes were cored with the APC system. The APCT-3 was not deployed because of the shallow sediment depth. PFT was pumped for the entire drilling/coring interval until the last core was on deck. APC system recovery for Site U1369 was 108%. A total of 10 cores were attempted while coring 46.1 m. The total length of core recovered at this site was 49.81 m (108.0% recovery).

Hole U1369A

Rig floor operations commenced at 1445 h on 22 November 2010. The trip to the seafloor was uneventful. The top drive was picked up and the drill string was spaced out and spudded at 0040 h on 23 November. The PFT pump was turned on to displace the drill string with the contamination testing fluid. The washdown hole was drilled to determine depth of basement. Mud line was established at 5290.5 mbrf by tagging with the bit. After drilling down, basement was established at 12.2 mbsf. The bit was pulled back above the seafloor, clearing the seafloor at 0125 h and ending Hole U1369A.

Hole U1369B

After clearing the seafloor, the center bit was pulled by wireline, the vessel was offset 20 m west, and the drill string was spaced out to spud Hole U1369B. After making up

the first APC core barrel, the core barrel was run to bottom on the wireline and Hole U1369B was spudded at 0350 h on 23 November. Seafloor depth was established at 5286.3 mbrf with a mudline core. APC coring continued to 15.9 mbsf. An XCB core barrel was dropped after an initial analysis from the science party based on concern that the deepest material recovered might not have been igneous in origin. Subsequent analysis verified the rock samples to be igneous in origin and the core barrel was pulled without advancing. Three cores were taken with a total recovery of 18.14 m (114.1%). After Core 329-U1369B-3H, the bit was tripped back to just above the seafloor, ending Hole U1369B at 1030 h. PFT was mixed with the drilling fluid (sea water) and pumped on all cores for contamination testing.

Hole U1369C

Hole U1369C began at 1030 h when the APC assembly cleared the seafloor after completing Hole U1369B. After offsetting the vessel 20 m north, Hole U1369C was spudded at 1135 h and advanced with the APC system to 14.6 mbsf before encountering basement. Seafloor was established at 5288.0 mbrf. PFT was mixed with the drilling fluid (sea water) and pumped on all cores for contamination testing. Three cores were taken with a total recovery of 16.1 m (110.3%). The drill string was tripped to just above the mudline, clearing the seafloor at 1530 h on 23 November and ending Hole U1369C.

Hole U1369D

Hole U1369D began at 1530 h when the APC assembly cleared the seafloor after completing Hole U1369C. After offsetting the vessel 20 m east, Hole U1369D was spudded at 1615 h on 23 November. The core liner was shattered and even though the core barrel extended 9.5 m, manganese nodules in the core catcher comprised the only material recovered. Hole U1369D was abandoned. Seafloor was established at 5288.0 mbrf using an offset from the previous hole. Recovery was limited to a 0.08 m core length and the advance was recorded as 0.1 m. Percentage of recovery is recorded as 80%. PFT was mixed with the drilling fluid (sea water) and pumped on all cores for contamination testing. The hole ended at 1615 h with the mudline shot.

Hole U1369E

Hole U1369E began at 1615 h on 23 November after the failed mudline core on Hole U1369D. The vessel was offset 20 m east of Hole U1369D. After making up the first APC core barrel, the core barrel was run to bottom on the wireline and Hole U1369E was spudded at 1745 h. Seafloor depth was established with a mudline core at 5288.8

mbrf. The APC system was used to take three cores to 15.5 mbsf with a 15.49 m recovery (99.9%). PFT was mixed with the drilling fluid (sea water) and pumped on all cores for contamination testing. The drill string was tripped to the surface, clearing the rotary table at 0645 h on 24 November. The rig floor and secured for the 625 nmi transit to the next site, ending Hole U1369F and Site U1369 at 0730 h on 24 November.

Transit to Site U1370

After a 56.5 h transit from Site U1369, covering 625 nmi and averaging 11.1 kt, the speed was reduced and thrusters were lowered. Dynamic positioning was initiated over Site U1370 at 1602 h on 26 November 2010. The position reference was a combination of GPS signals. No acoustic beacon was deployed, but a beacon remained on standby in the event of a loss of GPS satellite coverage. While automatic input into the dynamic positioning system was not possible because of a system malfunction, it was possible to manually hold the vessel in position to clear the seafloor with the BHA if necessary.

Site U1370

Six holes were drilled or cored at Site U1370. The first hole was a washdown hole drilled with the center bit in order to establish the sediment depth of 66.7 mbsf and any hard layers (chert) throughout the formation. Hole U1370B had one mudline core taken before coring problems forced abandonment of the hole. Hole U1370C was drilled to 7.8 mbsf, and the attempt to take a piston core failed. The last three holes were cored successfully with the APC system. The APCT-3 was deployed four times on Holes U1370D and U1370E. PFT for contamination testing was pumped from Hole U1370C onward until the last core was on deck. A total of 26 cores were attempted while coring 206.3 m. The total length of core recovered at this site was 214.59 m. The overall recovery for Site U1370 using the APC coring system was 104%.

Hole U1370A

Rig floor operations commenced at 1602 h on 26 November 2010. The trip to the seafloor was uneventful. The top drive was picked up, the drill string was spaced out, and the hole was spudded at 0230 h on 27 November. The washdown hole was drilled to determine depth of basement. Mudline was established as 5085.7 mbrf using an offset depth from Hole U1370B. After drilling down, basement was established at 5150.4 mbrf (64.7 mbsf). Basement depth was verified by drilling two additional meters into

the basement. The bit was pulled back above the seafloor, clearing the seafloor at 0620 h and ending Hole U1370A.

Hole U1370B

After clearing the seafloor, the center bit was pulled by wireline, the vessel was offset 20 m west, and the drill string was spaced out to spud Hole U1370B. After making up the first APC core barrel, the core barrel was run to bottom on the wireline and Hole U1370B was spudded at 0745 h on 27 November. Seafloor depth was established at 5085.7 mbrf with a mudline core. APC coring was terminated after the second core attempt. It appeared as if there was something blocking the seal-bore collar that was preventing the core barrel from seating. The center bit was deployed in order to verify a clean seal-bore assembly and to check flow against the slow circulating rates taken at the start of the hole. Subsequent problems determined that it was most likely the shear pins failing during the deployment of the core barrel. The hole was terminated and several remedial measures were implemented. One core was taken with a total recovery of 7.81 m (100.1%). After Core 329-U1370B-1H was recovered, the bit was tripped back to just above the sea floor, ending Hole U1370B at 1000 h on 27 November.

Hole U1370C

Hole U1370C began at 1000 h when the APC assembly cleared the seafloor after completing Hole U1370B. After offsetting the vessel 20 m north, an attempt to spud Hole U1370C was made. After multiple wireline runs and multiple attempts to spud Hole U1370C, the hole was spudded at 1810 h in an attempt to advance the hole and coring began. During the effort to continue coring, several remediation efforts were attempted. The root problem seemed to be shear pin failure during the wireline trip into the hole. Rig instrumentation indicated that the core line received increasingly high tension variation as the core line was run to greater depth. Variations were ~2500 lb of force. An extra shear pin was added to the system in an effort to land the core barrel with the shear pin assembly intact. This still failed. A 90° heading change was made to try to reduce the overall heave of the vessel. Decreasing weather and the heading change successfully reduced the heave by over a meter. In an attempt to dampen the tension variation, the compensator was opened for core barrel deployment. After a drilled advance of 7.8 m, the core barrel was finally deployed without the shear pin failure that had been experienced all day. With three shear pins installed and the core barrel landed, the mud pump pressure was insufficient to shear the pins and shoot the APC core barrel. Consequently, the core barrel was pulled to the surface and re-

dressed with new shear system components and two shear pins. Hole U1370C was abandoned and the bit cleared the seafloor at 2000 h on 27 November, ending Hole U1370C.

Hole U1370D

Hole U1370D began at 2000 h, when the APC assembly cleared the seafloor after completing Hole U1370C. After offsetting the vessel 20 m east, Hole U1370D was spudded at 2115 h on 27 November. Seafloor depth was established with a mudline core at 5084.7 mbrf. An APCT-3 measurement was taken on Core 329-U1370D-4H. The APC coring system was used to take eight cores to 68.2 mbsf with 70.26 m recovery (103%). After Core 8H, the bit was advanced and rotated into basement to verify basement depth (68.2 mbsf) and the bit was tripped back to just above the seafloor ending Hole U1370D at 1250 h on 28 November.

Hole U1370E

Hole U1370E began at 1250 h when the APC assembly cleared the seafloor after completing Hole U1370D. After offsetting the vessel 20 m east, Hole U1370E was spudded at 1445 h on 28 November. Seafloor depth was established with a mudline core at 5085.3 mbrf. An APCT-3 measurement was taken on Cores 329-U1370E-3H, 5H, and 6H. The APC system was used to take nine cores to 65.6 mbsf with a 70.2 m recovery (107%). PFT was mixed with the drilling fluid (sea water) and pumped on all cores for contamination testing. After Core 9H, the bit was advanced and rotated into basement to verify basement depth (65.6 mbsf) and the bit was tripped back to just above the seafloor, ending Hole U1370E at 0855 h on 29 November.

Hole U1370F

Hole U1370F began at 0855 h when the APC assembly cleared the seafloor after completing Hole U1370E. The vessel was offset 20 m south of Hole U1370E. After making up the first APC core barrel, the core barrel was run to bottom on the wireline and Hole U1370F was spudded at 1010 h. Seafloor depth was established with a mudline core at 5084.8 mbrf. The APC system was used to take eight cores to 64.7 mbsf with a 66.32 m recovery (102.5%). PFT was mixed with the drilling fluid (sea water) and pumped on all cores for contamination testing. After Core 329-U1370F-8H, the bit was advanced and rotated into basement to verify basement depth (64.7 mbsf). The drill string was tripped to the surface, clearing the rotary table at 0530 h on 30 November. The rig floor was secured for the 499 nmi transit to the next site, ending Hole U1370F and Site U1370 at 0600 h.

Transit to Site U1371

After a 51 h transit from Site U1370, covering 499 nmi and averaging 9.8 kt, the speed was reduced and thrusters were lowered. Dynamic positioning was initiated over Site U1371 at 0907 h on 2 December 2010. The position reference was a combination of GPS signals. No acoustic beacon was deployed, but a beacon remained on standby in the event of a loss of GPS satellite coverage. Whereas automatic input into the dynamic positioning system was not possible because of a system malfunction, it was possible to manually hold the vessel in position to clear the sea floor with the BHA if necessary.

Site U1371

Eight holes were drilled or cored at Site U1371. The first hole was a washdown hole drilled with the center bit in order to establish the sediment depth of 122.5 mbsf. The entire time on site was plagued by high vessel heave, which hindered the APC coring. The first APC hole at the site came back with a disturbed mudline core and was abandoned. The second attempt at a mudline resulted in an over penetration without securing mudline and was abandoned as well. The following three APC holes were successfully cored to refusal. With the remaining time, an additional two holes were cored for mudline cores. The APCT-3 was deployed five times on Hole U1371D. PFT was pumped from Hole U1371E onward until the last core was on deck. APC system recovery for Site U1371 was 94.9%. A total of 46 cores were attempted while coring 410.0 m. The total length of core recovered at Site U1370 was 389.01 m (94.9% recovery).

Hole U1371A

Rig floor operations commenced at 0907 h on 2 December 2010. The trip to the seafloor was uneventful. The top drive was picked up, the drill string was spaced out, and the hole was spudded at 1845 h on 2 December. The washdown hole was drilled to determine depth of basement. Mudline was established as 5316.0 mbrf using the drill bit–tagged depth. There were no anomalies detected during the washdown to basement. After drilling down, basement was established at 5438.5 mbrf (122.5 mbsf). Total depth of the hole was 5439.5 mbrf after the bit was advanced into basement to verify basement contact. The bit was pulled back above the seafloor, clearing the seafloor at 2350 h on 2 December and ending Hole U1371A.

Hole U1371B

After clearing the seafloor, the center bit was pulled by wireline, the vessel was offset 20 m west, and the drill string was spaced out to spud Hole U1371B. After making up the first APC core barrel, the core barrel was run to bottom on the wireline and fired from 5310 mbrf. The core barrel came back empty and the bit was repositioned to 5315 mbrf. Hole U1371B was spudded at 0300 h on 3 December. Seafloor depth was established at 5316.4 mbrf (5305.1 mbsl) with a mudline core. Vessel heave during spud in was ~4 m. The first mudline core was too disturbed for science and the hole was terminated. One core was taken with a total recovery of 8.15 m for an overall recovery in Hole U1371B of 100.6%. After Core 329-U1371B-1H, the vessel was moved 20 m north, ending Hole U1371B at 0300 h on 3 December.

Hole U1371C

Hole U1371C began at 0300 h after abandoning Hole U1371B. After offsetting the vessel 20 m north, Hole U1371C spudded at 0445 h. Core 329-U1371C-1H came back with a full core barrel and no obvious mudline. Shoot depth was 5312 mbrf, which was 3 m higher than the shoot depth for Hole U1371B. The best explanation for another mudline failure was the high heave (>4 m) at the time of spudding. One core was taken in Hole U1371C, with a total recovery of 9.85 m (103.5%). Hole U1371C was abandoned after the first core and the vessel was moved 20 m east on 3 December, ending Hole U1371C at 0445 h.

Hole U1371D

Hole U1371D was spudded 20 m east of Hole U1371C at 0635 h on 3 December. Seafloor depth was established with a mudline core at 5311.1 mbrf (5299.9 mbsl). Orientation with the Flexit tools was done on Cores 329-U1371D-1H through 11H. APCT-3 measurements were taken on Cores 4H–6H, 8H, and 10H. All temperature measurements returned good data. While pulling Core 6H, the coring line parted at the wire rope socket and the core barrel and sinker bars fell back inside the drill pipe. The wireline was removed from the hole and reheaded at surface. The aft sinker bars were installed and a rotary core barrel was dropped to "fish" the forward sinker bars. The sinker bars were recovered by wireline, and Core 6H was recovered. Total time from the incident to resumption of coring was 5.5 h. Coring continued until refusal on Core 14H. The APC system was used to take 14 cores to 126.0 mbsf with 126.87 m recovery (100.7%). After Core 14H, the bit was advanced and rotated into basement to verify basement depth. The bit was tripped back to just above the seafloor, ending Hole U1371D at 1330 h on 4 December.

Hole U1371E

Hole U1371E began with the ship offset 20 m east of Hole U1471D. Hole U1371E was spudded at 1605 h on 4 December. Seafloor depth was established with a mudline core at 5310.2 mbrf. The APC system was used to take 14 cores to 128.2 mbsf with a 118.16 m recovery (92.2%). Nonmagnetic core barrels were used for the first 12 cores. PFT was mixed with the drilling fluid (sea water) and pumped on all cores for contamination testing. After Core 329-U1371E-14H, the bit was advanced and rotated into basement to confirm basement depth and tripped back to just above the seafloor, ending Hole U1371E at 1100 h on 4 December.

Hole U1371F

Hole U1371F was offset 20 m south of Hole U1371E. After making up the first APC core barrel, it was run to bottom on the wireline and Hole U1371F was spudded at 1205 h on 5 December. Seafloor depth was established with a mudline core at 5308.3 mbrf. The APC system was used to take 14 cores to 130.6 mbsf with a 118.44 m recovery (90.7%). PFT was mixed with the drilling fluid (sea water) and pumped on all cores for contamination testing. After Core 329-U1371F-14H, the bit was advanced and rotated into basement to verify basement depth and APC advance. The drill string was tripped to just above the seafloor, ending Hole U1371F at 0655 h on 6 December.

Hole U1371G

Hole U1371G was offset 20 m south of Hole U1371F. After making up the first APC core barrel, the core barrel was run to bottom on the wireline and Hole U1371G was spudded at 0755 h on 6 December. Seafloor depth was established with a mudline core at 5314.1 mbrf. The APC system was used to take a single core to 1.4 mbsf with a 1.37 m recovery (97.9%). PFT was mixed with the drilling fluid (sea water) and pumped on for contamination testing. After taking mudline Core 329-U1371G-1H, a second core (test Core 329-U1371G-2H) was taken for training purposes. The drill string was tripped to just above the seafloor, ending Hole U1371G at 0945 h on 6 December.

Hole U1371H

Hole U1371H was offset 20 m west of Hole U1371G. After making up the first APC core barrel, the core barrel was run to bottom on the wireline and Hole U1371H was spudded at 1030 h on 6 December. Seafloor depth was established with a mudline core at 5310.3 mbrf. The APC system was used to take a single core to 6.2 mbsf with a 6.19 m recovery (99.8%). PFT was mixed with the drilling fluid (sea water) and

pumped in for contamination testing. After taking mudline Core 329-U1371H-1H, the drill string was tripped to the surface, clearing the rotary table at 2326 h on 6 December. The rig floor was secured for the 1172 nmi transit to Auckland, ending the final hole and site of Expedition 329 at 2326 h on 6 December.

Site summaries

Site U1365

The scientific objectives at Site U1365 are

1. To document the nature of subseafloor life in very old (>100 Ma) and slowly accumulating organic-poor sediments;
2. To test how oceanographic factors (such as surface ocean productivity, sedimentation rate and distance from shore) control variation in sedimentary habitats, activities, and communities from gyre center to gyre margin;
3. To quantify the extent to which subseafloor communities in organic-poor sediment are sustained by H_2 from radiolysis of water; and
4. To determine how basement habitats, potential activities, and, if measurable, communities vary with basalt age and hydrologic regime (from ridge crest to abyssal plain).

Site U1365 (5708 mbsl) is centrally located in ocean crust formed during the CNS. The tectonic history of this Australia-sized area is poorly constrained because correlatable magnetic seafloor anomalies are not present. Consequently, radiometric dating of the recovered basalt will provide important constraints on the tectonic and volcanic history of this region.

The complete sedimentary succession was recovered by APC coring in Hole U1365A. Excluding a drilled-over chert interval in the lower sediment column, complete successions were also recovered from Holes U1365B and U1365C. Core recovery in the underlying basalt was unusually high (75%). However, slow penetration (<1 m/h) allowed us to drill only ~50 m of basalt, preventing us from reaching sufficient depth below seafloor to deploy downhole logging tools.

Principal results

Sediment

The sedimentary succession at Site U1365 is composed of three units. Unit I consists of medium-brown zeolitic metalliferous pelagic clay (0–44 mbsf). Unit II consists of porcellanite and chert (44–65 mbsf). Unit III consists of dark brown metalliferous clay (65–75 mbsf) (Fig. **F15**).

Microbial cell counts are three or more orders of magnitude lower than at the same sediment depths in all sites previously cored by scientific ocean drilling and decline to near the minimum detection limit (MDL) at 15 mbsf. They are above the MDL (1.4×10^3 cells/cm^3) in many samples (and below the MDL in many other samples) for the remainder of Unit I (Fig. **F16**). Because the chert cannot be disaggregated, the presence or absence of cells cannot be determined in Unit II. Cell counts are consistently below the MDL in the metalliferous clay at the base of the sediment column (Unit III).

Dissolved oxygen is present throughout the entire sediment column at Site U1365. It declines most rapidly in the first several meters of the sediment column and then declines at increasingly lower rates with increasing depth in Unit I (Fig. **F17**). We could not measure its concentration in the chert and porcellanite of Unit II. Its concentration is essentially constant throughout Unit III.

Dissolved nitrate, dissolved phosphate, and dissolved inorganic carbon are also present throughout the sediment column. The increase in dissolved nitrate concentration (from ~35 to 45 µM) over the first 20 mbsf is consistent with nitrate production by oxygen-fueled reduction of organic matter (Fig. **F17**). Below the chert-dominated interval, dissolved nitrate concentration approximates the present deepwater value.

Dissolved hydrogen concentration is below detection throughout most of the sediment column (with the exception of a 30 nM peak centered at 30 mbsf).

The concentration of TN declines rapidly in the first 10 mbsf from 0.05 to 0.01 wt%. It then declines more slowly, until it drops consistently beneath its MDL (~0.007 wt%) at 38 mbsf. Consistently, TOC declines rapidly over the first few meters below seafloor (from ~0.2 to 0.05 wt%) and remains below 0.05 wt% for the remainder of the sediment column (Fig. **F18**).

Basalt

The drilled sequence of basement rock is composed of a series of massive basalt flows (Fig. **F14**). Massive flows at the top of deep-sea basement are unusual in ocean drilling history (e.g., Site 1256 and Site 1243 [interpreted as a lava pond]). The low-temperature alteration is similar to alteration in the uppermost basalt at other ocean drilling sites (Menard, Natland, Jordan, Orcutt, et al., 1987; Laverne et al., 1996; Teagle et al., 1996, 2006).

Relationships between igneous unit boundaries and alteration indicate that alteration at Site U1365 is strongly controlled by the structure of the basalt (Fig. **F14**). Ingress of seawater, secondary mineral precipitation, and wall-rock interaction is primarily restricted to regions between lava flows. A direct relationship between visual observations of alteration and NGR-based potassium content (Fig. **F14**) indicates that NGR can provide a more accurate and quantitative approach to estimating alteration extent than visual interpretation alone.

Secondary minerals provide evidence of both oxidative and oxygen-poor alteration. Some samples have undergone several stages of vein opening and halo emplacement. Minerals indicative of oxygen-poor alteration are most prevalent toward the base of the drilled basalt column.

Tubelike micro-scale weathering features occur in altered glass and discrete clusters or masses adjacent to fractures and iron oxyhydroxide (Fig. **F12**). Similar features have been observed in marine basaltic glass elsewhere and attributed to microbial origin (Fisk et al., 1998).

Multiple episodes of late-stage calcite precipitation and vein infill have occurred at Site U1365. These late fills suggest that alteration may be continuous or at least occur intermittently during the life of the ocean crust. Dissolved concentrations of magnesium and calcium in the lowermost sediment indicate that basalt-water interaction in the form of Mg exchange for Ca has occurred since seawater migrated into the formation. This exchange may continue to drive late-stage calcite precipitation.

General results

Downhole temperature was measured using the APCT-3. Six measurements give a least-squares thermal gradient of 76°C/km. This result closely agrees with the thermal gradient observed by site survey cruise KNOX-02RR of 74°C/km (Shipboard Scientific Party, 2007). The heat flow of 61 mW/m^2 is typical for crust of this age. Bottom water

temperature is 1.22°C and temperature at the sediment/basement interface is estimated to be 6.8°C. These temperatures are well within the range inhabited by psychrophilic microbes.

A wide range of microbiology experiments was initiated shipboard. Experiments on major microbial processes and cultivation of viable microbes were initiated on samples taken at selected depths ranging from near the sediment/water interface to nearly 50 m into the basaltic basement. Subsamples for shore-based biogeochemical and molecular ecological studies were routinely taken from all of the distinct lithologic units.

Site U1366

The scientific objectives at Site U1366 are

1. To document the habitats, metabolic activities, genetic composition, and biomass of microbial communities in subseafloor sediment with very low total activity;
2. To test how oceanographic factors control variation in sedimentary habitats, activities, and communities from gyre center to gyre margin;
3. To quantify the extent to which these sedimentary communities may be supplied with electron donors by water radiolysis; and
4. To assess from porewater chemistry how basement habitats and potential activities vary in the underlying basalt with crust age and sediment thickness (from ridge crest to abyssal plain).

Site U1366 (5127 mbsl) is located in ocean crust formed during the CNS. The complete sedimentary succession, from seafloor to underlying basalt, was recovered by APC coring in Hole U1366F. Partial successions, from seafloor to various depths, were also recovered from Holes U1366B–U1366E.

Principal results

The sediment at Site U1366 is primarily clay and is assigned to two lithologic units: zeolitic metalliferous pelagic clay (Unit I) and metalliferous clay (Unit II) (Fig. **F19**). The principal components of the sediment are smectite, mica-group members, phillipsite, and red-brown to yellow-brown semiopaque oxide (RSO). Manganese nodules are relatively common at the seafloor and at depth in Unit I. The nodules generally produce peaks in NGR, magnetic susceptibility, and gamma ray attenuation density.

Both clay and zeolite exhibit overall trends of decreasing abundance with increasing depth.

NGR core logging can be used to quantify in situ concentrations of potassium, ^{238}U-series isotopes and ^{232}Th-series isotopes (Fig. **F20**). Prominent NGR features at Site U1366 include (1) a pronounced peak in ^{238}U-series isotopes just below the seafloor and (2) NGR peaks associated with manganese nodules, which were temporarily removed from the core for additional NGR logging. The manganese nodules (at the seafloor and at depth) do not contribute to the ^{238}U-isotope peak just below the seafloor.

Cell counts for Site U1366 sediment are three or more orders of magnitude lower than at the same depths in all sediment cored gathered by previous scientific ocean drilling expeditions. Cell counts range from below the MDL (1.4×10^3 cells/cm^3) to nearly 10^4 cells/cm^3. They do not exhibit any consistent trend with depth (Fig. **F21**).

The concentration of TN declines steadily from 0.04 wt% at the seafloor to below detection at 15 mbsf. TOC declines downhole to ~0.03 wt% at 10.75 mbsf (Fig. **F22**). Dissolved oxygen is present throughout the entire sediment column. Its concentration drops rapidly by 20 µM in the first 3 mbsf and declines linearly with depth to ~110 µM at the sediment/basalt interface. Over the first ~10 mbsf, dissolved nitrate and DIC increase slightly in concentration (from ~35 to ~40 µM and ~2.5 to ~2.7 mM, respectively) (Fig. **F23A, F23B**). Both are relatively stable for the remainder of the sediment column. These gradual increases are consistent with oxygen-fueled reduction of organic matter in the first 10 mbsf. Dissolved hydrogen concentration is below detection throughout the first 15 m of the sediment column but rises by several tens of nanno mols as the basaltic basement is approached. Chloride concentrations increase monotonically from ~550 mM to reach a maximum of ~570 mM in the deepest 5 m of the sediment column (a 3% increase) (Fig. **F23C**). This increase is most likely due to relict glacial seawater and, possibly, hydration of the underlying basement.

A wide range of microbiology experiments was initiated shipboard. Experiments on major microbial processes and cultivations of viable microbes were initiated on samples taken at selected depths ranging from near the sediment/water interface to the sediment/basement contact. Subsamples for shore-based biogeochemical and molecular ecological studies were routinely taken from all of the distinct lithologic units.

Site U1367

Site U1367 was selected as a drilling target because (1) its microbial activities and cell counts were expected to be characteristic of a setting midway between the western gyre edge and the gyre center, and (2) its basement age renders it a reasonable location for documenting microbial habitability and testing the extent of basalt alteration and openness to flow in a thinly sedimented region of ~33.5 Ma basaltic basement.

The principal objectives at Site U1367 are

1. To document the habitats, metabolic activities, genetic composition, and biomass of microbial communities in subseafloor sediment with very low total activity;
2. To test how oceanographic factors control variation in sedimentary habitats, activities, and communities from gyre center to gyre margin;
3. To quantify the extent to which these sedimentary communities may be supplied with electron donors by water radiolysis; and
4. To determine how habitats, potential activities and, if measurable, communities in subseafloor basalt vary with crust age and hydrologic regime (from ridge crest to abyssal plain).

Site U1367 (4285 mbsl) is located in ocean crust formed during magnetic polarity Chron 13n (33.3–33.7 Ma; Gradstein et al., 2004). The complete sedimentary succession, from seafloor to underlying basalt, was recovered by APC coring in Holes U1367B–U1367E. The sediment/basalt contact varies by a few meters from hole to hole. The lowermost sediment and fragments of the underlying basalt were recovered by RCB coring in Hole U1367F. Core recovery of the basalt was unusually low (11%). Continuous infall of basaltic debris forced us to terminate the hole early, preventing us from reaching sufficient depth below seafloor to deploy downhole logging tools.

Principal results

Sediment

The sediment at Site U1367 is composed of 5.5–7 m of pelagic clay (Unit I) overlying ~16 m of Oligocene carbonate ooze (Unit II) (Fig. **F24**). The principal components of the clay are smectite and mica-group members, phillipsite (a zeolite), and RSO. The ooze is composed mainly of coccolithophores and RSO, accompanied by foraminifers. The clay and ooze differ significantly in several physical properties, including porosity, bulk density, electrical conductivity, magnetic susceptibility, and NGR. The

transition from clay to ooze is gradual. The depth of the sediment/basalt interface varies by ~3 m from hole to hole. Although unit thickness and composition vary from hole to hole, general sediment composition is very similar in each hole.

Microbial cell counts decline rapidly from ~10^5 cells/cm^3 at 0.15 mbsf to the MDL (10^3 cells/cm^3) at 2 mbsf. They are mostly below the MDL throughout the remaining sediment column.

The concentration of TN declines to below detection in the first 7 mbsf (from 0.03% to 0.0%). TOC declines from 0.17 to 0.02 wt% over the same interval. Dissolved nitrate, dissolved phosphate, and DIC are present throughout the sediment column (Fig. **F25**). Dissolved oxygen also occurs throughout the column. Dissolved hydrogen concentration is below detection in most of the clay but above detection in most samples of the carbonate.

Basalt

The recovered sequence of basement rock is composed of pillow basalt fragments with prominent chill margins. Secondary mineralization and wall-rock interaction is limited in the recovered basalt. However, it is likely that the most altered portions of the basalt were not recovered.

A wide range of microbiology experiments was initiated shipboard. Experiments on major microbial processes and cultivations of viable microbes were initiated on samples taken at selected depths ranging from near the sediment-water interface to ~30 m into the basaltic basement. Subsamples were routinely taken from all of the distinct lithologic units for postcruise molecular assays and microbiological experiments.

Site U1368

Site U1368 was selected as a drilling target because (1) its microbial activities and cell counts were expected to be characteristic of the gyre center and (2) its basement age renders it a reasonable location for testing the extent of microbial habitability and basalt alteration in a thinly sedimented region of ~13.5 Ma basaltic basement.

The principal objectives at Site U1368 are

1. To document the habitats, metabolic activities, genetic composition, and biomass of microbial communities in subseafloor sediment with very low total activity;

2. To test how oceanographic factors control variation in sedimentary habitats, activities, and communities from gyre center to gyre margin,
3. To quantify the extent to which these sedimentary communities may be supplied with electron donors by water radiolysis; and
4. To determine how habitats, potential activities, and, if measurable, communities in subseafloor basalt vary with crust age and hydrologic regime (from ridge crest to abyssal plain).

Site U1368 (3738 mbsl) is located in ocean crust formed during magnetic polarity Chron 5ABn (13.4–13.6 Ma; Gradstein et al., 2004). Most or all of the sedimentary succession was recovered by APC coring in Holes U1368B–U1368E. Basalt fragments were recovered from the basal cores of Holes U1368B and U1368D. The upper ~100 m of basalt was cored using RCB in Hole U1368F. Approximately 60 m of the basaltic basement was logged with both the triple combo and the FMS tool string.

Principal results

Sediment

The sediment at Site U1368 is 15–16 m thick and consists of calcareous ooze, pelagic clay, and lithic sand. An additional 1 m of volcaniclastic breccia was recovered from an interval between basalt flows, 80 m below the upper sediment/basalt interface. The principal components of the ooze are calcareous nannofossils accompanied by RSO and foraminifers (Fig. F26). Planktonic foraminiferal biostratigraphy indicates that the calcareous ooze spans from the middle Miocene to the middle Pliocene. Clay minerals are in relatively low abundance throughout the sediment. The lowermost sediment contains one to three sandy intervals that collectively contain a wide variety of minerals, including albite-anorthite, ankerite, augite, calcite, chlorite, hematite, and titanomagnetite. The volcaniclastic breccia contains altered basaltic lithic and vitric grains.

Microbial cell counts decline rapidly from 10^5 to 10^6 cells/cm^3 just below the seafloor to slightly more than 10^3 cells/cm^3 at ~5 mbsf. They hover near the MDL (10^3 cells/cm^3) for the remainder of the sediment column.

The concentration of TN declines to below detection in the first 10 cm below seafloor. TOC declines to 0.03 wt% over the first 0.5 mbsf and remains low for the remainder of the sediment column. Dissolved nitrate, dissolved phosphate, DIC, and dissolved oxygen are present throughout the sediment column. Dissolved hydrogen concentra-

tion is below detection for the first 9.4 mbsf but above detection in half of the samples at greater depth (Fig. F27).

Basalt

The recovered sequence of basement rock is composed of pillow basalt fragments with prominent chill margins.

Estimates of potassium content derived from downhole NGR logging agree closely with potassium concentration estimates derived from NGR logging of whole-round cores (Fig. F28).

A wide range of microbiology experiments was initiated shipboard. Experiments on major microbial processes and cultivations of viable microbes were initiated on samples from selected depths ranging from near the sediment/water interface to ~100 m into the basaltic basement. Subsamples were routinely taken from all of the distinct lithologic units for postcruise molecular assays and microbiological experiments.

Site U1369

Site U1369 was selected as a drilling target because (1) its microbial activities and cell counts were expected to be characteristic of midway between gyre center and the southern gyre edge and (2) its basement age renders it a reasonable location for testing the extent of sediment-basement interaction in a thinly sedimented region of ~58 Ma basaltic basement.

The principal objectives at Site U1369 are

1. To document the habitats, metabolic activities, genetic composition, and biomass of microbial communities in subseafloor sediment with very low total activity;
2. To test how oceanographic factors control variation in sedimentary habitats, activities, and communities from gyre center to gyre margin;
3. To quantify the extent to which these sedimentary communities may be supplied with electron donors by water radiolysis; and
4. To determine how sediment-basement exchange and potential activities in the basaltic basement vary with basement age and hydrologic regime (from ridge crest to abyssal plain).

Site U1369 is located in the South Pacific Gyre at 5277 mbsl. Basement age is estimated from extrapolated magnetic models and changes in spreading rate recorded by neighboring magnetic profiles. Our best estimate of the crustal age is ~58 Ma and corresponds to magnetic polarity Chron 25r (57.2–58.4 Ma; Gradstein et al., 2004). The sedimentary succession was recovered by APC coring in Holes U1369B, U1369C, and U1369E. Basalt fragments were recovered from the basal cores of these holes.

Principal results

Sediment

The sediment at Site U1369 consists of ~16 m of zeolitic metalliferous clay. The sediment is massive in texture and contains visible burrows throughout. The principal components of the clay are phillipsite, RSO, and clay (Fig. **F29**). Manganese nodules were recovered from the sediment/water interface and from deeper in the sediment column. Micro- and nannofossils are almost completely absent. The sediment/basalt interface consists of vitric sand overlying altered basalt. Sediment thickness and composition are fairly uniform from hole to hole.

Microbial cell counts decline rapidly from ~10^5 cells/cm^3 just below the seafloor to ~10^3 cells/cm^3 at ~2 mbsf (Fig. **F30**). They are below the MDL (~10^3 cells/cm^3) for the remainder of the sediment column.

TN and TOC decrease rapidly from near the seafloor to ~3 mbsf and are extremely low for the remainder of the sediment column. Dissolved oxygen, dissolved nitrate, dissolved phosphate, and DIC are present throughout the sediment column (Fig. **F31**). Dissolved hydrogen concentration is consistently low throughout the column.

A wide range of microbiology experiments was initiated shipboard. Experiments on major microbial processes and cultivations of viable microbes were initiated with samples from selected depths ranging from near the sediment/water interface to the sediment/basalt interface. Subsamples were routinely taken from all of the distinct lithologic units for postcruise molecular assays and microbiological experiments.

Site U1370

Site U1370 was selected as a drilling target because (1) its microbial activities and cell counts were expected to be characteristic of midway between gyre center and the southern gyre edge and (2) its basement age renders it a reasonable location for testing

the extent of sediment-basement interaction in a moderately sedimented region 74–80 Ma basaltic basement.

The principal objectives at Site U1370 are

1. To document the habitats, metabolic activities, genetic composition, and biomass of microbial communities in subseafloor sediment with low total activity;
2. To test how oceanographic factors control variation in sedimentary habitats, activities, and communities from gyre center to gyre margin;
3. To quantify the extent to which these communities may be supplied with electron donors by water radiolysis; and
4. To determine how sediment-basement exchange and potential activities in the basaltic basement vary with basement age and hydrologic regime (from ridge crest to abyssal plain).

Site U1370 is located in the South Pacific Gyre at 5074 mbsl. The coring site is located within magnetic polarity Chron 33n, so the crustal age may range from 73.6 to 79.5 Ma (Gradstein et al., 2004). The sedimentary succession was recovered by APC coring in Holes U1370D, U1370E, and U1370F. Altered basaltic fragments were recovered from the basal cores of Holes U1370D and U1370F.

Principal results

Sediment

The sediment at Site U1370 is ~70 m thick. The dominant lithology is dark brown zeolitic metalliferous pelagic clay (Fig. **F32**). The principal components of the clay are RSO, phillipsite, and smectite. Unit I lies between the sediment/water interface and the top of a nannofossil ooze (Unit II) at ~61 mbsf. Unit II is a relatively short (30–290 cm) pale yellow interval predominantly composed of coccolithophores, with trace phillipsite, and clay. Unit III is a thin clay interval containing 88% RSO and 12% clay that directly overlays the basaltic basement. Although volcanic glass is locally abundant (~43%) in Unit I, its overall abundance is only 7%, and it is completely absent in Units II and III. A large, fragmented manganese nodule was recovered in Hole U1370D at 10 mbsf, and fragments of a manganese-encrusted hardground were in recovered in Hole U1370F at 52 mbsf.

Overall sediment structure at Site U1370 is massive, although occasional laminations and thin beds are visible in the lower half of Unit I. *Planolites* (horizontal) burrows are faintly visible in most of the clay and *Trichichnus* (vertical) burrows blend the upper

and lower contacts of the nannofossil ooze and the overlying and underlying clay. Sediment thickness and composition are uniform from hole to hole.

The nannofossil ooze was deposited during early Paleocene foraminiferal Zone P1. Its occurrence in this deep-sea clay sequence is attributed to deepening of the CCD and lysocline during the interval of decreased planktonic carbonate precipitation that followed the end-Cretaceous mass extinction (D'Hondt, 2005).

Microbial cell counts were above the MDL (~10^3 cells/cm^3) throughout much of the sediment column.

The dissolved oxygen and nitrate profiles at Site U1370 (Fig. **F33**) exhibit much greater curvature than the profiles at previous Expedition 329 sites. Dissolved oxygen concentration decreases sharply in the first several meters below seafloor and then more gradually to 40 mbsf. Below that depth, it decreases monotonically from ~10 µM to a few micro mols at the sediment/basalt interface. The rate of increase in dissolved nitrate concentration from surface sediment to 20 mbsf is higher than at previous sites (U1365–U1369), suggesting that organic nitrogen oxidation in the sediment is greater here than at those sites. The changes in dissolved oxygen and nitrate throughout the upper sediment column are attributed to oxygen consuming organic oxidation by sedimentary microbes.

Basalt

Dissolved potassium concentration declines nearly linearly with depth in the sediment (Fig. **F34**), indicating a sink for dissolved potassium in the underlying basaltic basement. This sink is inferred to be basalt alteration (clay formation).

A wide range of microbiology experiments was initiated shipboard. Experiments on major microbial processes and cultivations of viable microbes were initiated with samples taken at selected depths ranging from near the sediment/water interface to the sediment/basalt interface. Subsamples were routinely taken from all of the distinct lithologic units for postcruise molecular assays and microbiological experiments.

Site U1371

Site U1371 was selected as a drilling target because (1) its microbial activities and cell counts were expected to be characteristic of the upwelling region just south of the

gyre and (2) its basement age renders it a reasonable location for testing the extent of sediment-basement interaction in a moderately sedimented region of 71.5–73 Ma basaltic basement.

The principal objectives at Site U1371 are

1. To document the nature of life in moderately slowly accumulating sediments of great age (as old as 73 Ma), where the surface ocean is characterized by moderate mean chlorophyll content (<3 mg/m^3);
2. To determine the extent to which basement age, thermal regime, and chemical transport through the 73 Ma basaltic basement affect microbial communities and biogeochemical processes in the sediment and the extent to which chemical transport and microbial activities in the sediment affect the alteration and habitability of the basaltic basement;
3. To provide a much higher activity standard of comparison for the sites within the gyre (Sites U1365–U1370); and
4. To test the extent to which life in this sediment may be supplied with an electron donor (dissolved hydrogen) by radiolysis of water.

Site U1371 is located in the South Pacific Gyre at ~5300 mbsl. The coring site is located within magnetic polarity Chron 32n.2n, so the crustal age may range from 71.5 to 72.9 Ma (Gradstein et al., 2004). Based on a tectonic reconstruction of the region by Larson et al. (2002), the crust was accreted along the Pacific-Phoenix spreading center at ~73 Ma. The sedimentary succession was recovered by APC coring in Holes U1371D–U1371F. Additional mudline cores were recovered in Holes U1371B, U1371C, U1371G, and U1371H. Altered basaltic fragments were recovered from the basal core of Hole U1371F.

Principal results

Sediment

The sediment at Site U1371 consists of ~130 m of diatom ooze and pelagic clay, divided into two units based on their sharply contrasting mineralogy (Fig. **F35**). Unit I is ooze with average diatom and clay content of 56% and 17%, respectively. It is 104–107 m thick and contains numerous ash layers and multiple thin hardgrounds. Unit II is a blend of clay (32%), zeolite (30%), and red-brown to yellow-brown semiopaque iron-manganese oxyhydroxides (15%). The transition from ooze to clay constitutes the upper 5 m of Unit II; this portion of Unit II contains as much as 26% diatoms.

Other minor sedimentary components at Site U1371 include quartz, pyrite, manganese oxide/hydroxide, radiolarians, spicules, and silicoflagellates.

The clay-bearing diatom ooze and pelagic clay at Site U1371 form interbedded intervals of highly fossiliferous and clay-rich layers. Bioturbation is a prominent feature of the sediment, causing diffuse boundaries on most beds. Overall sediment thickness and composition appear to be broadly uniform from hole to hole.

Microbial cell counts were above the MDL (~10^3 cells/cm^3) throughout much of the sediment column.

Profiles of dissolved chemicals clearly indicate that most of the sediment column is anoxic, with thin oxic zones at the top and bottom of the column (Fig. **F36**). Manganese is a prominent net electron acceptor throughout most of the column. Dissolved oxygen concentration decreases rapidly within the first meter below seafloor and is below detection by ~5 mbsf. Below that depth, it is indistinguishable from zero until to a few meters above the sediment/basalt interface, when it rises to a few micro mols. Dissolved oxygen content generally matches sediment color, with dissolved oxygen present in the brown sediment at the top and bottom of the column but indistinguishable from zero throughout the gray sediment that characterized most of the column. Dissolved nitrate disappears within 2.5 mbsf but re-appears above the sediment/basalt interface, from 105 to 120 mbsf (the deepest sample analyzed for nitrate). Dissolved ammonium rises from 0.35 µM at 0.15 mbsf to a maximum of ~55 µM between 30 and 65 mbsf and then decreases slightly to 40 µM at 97 mbsf (no deeper samples were analyzed for ammonium). Dissolved manganese strongly increases to ~360 µM in the uppermost 3 mbsf, exhibits four broad maxima and three local minima within the column, and decreases to ~70 µM at ~128 mbsf. Redox potential, measured by electrode, broadly mirrors the dissolved manganese profile, with positive potential at the top and bottom of the sediment column and generally negative (but sometimes low positive) potential throughout most of the column. Three minima in redox potential within the column correspond to the local minima in dissolved manganese concentration.

Throughout the sediment column, concentrations of dissolved phosphate and DIC are much higher at Site U1371 than at equivalent sediment depths at the sites within the gyre (Sites U1365–U1370). Concentrations of these chemical species peak a few meters below seafloor.

Shipboard studies of Site U1371 found at least four additional results of note. First, the presence of pyrite in the first 0–10 m of the sediment column suggests that sulfate and iron reduction have occurred in the near-seafloor zones of oxygen, nitrate, and manganese reduction. Second, the sulfate anomaly profile suggests that sulfate reduction and manganese reduction may broadly co-occur within the column. Third, dissolved oxygen and dissolved manganese appear to co-exist for at least 13 m in the lowermost sediment column. Fourth, dissolved oxygen and dissolved hydrogen also appear to co-exist in the lowermost sediment column. Postcruise studies will test (1) the co-occurrence of sulfate reduction, iron reduction, and other redox processes in this sediment column and (2) explanations of the co-occurrence of dissolved oxygen, manganese, and hydrogen deep in the column.

Basalt

The presence of dissolved oxygen, nitrate, phosphate, and DIC in the lowermost sediment indicates that life is not inhibited in the upper basaltic basement by absence of electron acceptors, major nutrients, or carbon.

Dissolved potassium concentration declines with depth in the sediment, indicating a sink for dissolved potassium in the underlying basaltic basement. This sink is inferred to be basalt alteration (clay formation).

A wide range of microbiology experiments was initiated shipboard. Experiments on major microbial processes and cultivations of viable microbes were initiated with samples taken at selected depths ranging from near the sediment/water interface to the sediment/basalt interface. Subsamples were routinely taken from all of the distinct lithologic units for postcruise molecular assays and microbiological experiments.

References

Alt, J.C., France-Lanord, C., Floyd, P.A., Castillo, P., and Galy, A., 1992. Low-temperature hydrothermal alteration of Jurassic ocean crust, Site 801. *In* Larson, R.L., Lancelot, Y., et al., *Proc. ODP, Sci. Results,* 129: College Station, TX (Ocean Drilling Program), 415–427. **doi:10.2973/odp.proc.sr.129.132.1992**

Anderson, R.N., and Skilbeck, J.N., 1981. Oceanic heat flow. *In* Emiliani, C. (Ed.), *The Sea* (Vol. 7): *The Oceanic Lithosphere:* New York (Wiley), 489–524.

Bach, W., and Edwards, K.J., 2003. Iron and sulfide oxidation within the basaltic ocean crust: implications for chemolithoautotrophic microbial biomass production. *Geochim. Cosmochim. Acta,* 67(20):3871–3887. **doi:10.1016/S0016-7037(03)00304-1**

Barr, S.R., Révillon, S., Brewer, T.S., Harvey, P.K., and Tarney, J., 2002. Determining the inputs to the Mariana Subduction Factory: using core-log integration to reconstruct basement lithology at ODP Hole 801C. *Geochem., Geophys., Geosyst.,* 3(11):8901. **doi:10.1029/2001GC000255**

Behrenfeld, M.J., and Falkowski, P.G., 1997. Photosynthetic rates derived from satellite-based chlorophyll concentration. *Limnol. Oceanogr.,* 42(1):1–20.

Blair, C.C., D'Hondt, S., Spivack, A.J., and Kingsley, R.H., 2007. Radiolytic hydrogen and microbial respiration in subsurface sediments. *Astrobiology,* 7(6):951–970. **doi:10.1089/ast.2007.0150**

Broecker, W.S., 1982. Ocean chemistry during glacial time. *Geochim. Cosmochim. Acta,* 46(10):1689–1705. **doi:10.1016/0016-7037(82)90110-7**

Cowen, J.P., Giovannoni, S.J., Kenig, F., Johnson, H.P., Butterfield, D., Rappé, M.S., Hutnak, M., and Lam, P., 2003. Fluids from aging ocean crust that support microbial life. *Science,* 299(5603):120–123. **doi:10.1126/science.1075653**

Debierne, A., 1909. Radioactivitié: sur la decomposition de l'eau par les sel de radium. *C. R. Acad. Sci.,* 148:703–705.

D'Hondt, S., 2005. Consequences of the Cretaceous/Paleogene mass extinction for marine ecosystems. *Annu. Rev. Ecol. Evol. Syst.,* 36(1):295–317. **doi:10.1146/annurev.ecolsys.35.021103.105715**

D'Hondt, S., Jørgensen, B.B., Miller, D.J., Batzke, A., Blake, R., Cragg, B.A., Cypionka, H., Dickens, G.R., Ferdelman, T., Hinrichs, K.-U., Holm, N.G., Mitterer, R., Spivack, A., Wang, G., Bekins, B., Engelen, B., Ford, K., Gettemy, G., Rutherford, S.D., Sass, H., Skilbeck, C.G., Aiello, I.W., Guerin, G., House, C.H., Inagaki, F., Meister, P., Naehr, T., Niitsuma, S., Parkes, R.J., Schippers, A., Smith, D.C., Teske, A., Wiegel, J., Naranjo Padillo, C., and Solis Acosta, J.L., 2004. Distributions of microbial activities in deep subseafloor sediments. *Science,* 306(5705):2216–2221. **doi:10.1126/science.1101155**

D'Hondt, S., Rutherford, S., and Spivack., A.J., 2002. Metabolic activity of the subsurface life in deep-sea sediments. *Science,* 295(5562):2067–2070. **doi:10.1126/science.1064878**

D'Hondt, S., Spivack, A.J., Pockalny, R., Ferdelman, T.G., Fischer, J.P., Kallmeyer, J., Abrams, L.J., Smith, D.C., Graham, D., Hasiuk, F., Schrum, H., and Stancine, A.M., 2009. Subseafloor sedimentary life in the South Pacific Gyre. *Proc. Natl. Acad. Sci. U. S. A.,* 106(28):11651–11656. **doi:10.1073/pnas.0811793106**

D'Hondt, S.L., Jørgensen, B.B., Miller, D.J., et al., 2003. *Proc. ODP, Init. Repts.,* 201: College Station, TX (Ocean Drilling Program). **doi:10.2973/odp.proc.ir.201.2003**

D'Hondt, S., Inagaki, F., and Alvarez Zarikian, C., 2010. South Pacific Gyre Microbiology. *IODP Sci. Prosp.,* 329. **doi:10.2204/iodp.sp.329.2010**

Durbin, A.M., and Teske, A., 2010. Sediment-associated microdiversity within the Marine Group I Crenarchaeota. *Environ. Microbiol. Rep.,* 2(5):693–703. **doi:10.1111/j.1758-2229.2010.00163.x**

Edwards, K.J., Rogers, D.R., Wirsen, C.O., and McCollom, T.M., 2003. Isolation and characterization of novel psychrophilic, neutrophilic, Fe-oxidizing, chemolithoauto-trophic alpha- and gamma-Proteobacteria from the Deep Sea. *Appl. Environ. Microbiol.* 69(5):2906–2913. **doi:10.1128/AEM.69.5.2906-2913.2003**

Fischer, J.P., Ferdelman, T.G., D'Hondt, S., Røy, H., and Wenzhöfer, F., 2009. Oxygen penetration deep into the sediment of the South Pacific gyre. *Biogeosciences*, 6:1467–1478. **http://www.biogeosciences.net/6/1467/2009/bg-6-1467-2009.pdf**

Fisher, A.T., and Becker, K., 2000. Channelized fluid flow in oceanic crust reconciles heat-flow and permeability data. *Nature (London, U. K.),* 403(6765):71–74. **doi:10.1038/47463**

Fisher, A.T., and Von Herzen, R.P., 2005. Models of hydrothermal circulation within 106 Ma seafloor: constraints on the vigor of fluid circulation and crustal properties, below the Madeira Abyssal Plain. *Geochem., Geophys., Geosyst.,* 6(11):Q11001. **doi:10.1029/2005GC001013**

Fisk, M.R., Giovannoni, S.J., and Thorseth, I.H., 1998. Alteration of oceanic volcanic glass: textural evidence of microbial activity. *Science,* 281(5379):978–980. **doi:10.1126/science.281.5379.978**

Furnes, H., and Staudigel, H., 1999. Biological mediation in ocean crust alteration: how deep is the deep biosphere? *Earth Planet. Sci. Lett.,* 166(3–4):97–103. **doi:10.1016/S0012-821X(99)00005-9**

Gallahan, W.E., and Duncan, R.A., 1994. Spatial and temporal variability in crystallization of celadonites with the Troodos ophiolite, Cyprus: implications for low-temperature alteration of the oceanic crust. *J. Geophys. Res., [Solid Earth],* 99(B2):3147–3161. **doi:10.1029/93JB02221**

Gieskes, J.M., and Boulègue, J., 1986. Interstitial water studies, Leg 92. *In* Leinen, M., Rea, D.K., et al., *Init. Repts. DSDP,* 92: Washington, DC (U.S. Govt. Printing Office), 423–429. **doi:10.2973/dsdp.proc.92.124.1986**

Gradstein, F.M., Ogg, J.G., and Smith, A.G. (Eds.), 2004. *A Geologic Time Scale 2004:* Cambridge (Cambridge Univ. Press). **http://cambridge.org/uk/catalogue/catalogue.asp?isbn=9780521781428**

Hauff, F., Hoernle, K., and Schmidt, A., 2003. Sr-Nd-Pb composition of Mesozoic Pacific oceanic crust (Site 1149 and 801, ODP Leg 185): implications for alteration of ocean crust and the input into the Izu-Bonin-Mariana subduction system. *Geochem., Geophys., Geosyst.,* 4(8):8913. **doi:10.1029/2002GC000421**

Inagaki, F., Nunoura, T., Nakagawa, S., Teske, A., Lever, M., Lauer, A., Suzuki, M., Takai, K., Delwiche, M., Colwell, F.S., Nealson, K.H., Horikoshi, K., D'Hondt, S., and Jørgensen, B.B., 2006. Biogeographical distribution and diversity of microbes in methane hydrate-bearing deep marine sediments on the Pacific Ocean margin. *Proc. Natl. Acad. Sci. U. S. A.,* 103(8):2815–2820. **doi:10.1073/pnas.0511033103**

Jacobson, R.S., 1992. Impact of crustal evolution on changes of the seismic properties of the uppermost ocean crust. *Rev. Geophys.,* 30(1):23–42. **doi:10.1029/91RG02811**

Jahnke, R.A., 1996. The global ocean flux of particulate organic carbon: areal distribution and magnitude. *Global Biogeochem. Cycles,* 10(1):71–88. **doi:10.1029/95GB03525**

Jarrard, R.D., Abrams, L.J., Pockalny, R.A., Larson, R.L., and Hirono, T., 2001. Physical properties of upper oceanic crust: ODP Hole 801C and the waning of hydrothermal circulation.

Eos, Trans. Am. Geophys. Union, 82(47)(Suppl.):V21C-0980. (Abstract) **http://www.agu.org/meetings/fm01/waisfm01.html**

Kelley, K.A., Plank, T., Ludden, J., and Staudigel, H., 2003. Composition of altered oceanic crust at ODP Sites 801 and 1149. *Geochem., Geophys., Geosyst.,* 4(6)8910. **doi:10.1029/2002GC000435**

Koppers, A.A.P., Staudigel, H., and Duncan, R.A., 2003. High-resolution $^{40}Ar/^{39}Ar$ dating of the oldest oceanic basement basalts in the western Pacific basin. *Geochem., Geophys., Geosyst.,* 4(11):8914. **doi:10.1029/2003GC000574**

Larson, R.L., and Olson, P., 1991. Mantle plumes control magnetic reversal frequency. *Earth Planet. Sci. Lett.,* 107(3–4):437–447. **doi:10.1016/0012-821X(91)90091-U**

Larson, R.L., Pockalny, R.A., Viso, R.F., Erba, E., Abrams, L.J., Luyendyk, B.P., Stock, J.M., and Clayton, R.W., 2002. Mid-Cretaceous tectonic evolution of the Tongareva triple junction in the southwestern Pacific Basin. *Geology,* 30(1):67–70. **doi:10.1130/0091-7613(2002)030<0067:MCTEOT>2.0.CO;2**

Laverne, C., Belarouchi, A., and Honnorez, J., 1996. Alteration mineralogy and chemistry of the upper oceanic crust from Hole 896A, Costa Rica rift. *In* Alt, J.C., Kinoshita, H., Stokking, L.B., and Michael, P.J. (Eds.), *Proc. ODP, Sci. Results,* 148: College Station, TX (Ocean Drilling Program), 151–170. **doi:10.2973/odp.proc.sr.148.127.1996**

Leinen, M., Rea, D.K., et al., 1986. *Init. Repts. DSDP,* 92: Washington, DC (U.S. Govt. Printing Office). **doi:10.2973/dsdp.proc.92.1986**

Lin, L.-H., Hall, J., Lippmann-Pipke, J., Ward, J.A., Sherwood Lollar, B., DeFlaun, M., Rothmel, R., Moser, D., Gihring, T.M., Mislowack, B., and Onstott, T.C., 2005. Radiolytic H_2 in continental crust: nuclear power for deep subsurface microbial communities. *Geochem., Geophys., Geosyst.,* 6(7):Q07003. **doi:10.1029/2004GC000907**

Lin, L.-H., Slater, G.F., Sherwood Lollar, B., Lacrampe-Couloume, G., and Onstott, T.C., 2005. The yield and isotopic composition of radiolytic H_2, a potential energy source for the deep subsurface biosphere. *Geochim. Cosmochim. Acta,* 69(4):893–903. **doi:10.1016/j.gca.2004.07.032**

Lipp, J.S., and Hinrichs, K.-U., 2009. Structural diversity and fate of intact polar lipids in marine sediments. *Geochim. Cosmochim. Acta,* 73(22):6816–6833. **doi:10.1016/j.gca.2009.08.003**

Loper, D.E., and McCartney, K., 1986. Mantle plumes and the periodicity of magnetic field reversals. *Geophys. Res. Lett.,* 13(13):1525–1528. **doi:10.1029/GL013i013p01525**

Menard, H.W., Natland, J.H., Jordan, T.H., Orcutt, J.A., et al., 1987. *Init. Repts. DSDP,* 91: Washington, DC (U.S. Govt. Printing Office). **doi:10.2973/dsdp.proc.91.1987**

Morel, A., Gentili, B., Claustre, H., Babin, M., Bricaud, A., Ras, J., and Tiéche, F., 2007. Optical properties of the "clearest" natural waters. *Limnol. Oceanogr.,* 52(1):217–229.

Ocean Studies Board and Earth and Life Studies, 2003. *Enabling Ocean Research in the 21st Century: Implementation of a Network of Ocean Observatories*: Washington, DC (National Academies Press). **http://www.nap.edu/openbook.php?isbn=0309089905**

Parkes, R.J., Cragg, B.A., and Wellsbury, P., 2000. Recent studies on bacterial populations and processes in subseafloor sediments: a review. *Hydrogeol. J.,* 8(1):11–28. **doi:10.1007/PL00010971**

Parsons, B., and Sclater, J.G., 1977. An analysis of the variation of ocean floor bathymetry and heat flow with age. *J. Geophys. Res., [Solid Earth],* 82(5):803–827. **doi:10.1029/JB082i005p00803**

Pedersen, K., 1996. Microbial life in granite rock [presented at the 1996 International Symposium on Subsurface Microbiology (ISSN-96), Davos, Switzerland, 15–21 September 1996].

Pick, T., and Tauxe, L., 1993. Geomagnetic paleointensities during the Cretaceous normal superchron measured using submarine basaltic glass. *Nature (London, U. K.),* 366(6452):238–242. **doi:10.1038/366238a0**

Plank, T., and Langmuir, C.H., 1998. The chemical composition of subducting sediment and its consequences for the crust and mantle. *Chem. Geol.,* 145(3–4):325–394. **doi:10.1016/S0009-2541(97)00150-2**

Pockalny, R.A, and Larson, R.L., 2003. Implications for crustal accretion at fast spreading ridges from observations in Jurassic oceanic crust in the western Pacific. *Geochem., Geophys., Geosyst.,* 4(1):8903. **doi:10.1029/2001GC000274**

Révillon, S., Barr, S.R., Brewer, T.S., Harvey, P.K., and Tarney, J., 2002. An alternative approach using integrated gamma-ray and geochemical data to estimate the inputs to subduction zones from ODP Leg 185, Site 801. *Geochem., Geophys., Geosyst.,* 3(12):8902. **doi:10.1029/2002GC000344**

Shipboard Scientific Party, 2000. Site 1149. *In* Plank, T., Ludden, J.N., Escutia, C., et al., *Proc. ODP, Init. Repts.,* 185: College Station, TX (Ocean Drilling Program), 1–190. **doi:10.2973/odp.proc.ir.185.104.2000**

Shipboard Scientific Party, 2003. Explanatory notes. *In* D'Hondt, S.L., Jørgensen, B.B., Miller, D.J., et al., *Proc. ODP, Init. Repts.,* 201: College Station, TX (Ocean Drilling Program), 1–103. **doi:10.2973/odp.proc.ir.201.105.2003**

Shipboard Scientific Party, 2007. Site reports for South Pacific Gyre Expedition KNOX-02RR (R/V *Roger Revelle,* 12/06–1/07).

Smith, W.H.F., and Sandwell, D.T., 1997. Global sea floor topography from satellite altimetry and ship depth soundings. *Science,* 277(5334):1956–1962. **doi:10.1126/science.277.5334.1956**

Sørensen, K.B., Lauer, A., and Teske, A., 2004. Archaeal phylotypes in a metal-rich and low-activity deep subsurface sediment of the Peru Basin, ODP Leg 201, Site 1231. *Geobiology,* 2(3):151–161. **doi:10.1111/j.1472-4677.2004.00028.x**

Staudigel, H., Yayanos, A., Chastain, R., Davies, G., Verdurmen, E.A.T., Schiffman, P., Bourcier, R., and De Baar, H., 1998. Biologically mediated dissolution of volcanic glass in seawater. *Earth Planet. Sci. Lett.,* 164(1–2):233–244. **doi:10.1016/S0012-821X(98)00207-6**

Stein, C.A., and Stein, S., 1994. Constraints on hydrothermal heat flux through the oceanic lithosphere from global heat flow. *J. Geophys. Res., [Solid Earth],* 99(B2):3081–3095. **doi:10.1029/93JB02222**

Tarduno, J.A., Cottrell, R.D., and Smirnov, A.V., 2001. High geomagnetic intensity during the mid-Cretaceous from Thellier analyses of single plagioclase crystals. *Science,* 291(5509):1779–1783. **doi:10.1126/science.1057519**

Taylor, B., 2006. The single largest oceanic plateau: Ontong Java–Manihiki–Hikurangi. *Earth Planet. Sci. Lett.,* 241(3–4):372–380. **doi:10.1016/j.epsl.2005.11.049**

Teagle, D.A.H., Alt, J.C., Bach, W., Halliday, A.N., and Erzinger, J., 1996. Alteration of upper ocean crust in a ridge-flank hydrothermal upflow zone: mineral, chemical, and isotopic constraints from Hole 896A. *In* Alt, J.C., Kinoshita, H., Stokking, L.B., and Michael, P.J. (Eds.), *Proc. ODP, Sci. Results,* 148: College Station, TX (Ocean Drilling Program), 119–150. **doi:10.2973/odp.proc.sr.148.113.1996**

Teagle, D.A.H., Alt, J.C., Umino, S., Miyashita, S., Banerjee, N.R., Wilson, D.S., and Expedition 309/312 Scientists, 2006. *Proc. IODP,* 309/312: Washington, DC (Integrated Ocean Drilling Program Management International, Inc.). **doi:10.2204/iodp.proc.309312.2006**

Von Herzen, R.P., 2004. Geothermal evidence for continuing hydrothermal circulation in older (>60 Ma) ocean crust. *In* Davis, E.E., and Elderfield, H. (Eds.) *Hydrogeology of the Oceanic Lithosphere:* Cambridge (Cambridge Univ. Press), 414–450.

Whitman, W.B., Coleman, D.C., and Wiebe, W.J., 1998. Prokaryotes: the unseen majority. Proc. Natl. Acad. Sci. U. S. A., 95(12):6578–6583. **doi:10.1073/pnas.95.12.6578**

Table T1. Expedition 329 operations summary.

Hole	Latitude	Longitude	Water depth (mbsl)	Penetration (m)	Cored (m)	Recovered (m)	Recovery (%)	Drilled (m)	Cores (*N*)	Time on hole (h)	Time on site (days)	Comments
U1365A	23°51.0493′S	165°38.6624′W	5695.6	75.5	75.5	74.06	98	0	26	80.25		Washdown hole - no cores
U1365B	23°51.0388′S	165°38.6629′W	5694.7	75.6	54.6	55.79	102	21	8	22		
U1365C	23°51.0377′S	165°38.6502′W	5696.7	74.8	48.8	39.67	81	26	8	21.75		
U1365D	23°51.0359′S	165°38.6381′W	5693.7	19	19	18.89	99	0	2	16		
U1365E	23°51.0489′S	165°38.6420′W	5693.7	124.2	53.2	39.66	75	71	11	144.75		
		Site U1365 totals:		369.1	251.1	228.07	91	118	55	284.75	11.86	
U1366A	26°03.0945′S	156°53.6591′W	5135	17.8	0	0	0	17.8	0	10.5		Washdown hole - no cores
U1366B	26°03.0950′S	156°53.6714′W	5130.8	17.2	17.2	17.31	101	0	2	4.25		
U1366C	26°03.0845′S	156°53.6700′W	5129.5	25	25	25.42	102	0	3	4.25		
U1366D	26°03.0850′S	156°53.6652′W	5126.1	20.9	20.9	18.86	90	0	4	6.25		
U1366E	26°03.0843′S	156°53.6825′W	5127.8	4.7	4.7	4.71	100	0	1	0.75		
U1366F	26°03.0836′S	156°53.6937′W	5127	30.1	30.1	30.15	100	0	4	18		
		Site U1366 totals:		115.7	97.9	96.45	98.6	17.8	14	44	1.83	
U1367A	26°28.8972′S	137°56.3646′W	4290.9	21.2	0	0	0	21.2	0	9.25		Washdown hole - no cores
U1367B	26°28.8966′S	137°56.3777′W	4288.9	22.3	22.3	22.31	100	0	4	6.5		
U1367C	26°28.8860′S	137°56.3783′W	4288.2	26.7	26.7	27.01	101	0	4	5.25		
U1367D	26°28.8861′S	137°56.3659′W	4288.1	25.5	25.5	24.54	96	0	4	7		
U1367E	26°28.8856′S	137°56.3538′W	4287.6	24.4	24.4	23.15	95	0	3	11		
U1367F	26°28.8960′S	137°56.3538′W	4288.9	55.5	38.5	4.33	11	17	5	63.75		
		Site U1367 totals:		175.6	137.4	101.34	80.6	38.2	20	102.75	4.28	
U1368A	27°55.0017′S	123°09.6562′W	3740	13.6	0	0	0	13.6	0	10.25		Washdown hole - no cores
U1368B	27°55.0024′S	123°09.6679′W	3739.1	16	16	15.84	99	0	3	5		
U1368C	27°54.9916′S	123°09.6681′W	3738.5	16.3	16.3	16.34	100	0	2	2.25		
U1368D	27°54.9920′S	123°09.6561′W	3739.1	15	15	15.04	100	0	2	2.25		
U1368E	27°54.9918′S	123°09.6442′W	3740.9	10.6	10.6	10.58	100	0	2	8.5		
U1368F	27°55.0021′S	123°09.6433′W	3741	115.1	115.1	31.74	28	0	14	112.5		
		Site U1368 totals:		186.6	173	89.54	85.4	13.6	23	140.75	5.86	
U1369A	39°18.6177′S	139°48.0383′W	5279.4	12.2	0	0	0	12.2	0	10.5		Washdown hole - no cores
U1369B	39°18.6178′S	139°48.0522′W	5275.2	15.9	15.9	18.14	114	0	3	9		
U1369C	39°18.6070′S	139°48.0519′W	5276.9	14.6	14.6	16.1	110	0	3	5		
U1369D	39°18.6069′S	139°48.0378′W	5276.9	0.1	0.1	0.08	80	0	1	0.75		
U1369E	39°18.6070′S	139°48.0246′W	5277.7	15.5	15.5	15.49	100	0	3	15.25		
		Site U1369 totals:		58.3	46.1	49.81	101	12.2	10	40.5	1.69	
U1370A	41°51.1289′S	153°06.3799′W	5074.6	66.7	0	0	0	66.7	0	14.25		Washdown hole - no cores
U1370B	41°51.1285′S	153°06.3953′W	5074.6	7.8	7.8	7.81	100	0	1	3.75		
U1370C	41°51.1171′S	153°06.3975′W	5074.6	7.8	0	0	0	7.8	0	10		
U1370D	41°51.1156′S	153°06.3812′W	5073.6	68.2	68.2	70.26	103	0	8	16.75		
U1370E	41°51.1158′S	153°06.3668′W	5074.2	65.6	65.6	70.2	107	0	9	20.25		
U1370F	41°51.1267′S	153°06.3674′W	5073.6	64.7	64.7	66.32	103	0	8	21		
		Site U1370 totals:		280.8	206.3	214.59	82.6	74.5	26	86	3.58	
U1371A	45°57.8492′S	163°11.0513′W	5316	123.5	0	0	0	123.5	0	14.75		Washdown hole - no cores
U1371B	45°57.8509′S	163°11.0673′W	5316.35	8.1	8.1	8.15	101	0	1	3.25		
U1371C	45°57.8404′S	163°11.0684′W	5312	9.5	9.5	9.83	103	0	1	1.75		
U1371D	45°57.8394′S	163°11.0512′W	5311.09	126	126	126.87	101	0	14	32.75		
U1371E	45°57.8397′S	163°11.0365′W	5310.24	128.2	128.2	118.16	92	0	14	21.5		
U1371F	45°57.8502′S	163°11.0369′W	5308.32	130.6	130.6	118.44	91	0	14	20		
U1371G	45°57.8637′S	163°11.0360′W	5314.13	1.4	1.4	1.37	98	0	1	2.75		
U1371H	45°57.8648′S	163°11.0512′W	5310.31	6.2	6.2	6.19	100	0	1	16.5		
		Site U1371 totals:		533.5	410	389.01	98	123.5	46	113.25	1.83	
Total holes: 42		Expedition 329 totals:		1719.6	1321.8	1168.81	88	397.8	194			

Figure F1. Map of annual chlorophyll-a (Chl-a) concentrations overlain by the proposed site locations (circled numbers; corresponds to site number). White lines = basement age in 10 m.y. increments. As illustrated by paleoposition histories of proposed Sites SPG-1 and SPG-12 (black lines), paleopositions determined with a fixed hotspot reference frame indicate that proposed Sites SPG-1–SPG-10 have been in the gyre for tens of millions of years and proposed Site SPG-12 has been at the gyre margin for tens of millions of years.

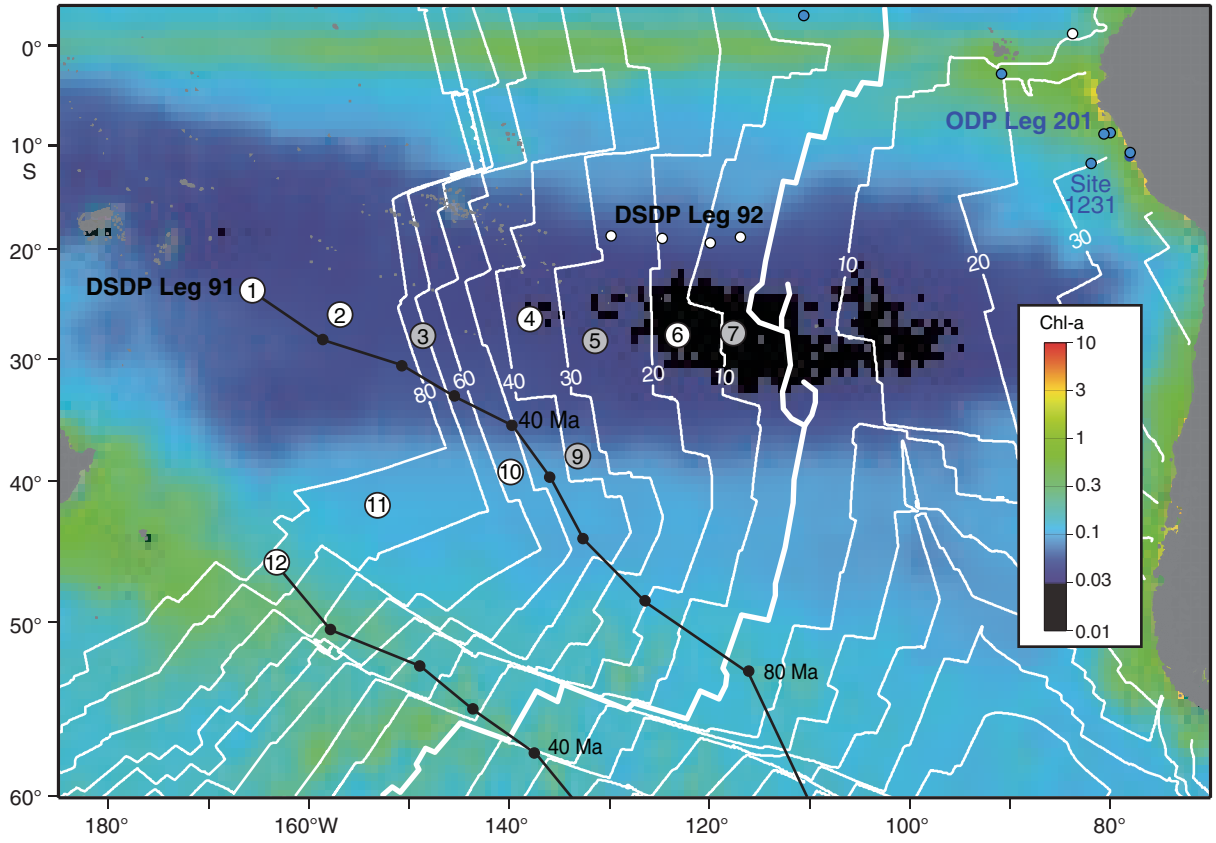

Figure F2. South Pacific seafloor bathymetry map (Smith and Sandwell, 1997) illustrating tectonic setting and location of sites drilled during Expedition 329 (circled numbers; corresponds to proposed site number). White circles = nearest DSDP drill sites; blue circles = nearest ODP drill sites.

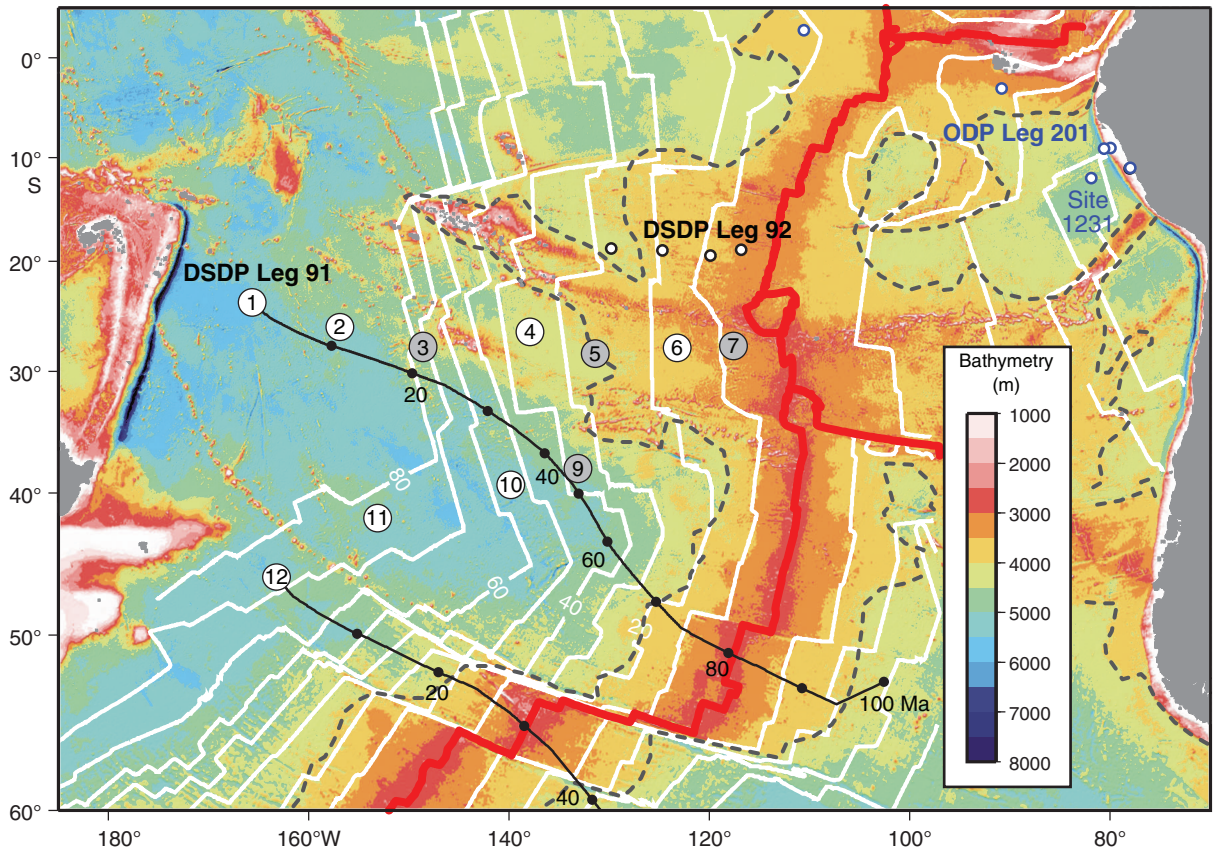

Figure F3. Subseafloor cell concentrations in shallow sediment at Expedition 329 sites (open circles = data from Sites U1365–U1370, open triangles = data from Site U1371, just outside the gyre) and at all previously counted ODP/IODP sites (solid circles) (D'Hondt et al., 2009). Site U1371 is the only Cruise KNOX-02RR site at which concentrations approach previous ODP/IODP values.

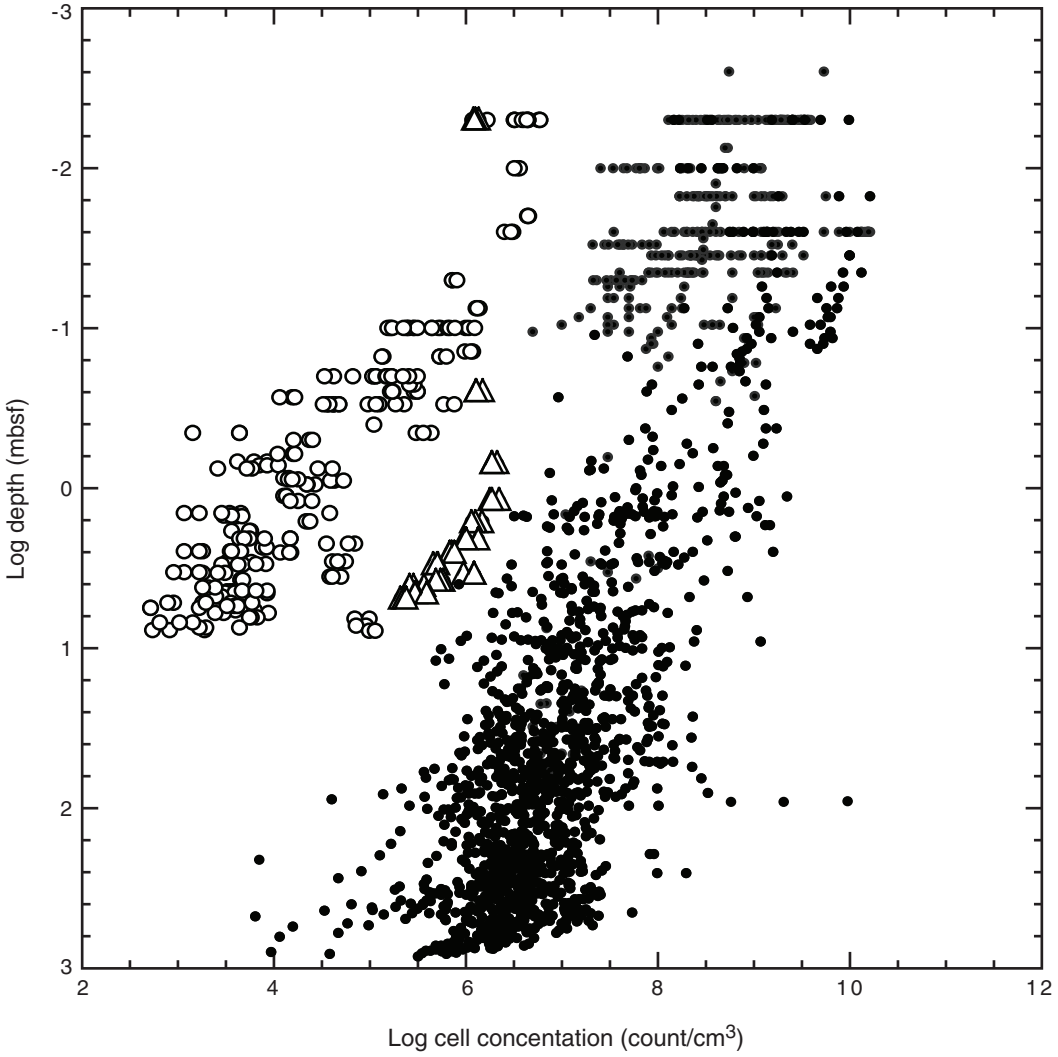

Figure F4. Dissolved (**A**) oxygen (O_2) and (**B**) nitrate (NO_3^-) profiles in the shallow sediment at Expedition 329 sites and Cruise KNOX-02RR proposed sites not drilled during Expedition 329 (D'Hondt et al., 2009).

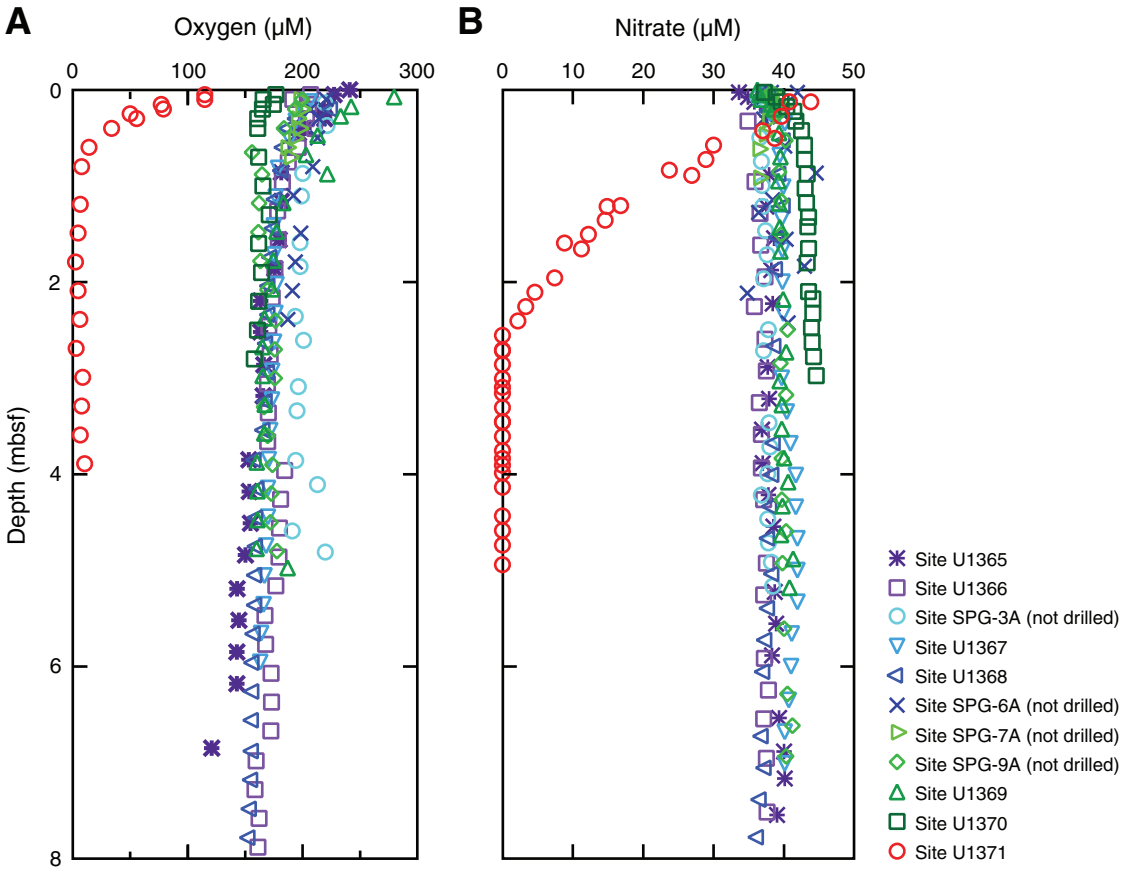

Figure F5. Model for relative rates of organic carbon (OC) oxidation and radiolytic H_2 oxidation with depth. Dotted pink line = maximum depth below seafloor cored curing Cruise KNOX-02RR. Radiolytic H_2 may provide more than half of the electron donors at some proposed sites (D'Hondt et al., 2009). Because organic carbon is oxidized at highest rates in the youngest sediment, at some depth below seafloor (dashed blue line), microbial oxidation of radiolytic H_2 may exceed oxidation of buried organic carbon. At still greater depth (solid green line), reactive organic matter may be depleted and radiolytic H_2 may be the sole electron donor. These predictions can only be tested by drilling the entire sediment column.

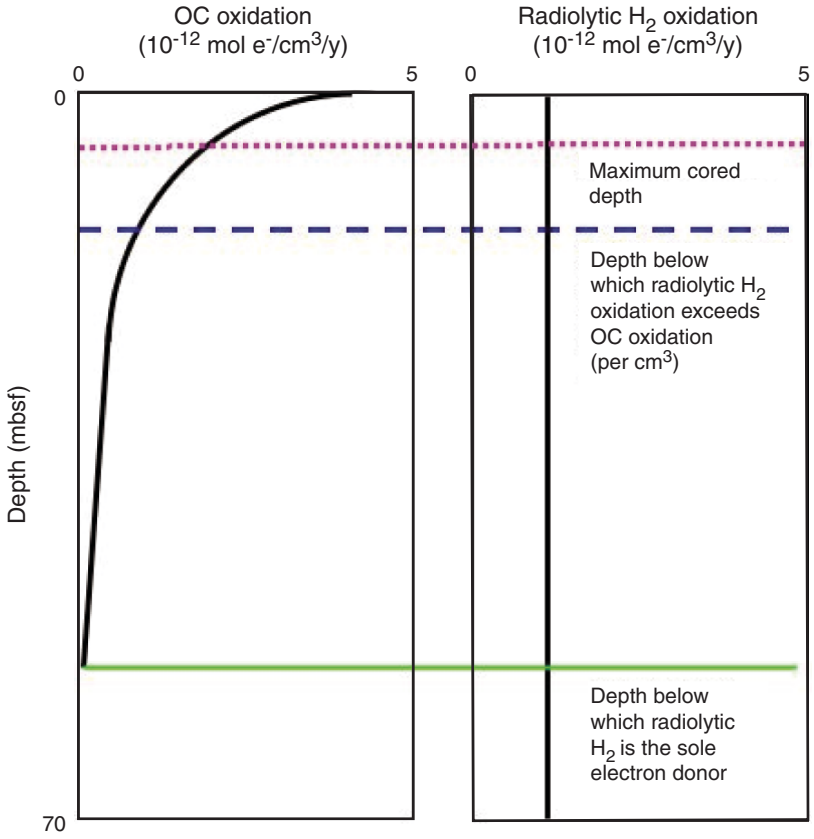

Figure F6. Models of radiolytic H_2 concentrations with depth. If H_2 is microbially oxidized, its concentration will be below our detection limit (pink line = concentrations measured at Site U1370 during Cruise KNOX-02RR [below detection limit of 3.5×10^{-8} M]. Other lines indicate predicted concentrations if the H_2 is not oxidized (e.g., if sediment is sterile), but radioactivity and porosity are constant throughout the sediment (blue line = diffusive loss of H_2 to both overlying ocean and underlying basement aquifer, red line = diffusive loss to the overlying ocean but basement is impermeable to chemical exchange). The constancy of radioactivity and porosity with depth and the concentrations of dissolved H_2 at depth can only be tested by drilling to basement.

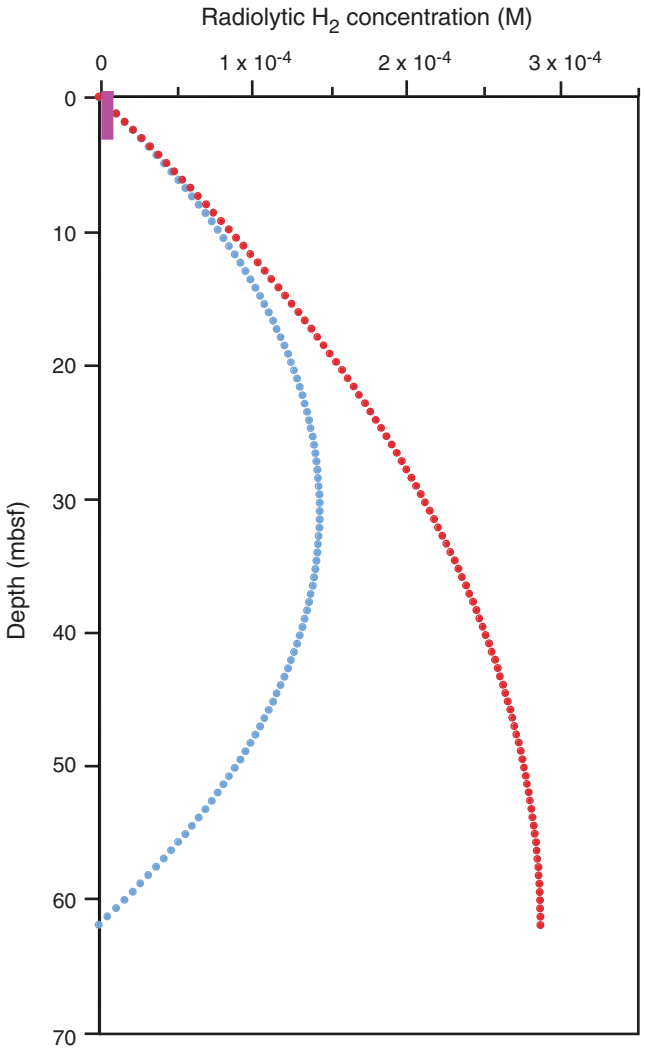

Figure F7. Surface heat flow data from Cruise Knox-02RR survey sites [Cruise Knox-02RR Shipboard Science Party, unpubl. data] superimposed on the compilation data of Stein and Stein (1994). Red circles = primary drilling sites, light blue circles = secondary sites, red arrows = primary sites for basement drilling. Heavy black line = expected heat flow for conductive crust in the absence of advection. No Cruise Knox-02RR data are available for Sites U1370 or U1371 because of technical failure and thermistor loss. Proposed Sites SPG3, SPG6, and SPG9 were not drilled during Expedition 329.

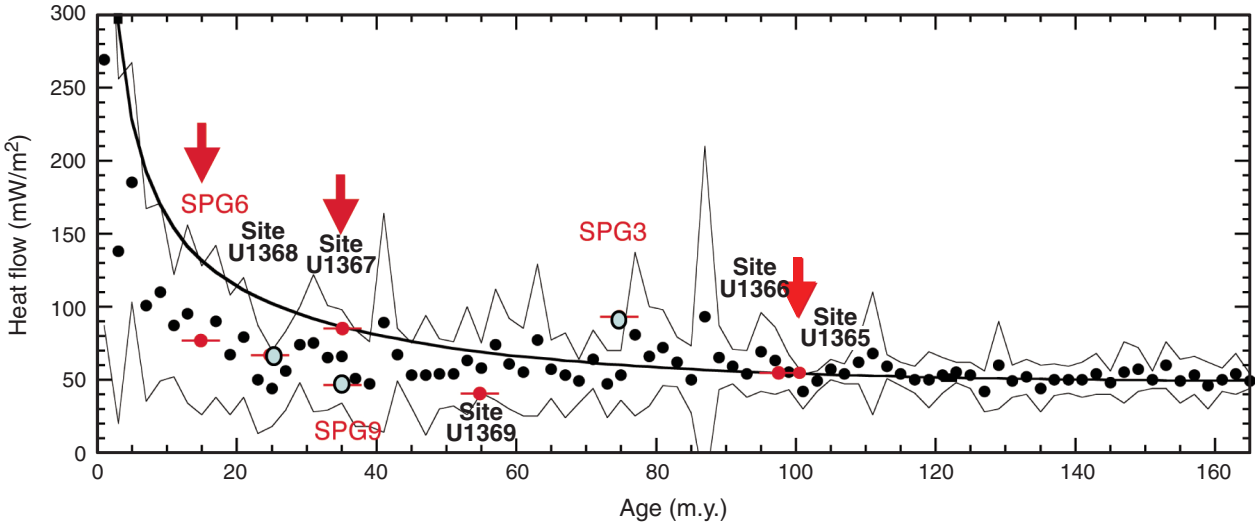

Figure F8. Representative lithologic columns, Sites U1365–U1371.

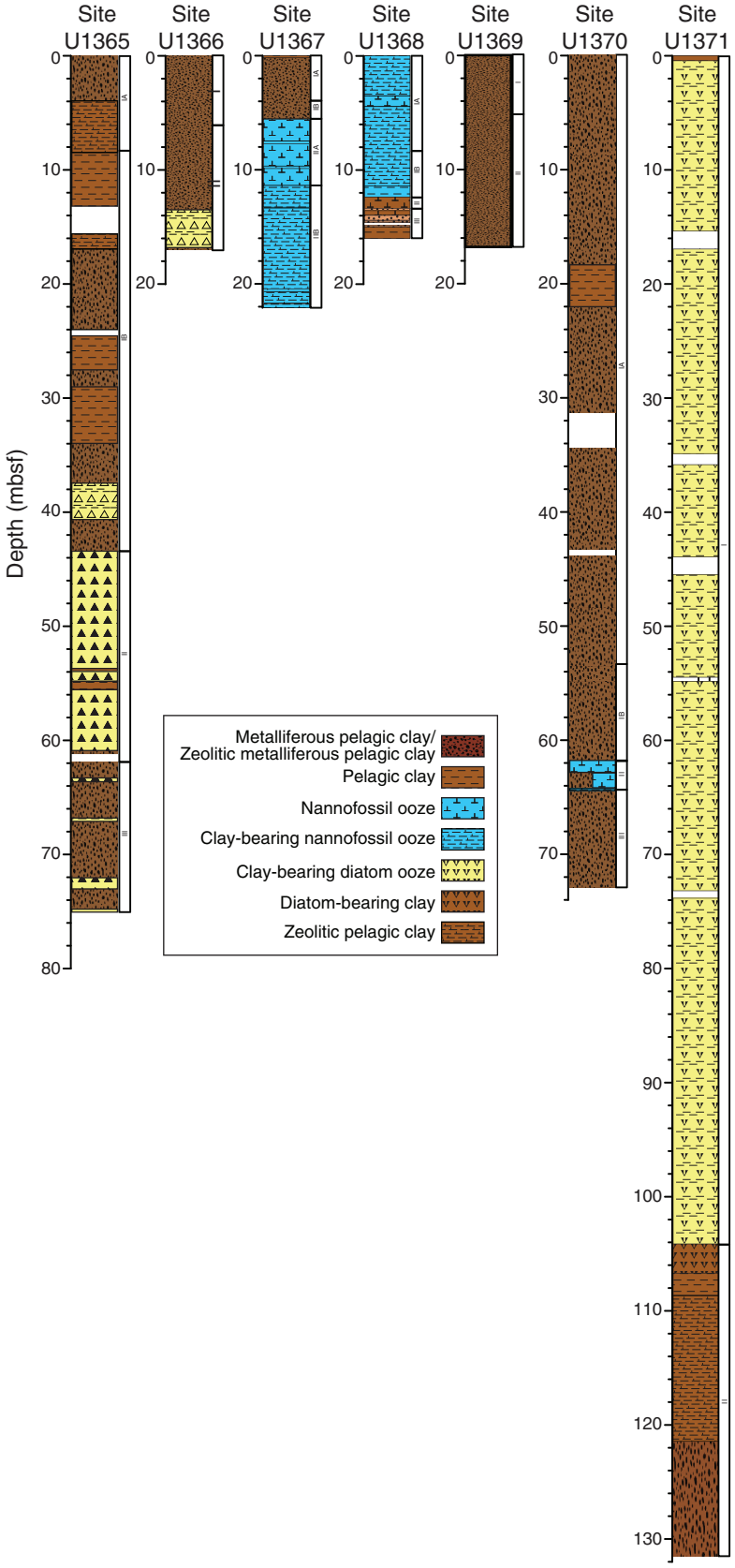

Figure F9. Plots of dissolved chemicals vs. depth, Sites U1365–U1371. **A.** Dissolved oxygen. **B.** Dissolved nitrate. **C.** Dissolved phosphate. **D.** Dissolved inorganic carbon (DIC).

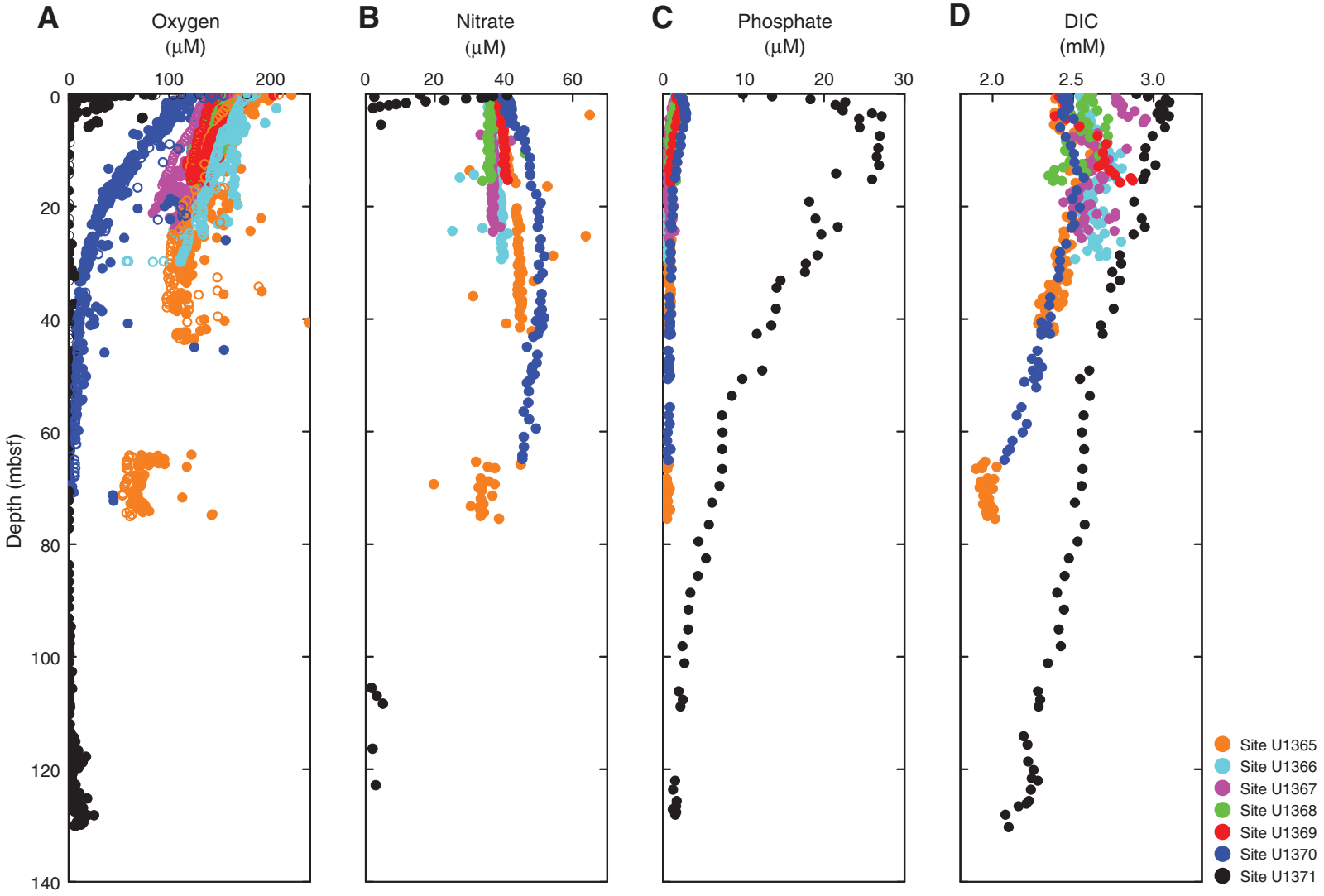

Figure F10. Plots of electron donor concentrations vs. depth, Sites U1365–U1371. **A.** Total organic carbon (TOC; solid phase). **B.** Total nitrogen (TN; solid-phase organic nitrogen). **C.** Dissolved H_2.

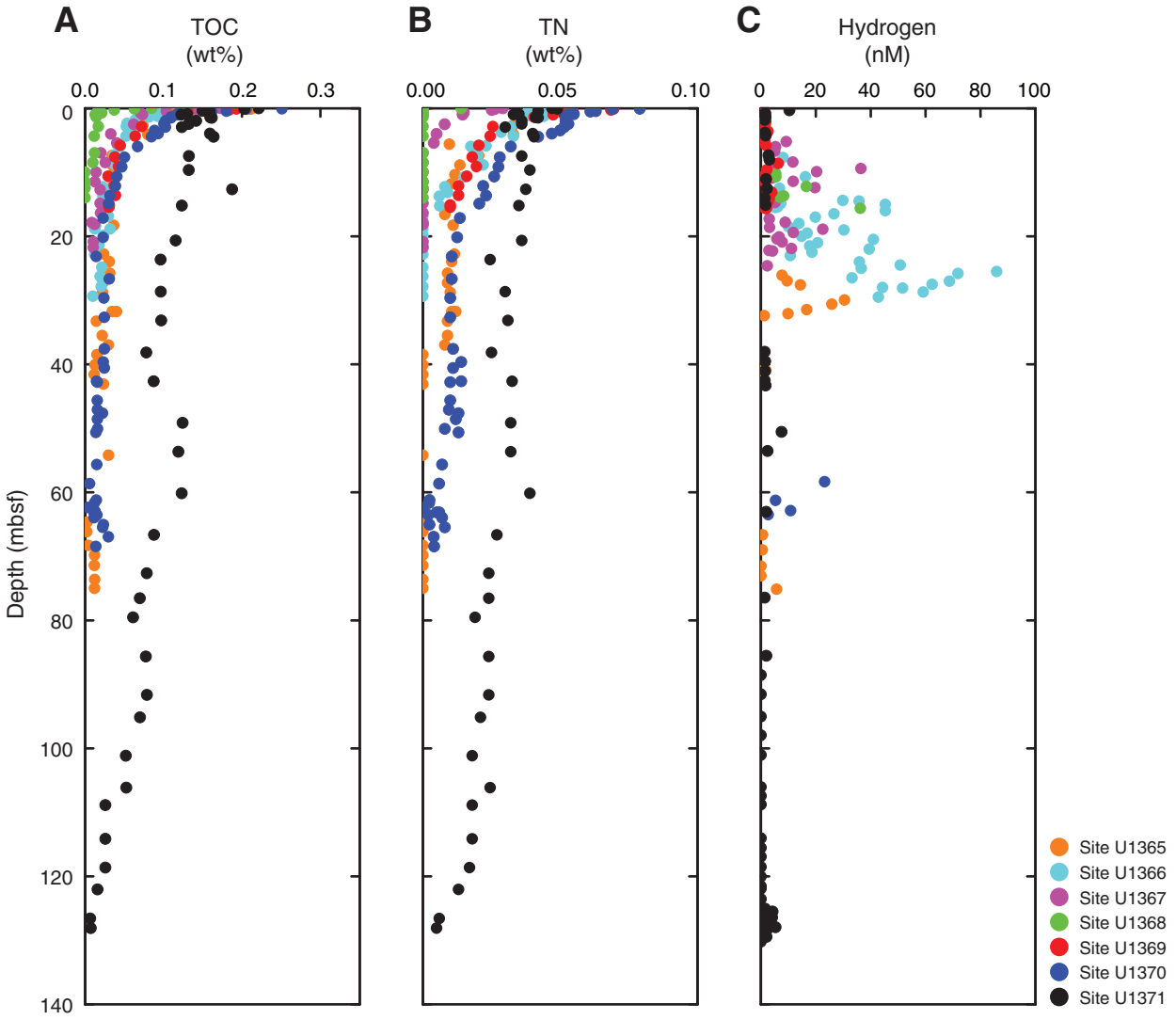

Figure F11. Plot of microbial cell counts vs. depth, Sites U1365–U1371. MDL = minium detection limit.

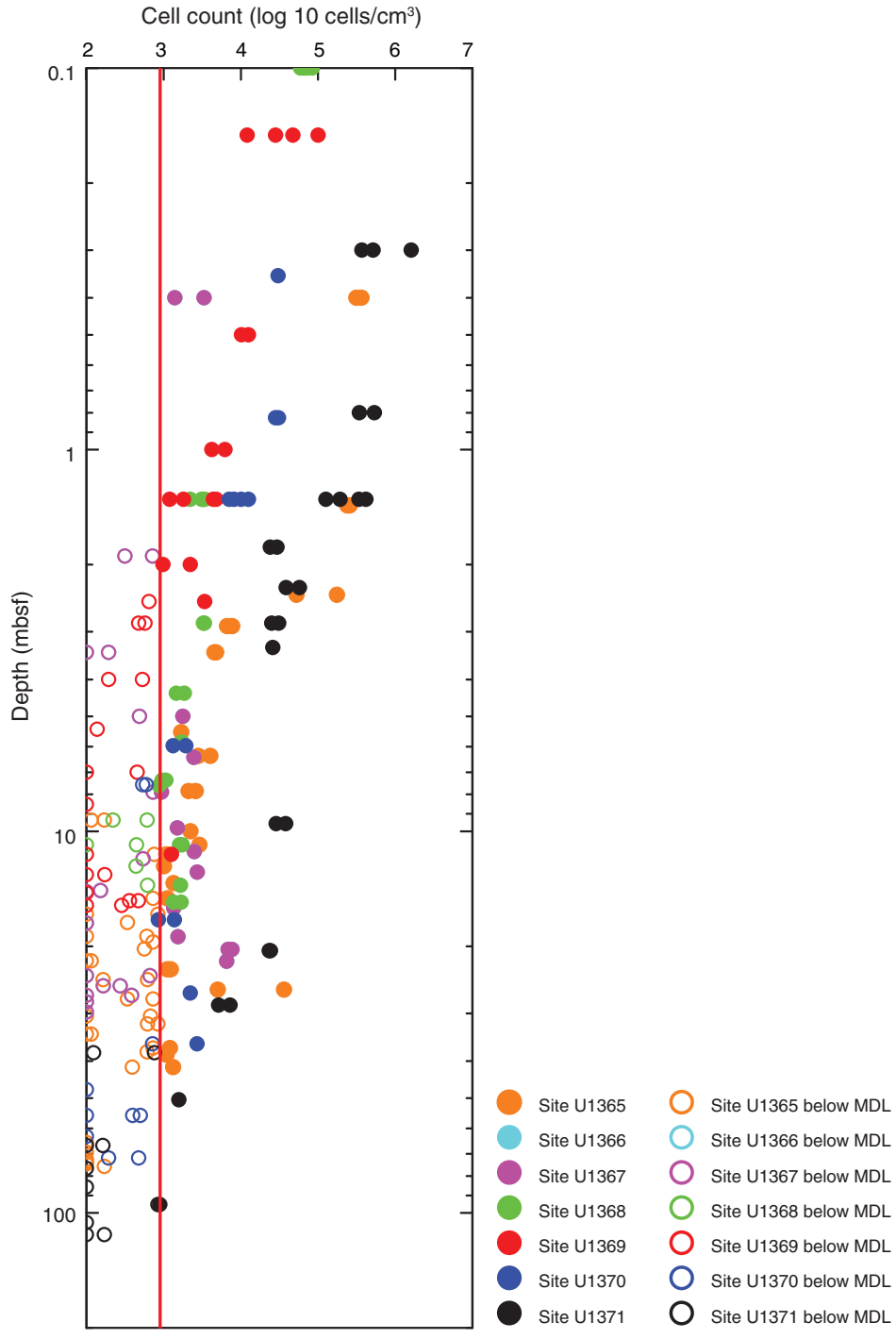

Figure F12. Photograph of potential biogenic alteration features within a hyaloclastite breccia, Site U1365. Altered basaltic glass with tubelike micro-scale weathering features (Sample 329-U1365E-8R-4, 3–6 cm; hyaloclastite breccia). Fe-Ox = iron oxyhydroxides. Plane-polarized light; 700× magnification

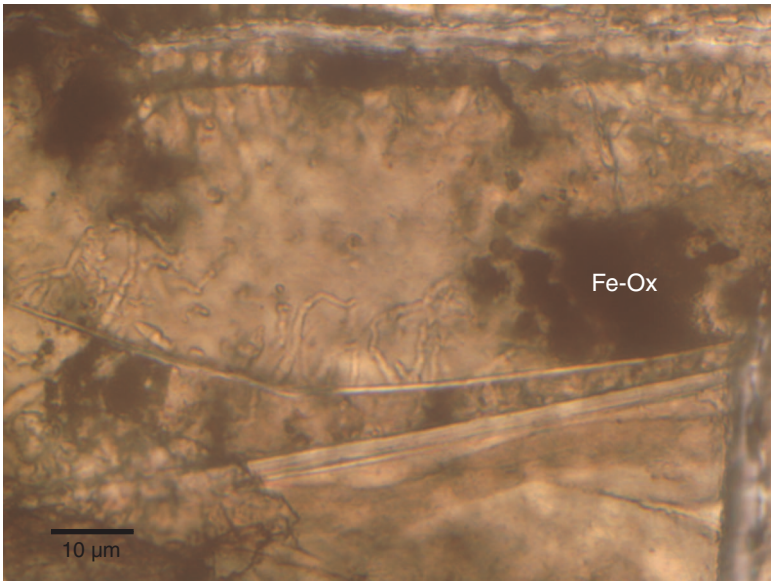

Figure F13. Profile of dissolved potassium, Sites U1365, U1370, and U1371.

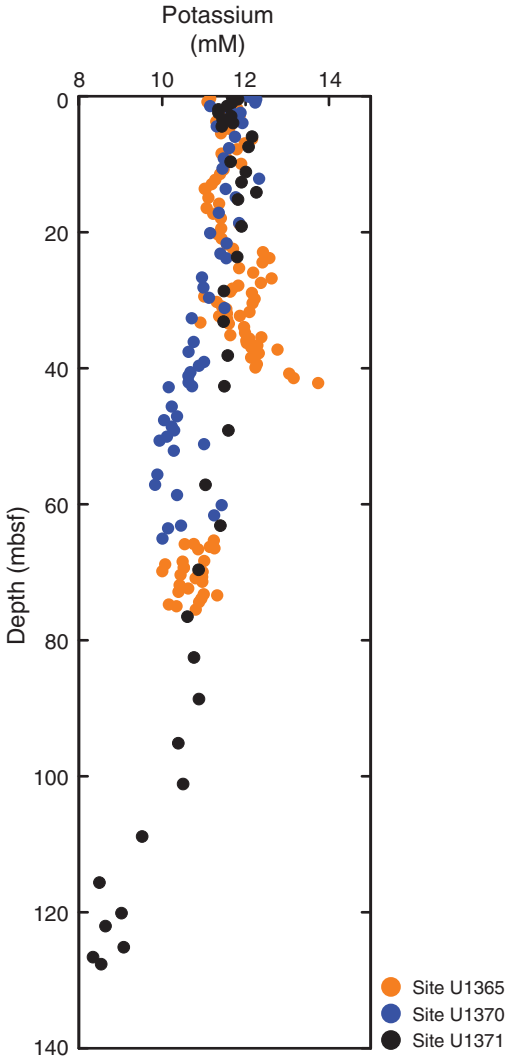

Figure F14. Illustration of relationship between igneous units, visually observed alteration intensity, and percent potassium content (determined by NGR core logging), Hole U1365E.

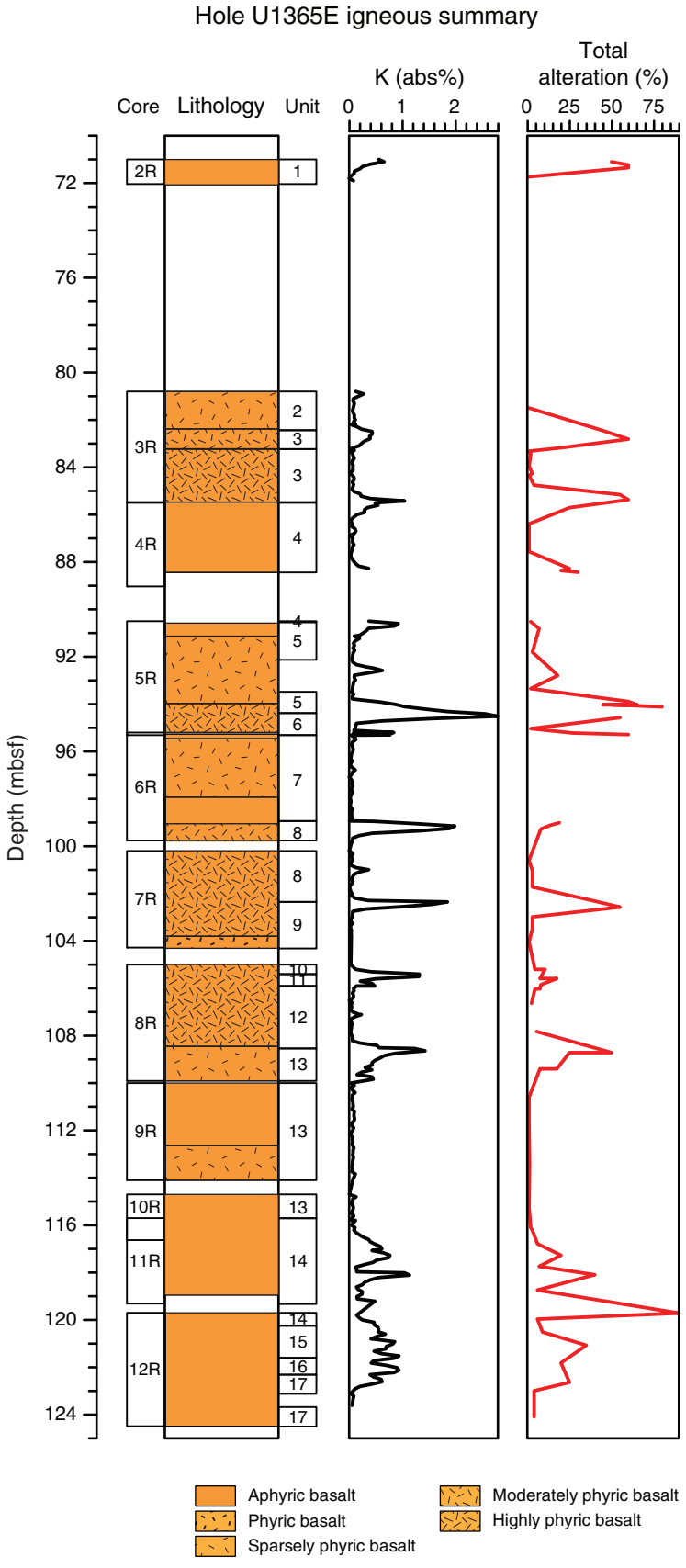

Figure F15. Summary of lithologic units and modal composition of minerals at Site U1365 based on the complete coring recovery of Hole U1365A. RSO = red-brown to yellow-brown semiopaque oxide.

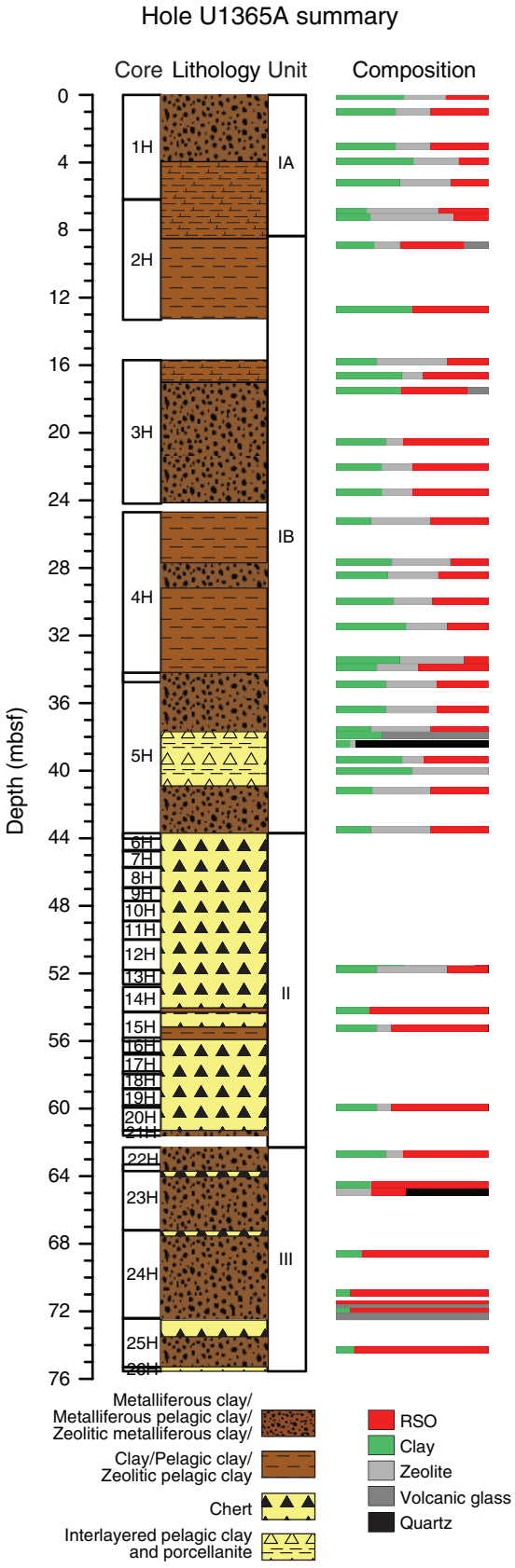

Figure F16. Plot of microbial cell count, Site U1366. Solid circles = microbial cell abundances quantified by epifluorescence microscopy (direct counts), open circles = cell counts below minimum detection limit (red line). Cell counts below the blank are shown as 102 cells/cm^3 in order to present them in the graph.

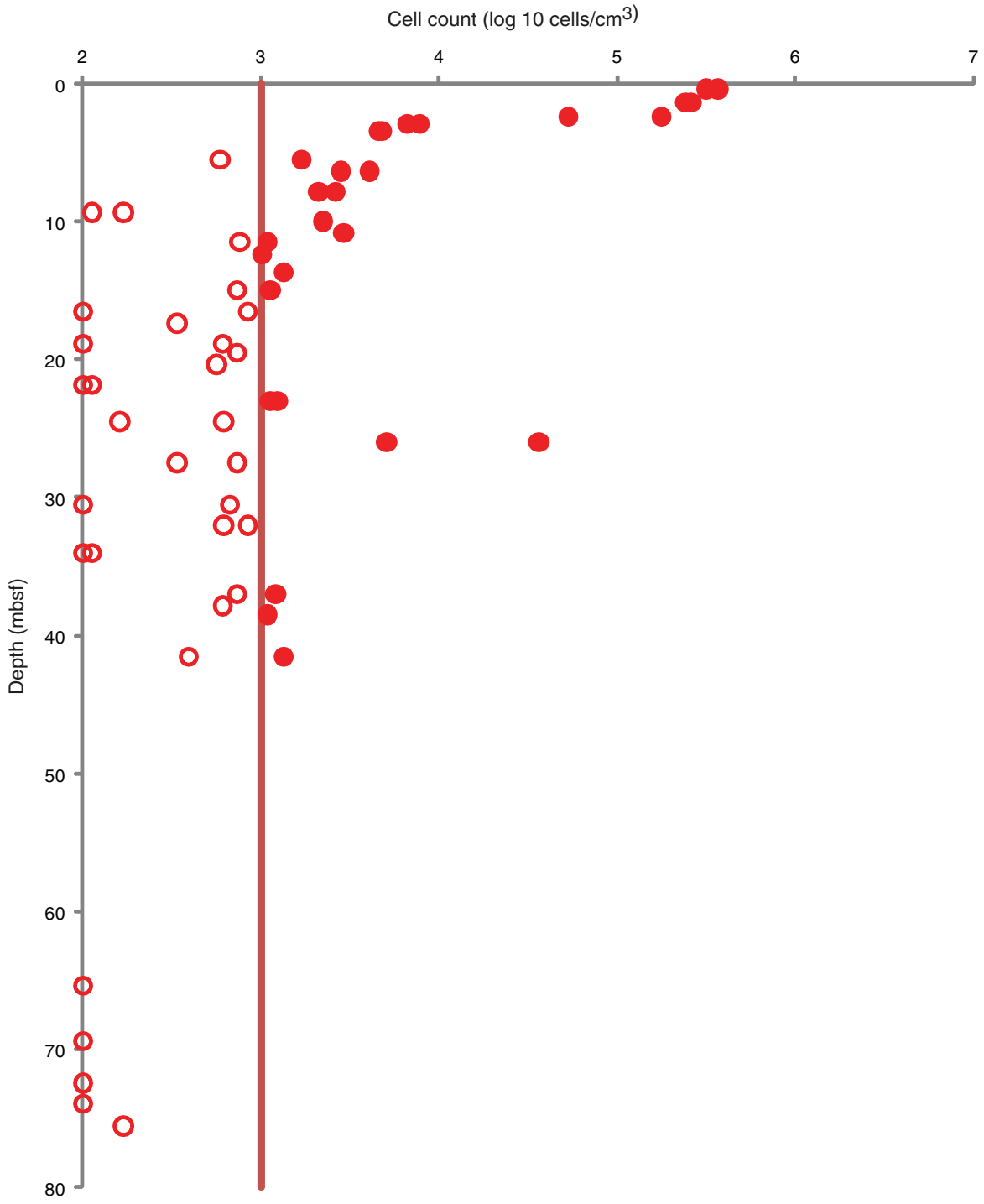

Figure F17. Profiles of dissolved oxygen and dissolved nitrate, Site U1365. **A.** Dissolved oxygen concentrations on all cores, Holes U1365A and U1365B. The figure includes measurements from core intervals that were observed before or during measurement to be compromised by core disturbance (flow-in, seawater intrusion, etc.). They are included to illustrate effects of core disturbance on dissolved oxygen measurements. **B.** Dissolved nitrate concentrations, Holes U1365B and U1365C.

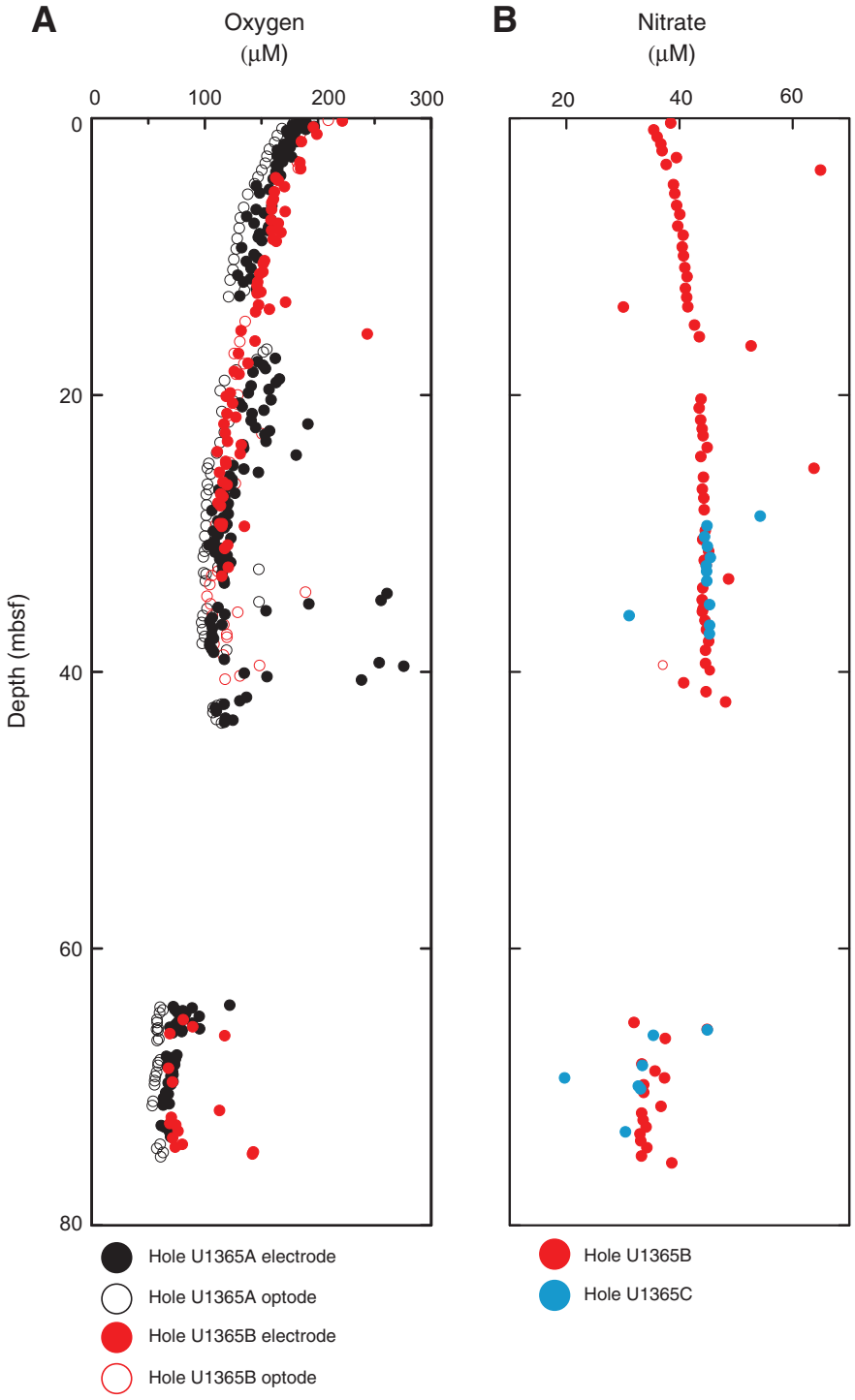

Figure F18. Plots of solid-phase nitrogen and carbon content, Hole U1365A. **A.** Total nitrogen (TN). **B.** Total organic carbon (TOC).

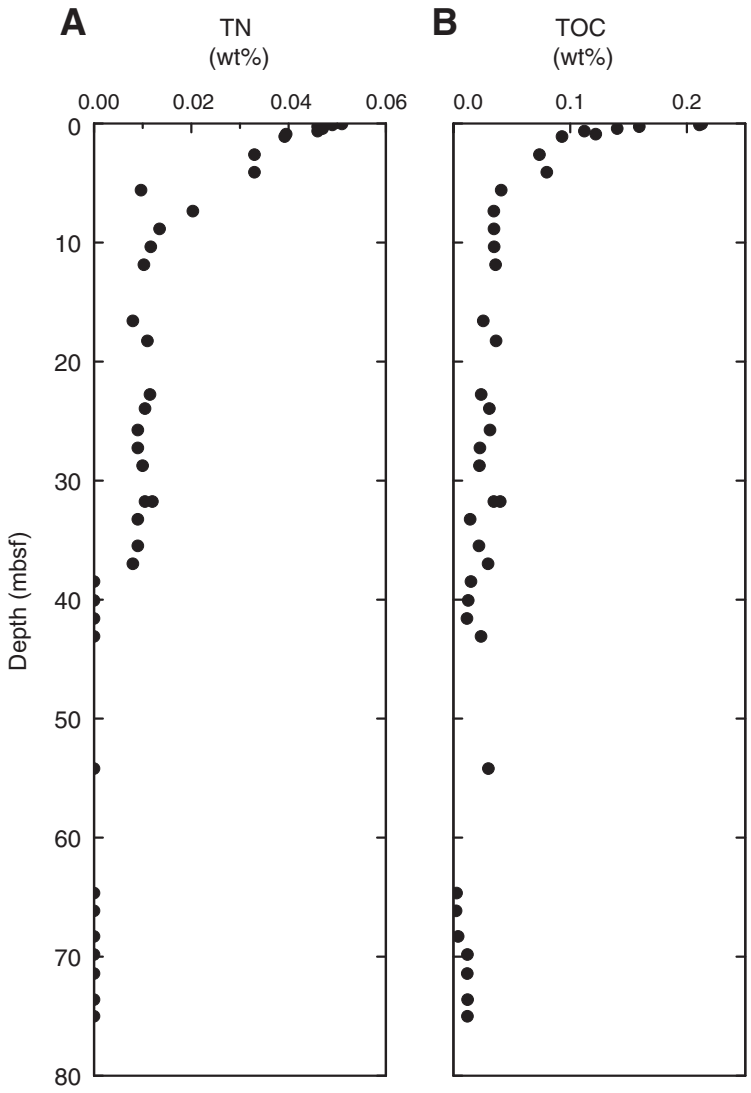

Figure F19. Summary of lithologic units and modal composition of minerals at Site U1366 based on the complete coring recovery of Hole U1366B. RSO = red-brown to yellow-brown semiopaque oxide.

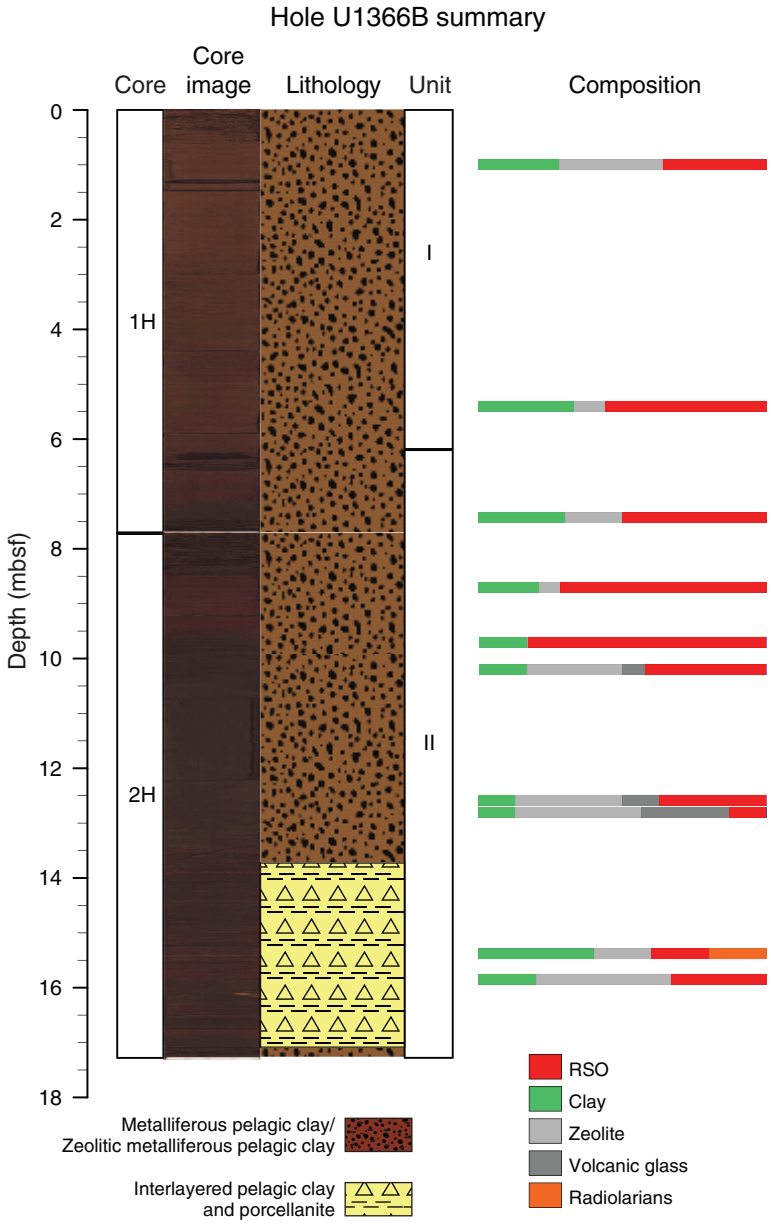

Figure F20. Plots of natural gamma radiation (NGR) core logs from the uppermost 1.5 m of Hole U1366E. Each data point is integrated over 20 cm. Dashed lines show manganese nodule concentrations of ^{238}U-series isotopes, ^{232}Th-series isotopes, and their ratio. **A.** NGR count. **B.** Concentration of ^{238}U-series isotopes. **C.** Concentration of ^{232}Th-series isotopes. **D.** Ratio of ^{238}U-series isotopes to ^{232}Th-series isotopes.

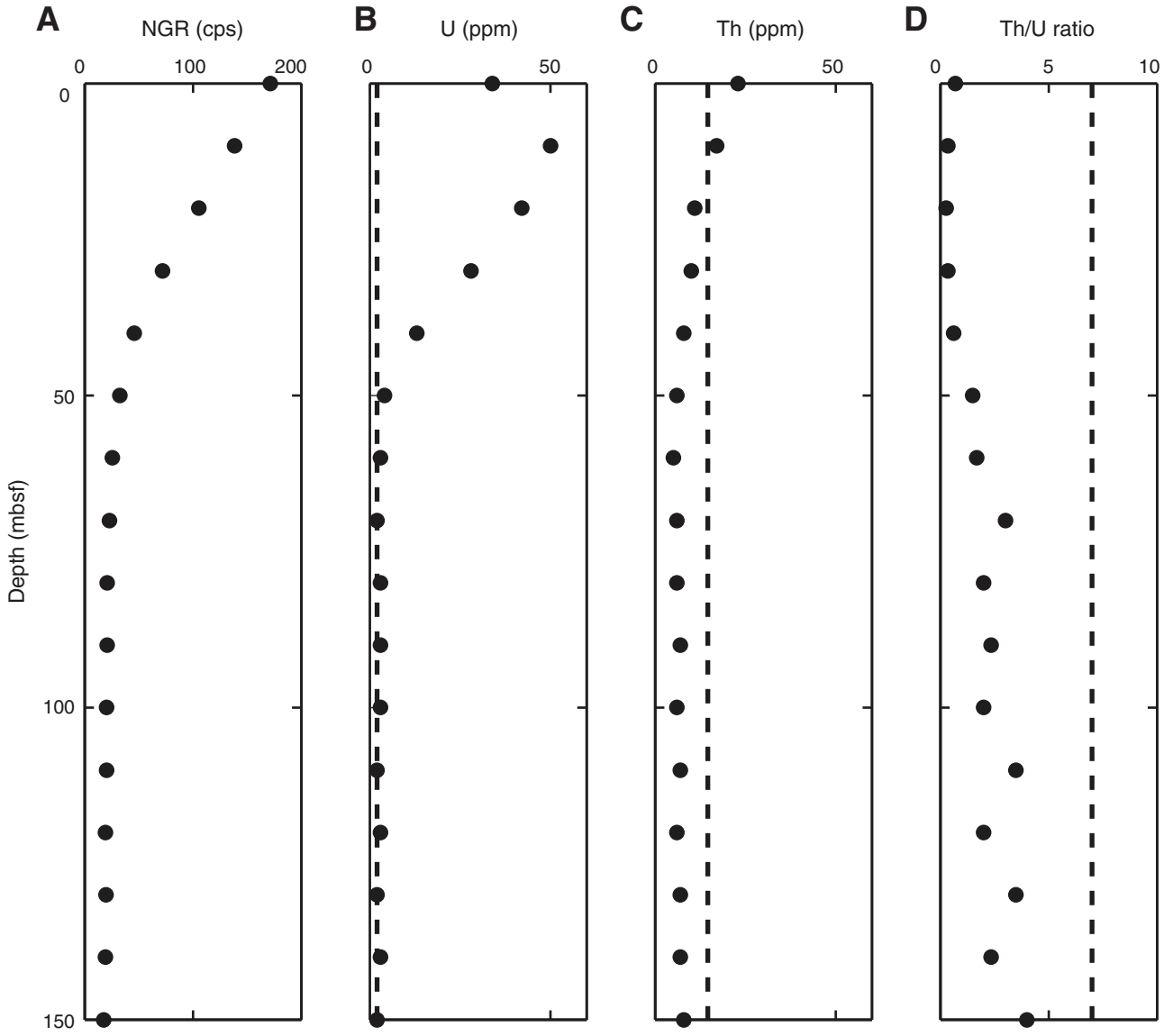

Figure F21. Plot of microbial cell counts, Site U1366. Solid circles = microbial cell abundances quantified by epifluorescence microscopy (direct counts), open circles = direct counts below minimum detection limit (red line). Cell counts below the blank are shown as 102 cells/cm^3 in order to present them in the graph.

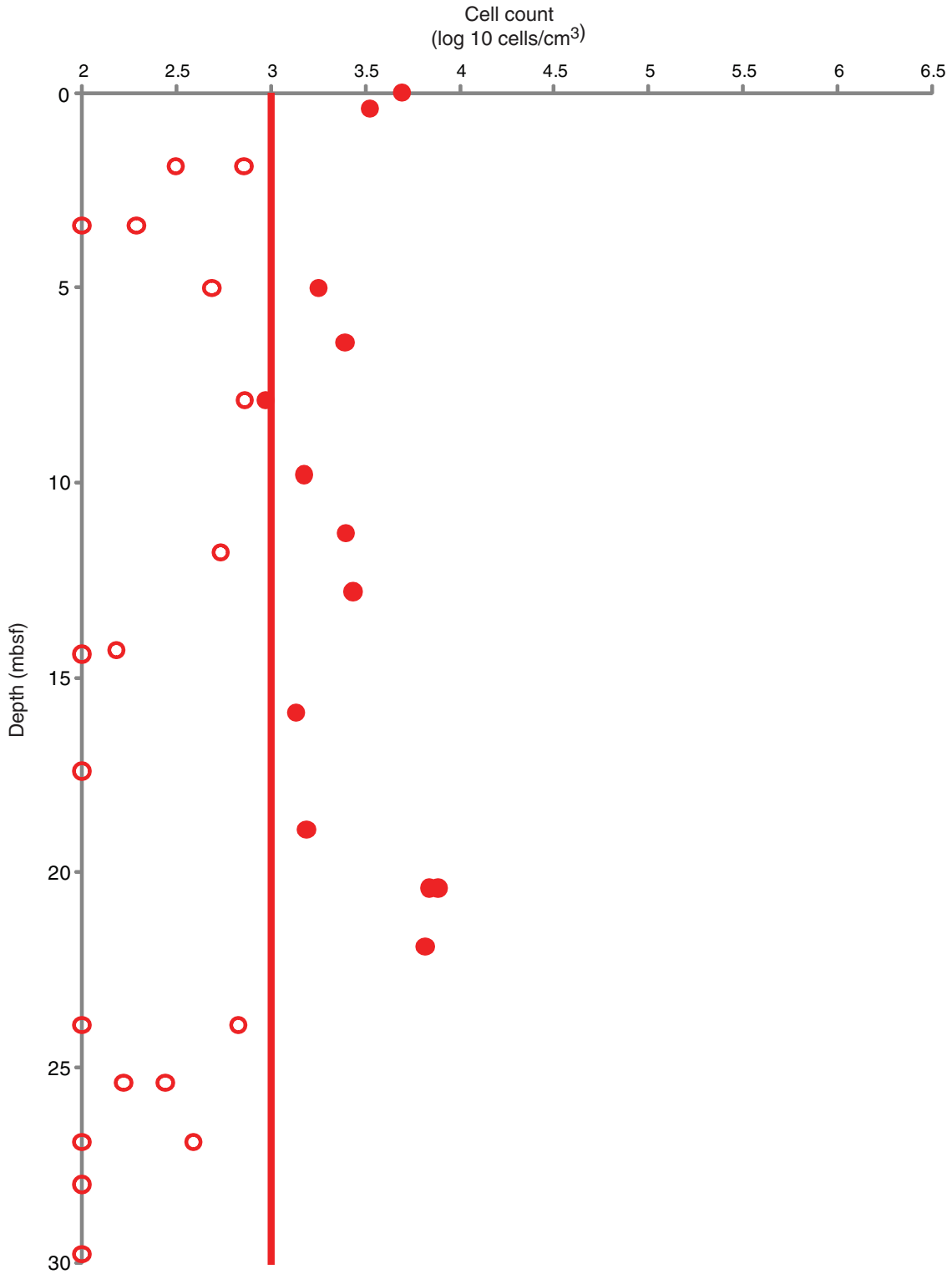

Figure F22. Plots of solid-phase nitrogen and carbon content, Holes U1366D and U1366F. **A.** Total nitrogen (TN). **B.** Total organic carbon (TOC). WTF = whole round taken fast.

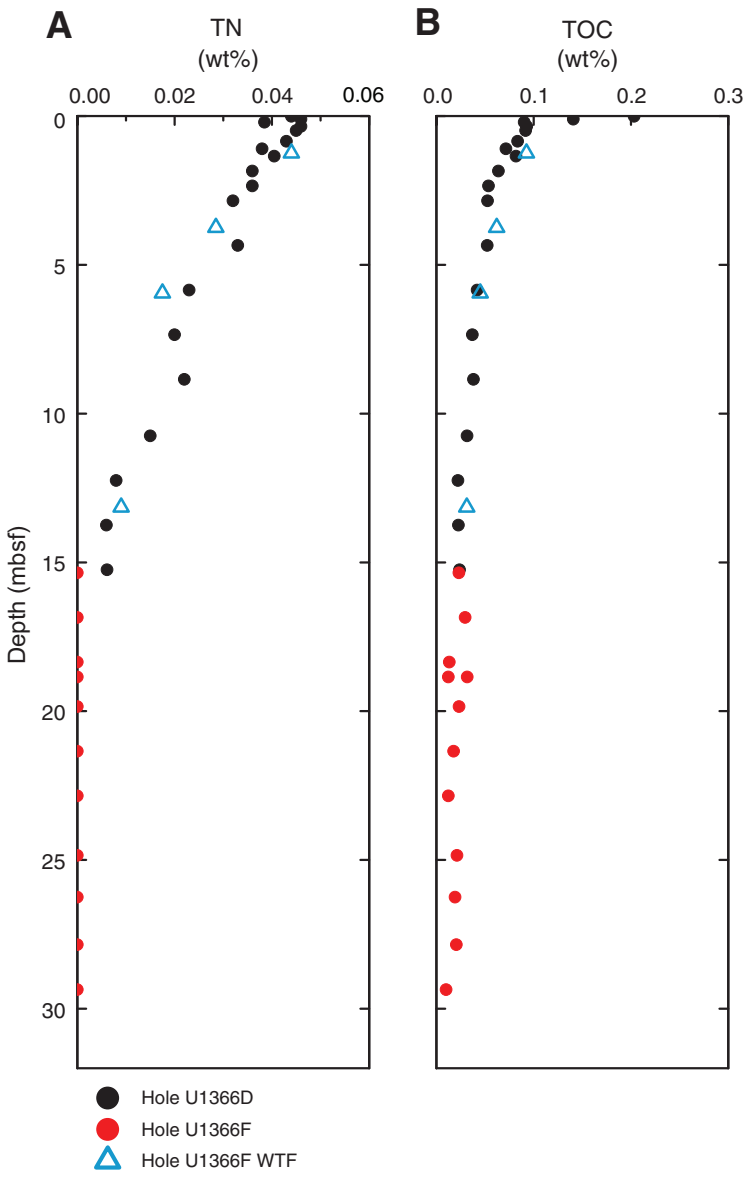

Figure F23. Profiles of (**A**) dissolved nitrate, (**B**) dissolved inorganic carbon (DIC), and (**C**) dissolved chloride concentrations, Holes U1366D and U1366F. Circles = samples taken as whole rounds in the hold-level core refrigerator, triangles = "whole round stored shorter" (WSS) samples taken as whole rounds in the hold deck refrigerator and immediately delivered to the geochemistry laboratory for squeezing porewater.

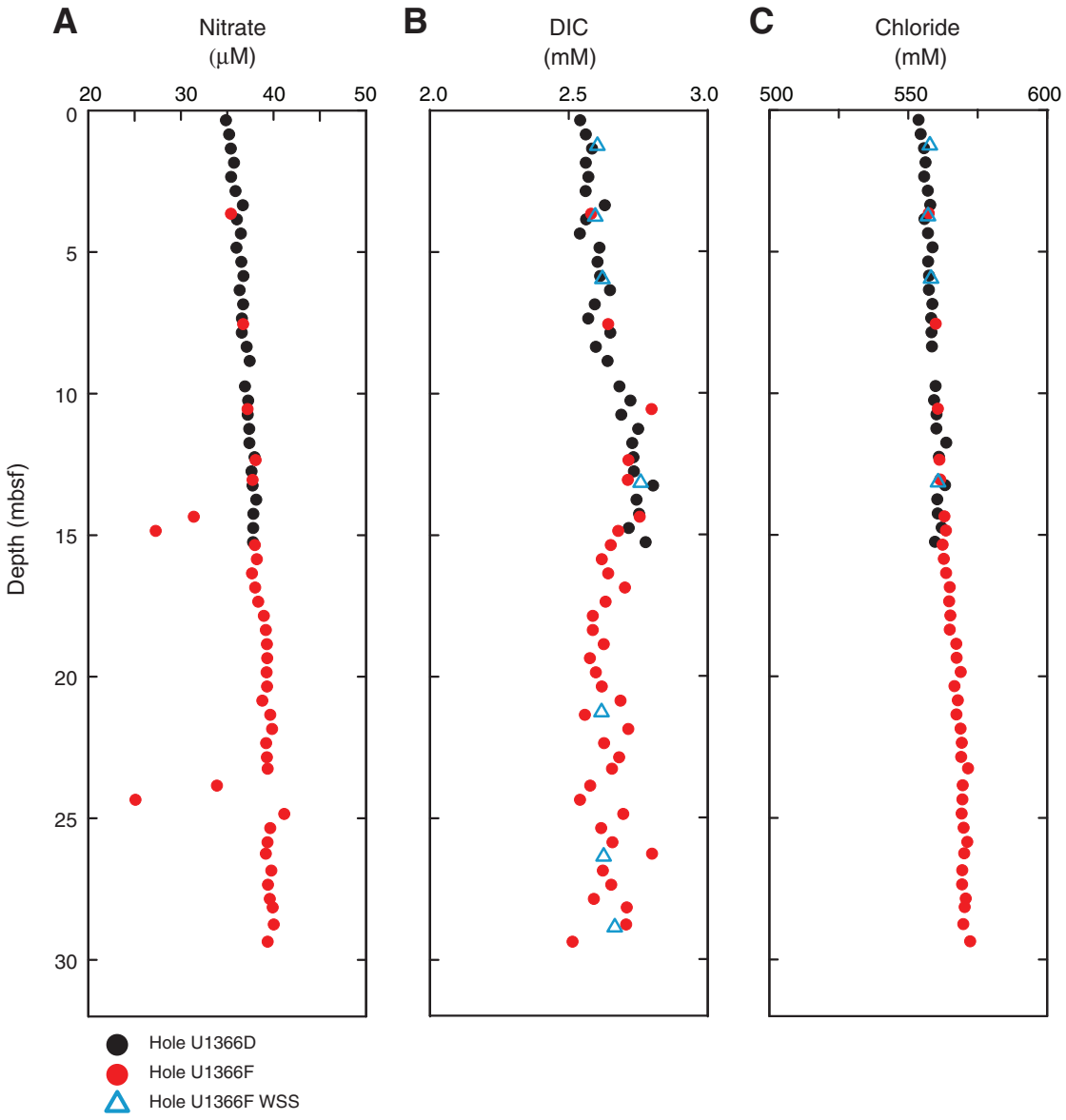

Figure F24. Summary of lithologic units and modal composition of minerals, Hole U1367B. RSO = red-brown to yellow-brown semiopaque oxide.

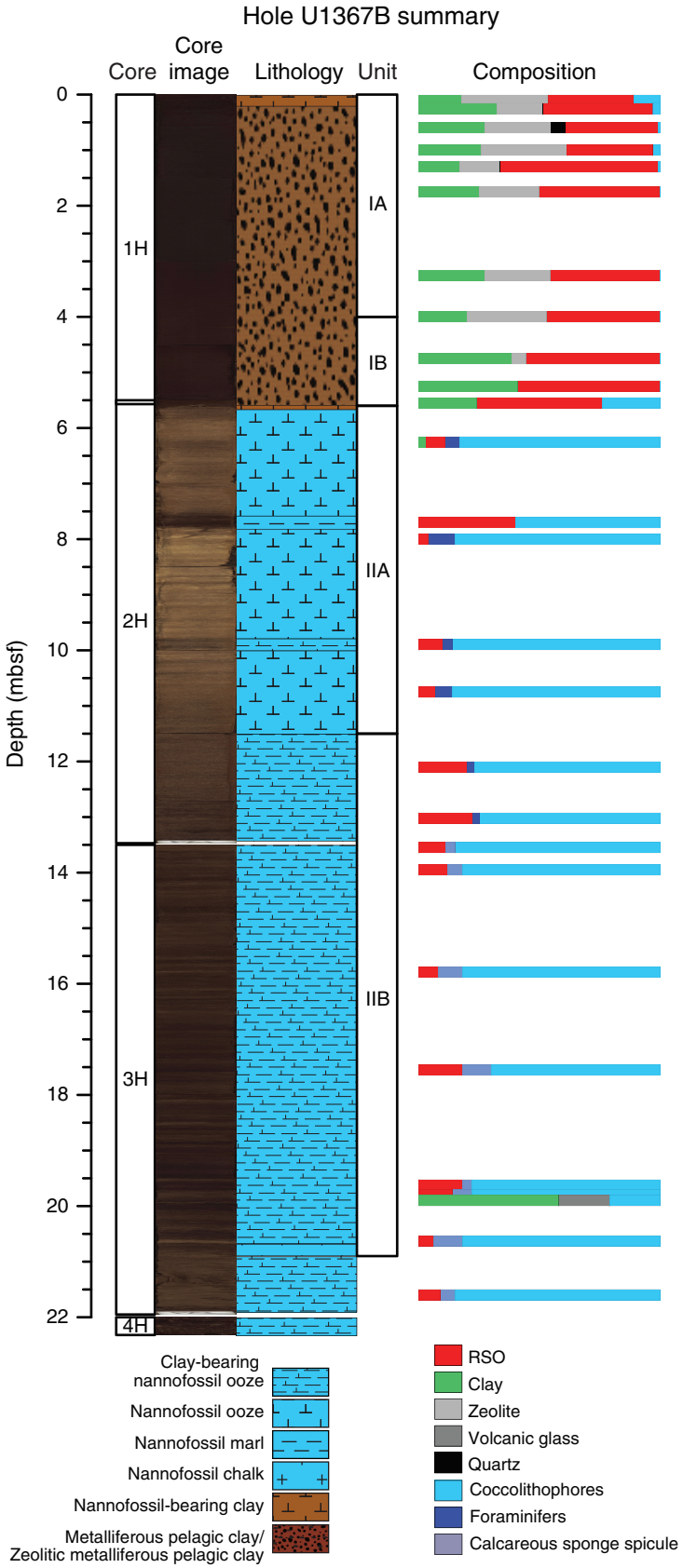

Figure F25. Profiles of (**A**) dissolved nitrate, (**B**) dissolved phosphate, and (**C**) dissolved inorganic carbon (DIC) concentrations, Holes U1366C and U1366D. Circles = samples taken as whole rounds in the hold-level core refrigerator, triangles = samples taken as whole rounds directly from the catwalk and immediately delivered to geochemistry laboratory for squeezing porewater.

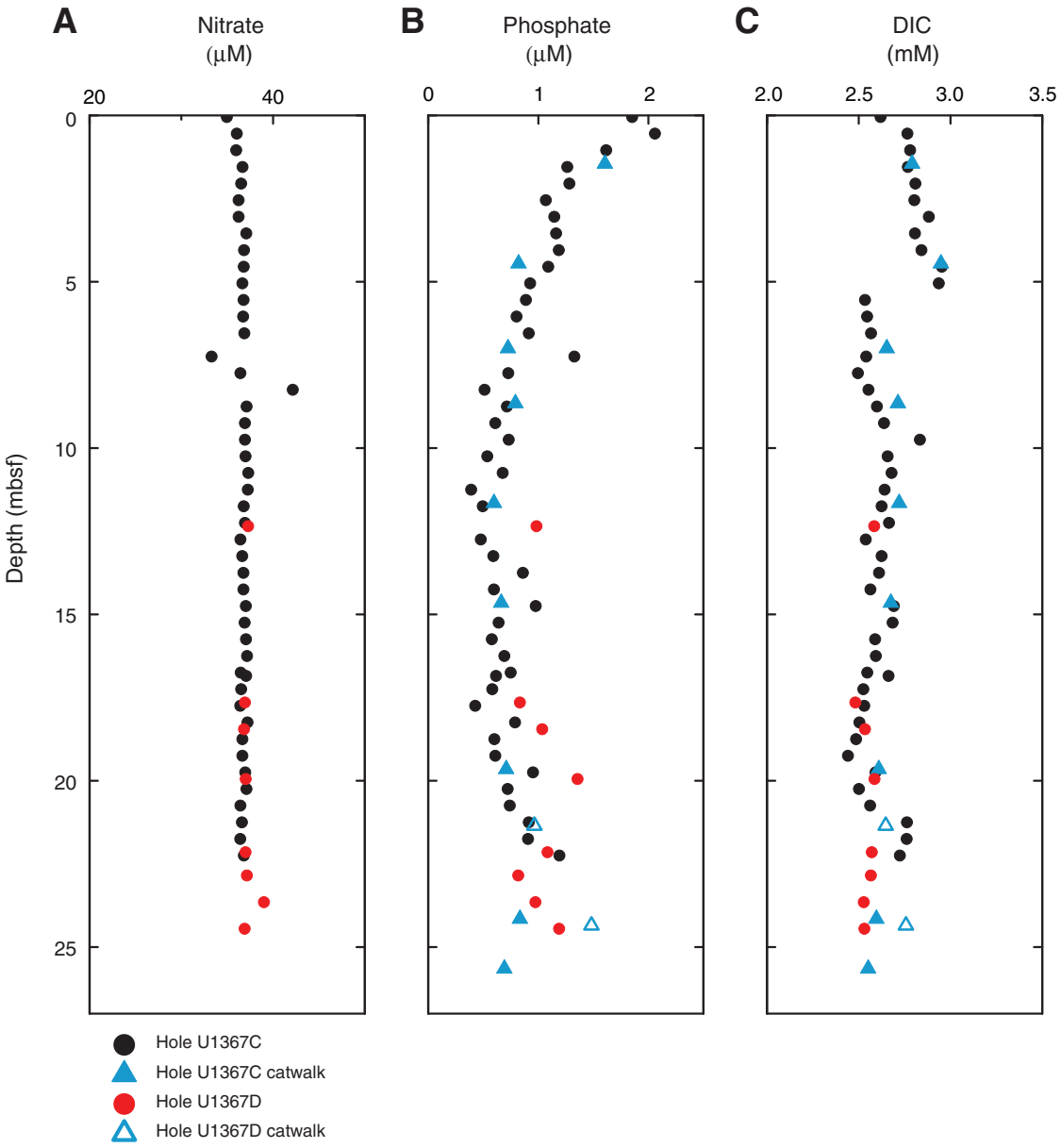

Figure F26. Summary of lithologic units and modal composition of minerals, Hole U1368B. RSO = red-brown to yellow-brown semiopaque oxide.

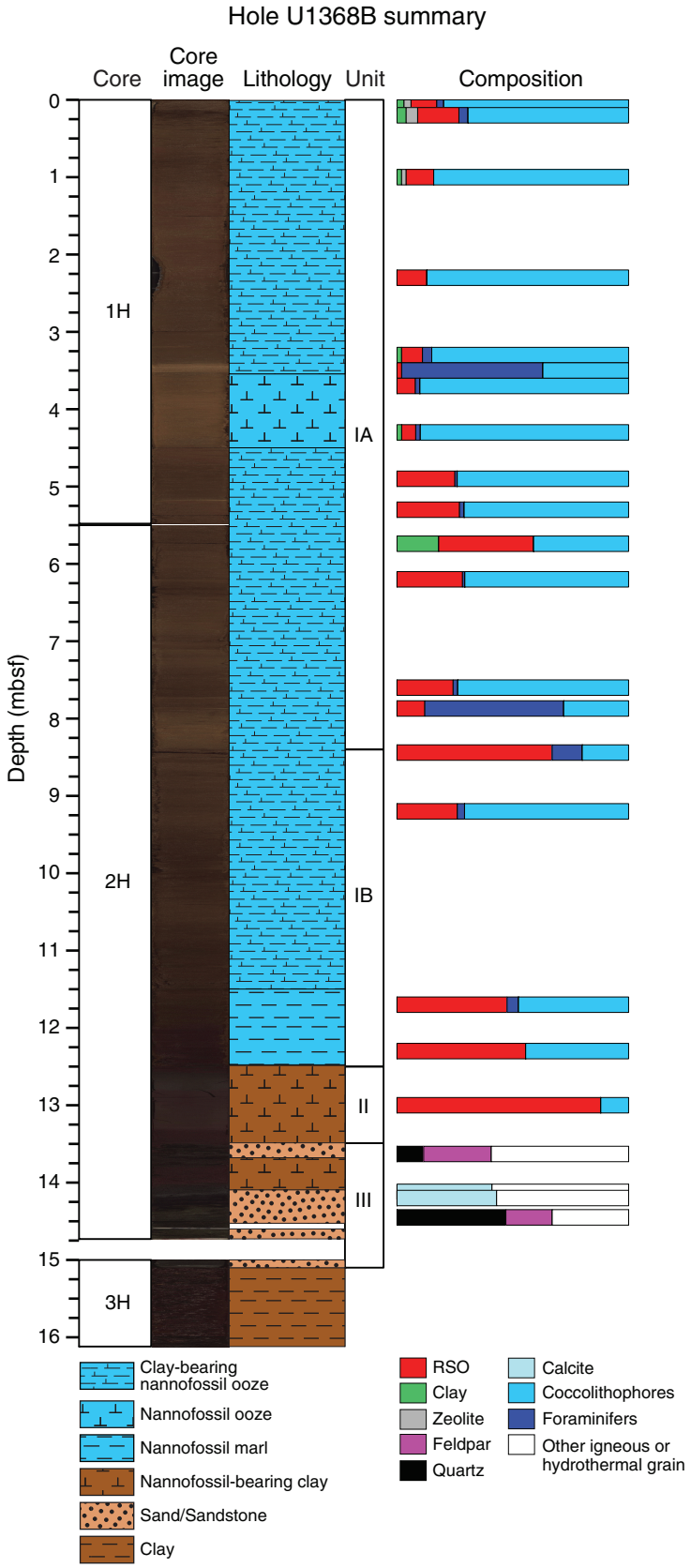

Figure F27. Profile of dissolved hydrogen, Hole U1368C. Circles = samples taken as whole rounds in the core refrigerator of the hold deck, triangles = samples taken as whole rounds directly from the catwalk.

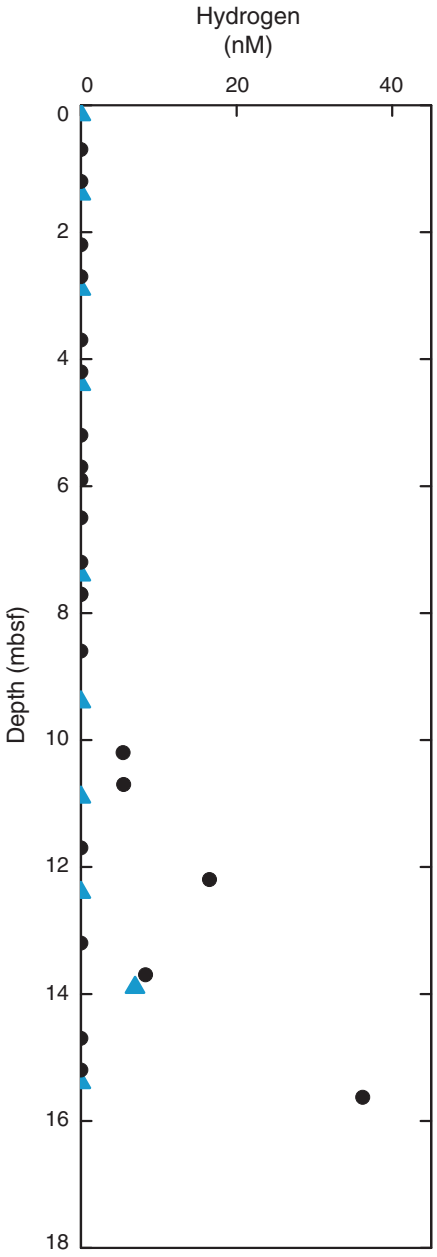

Figure F28. Profile of downhole NGR-based potassium concentration (purple) vs. whole-round core NGR-based potassium concentration (green).

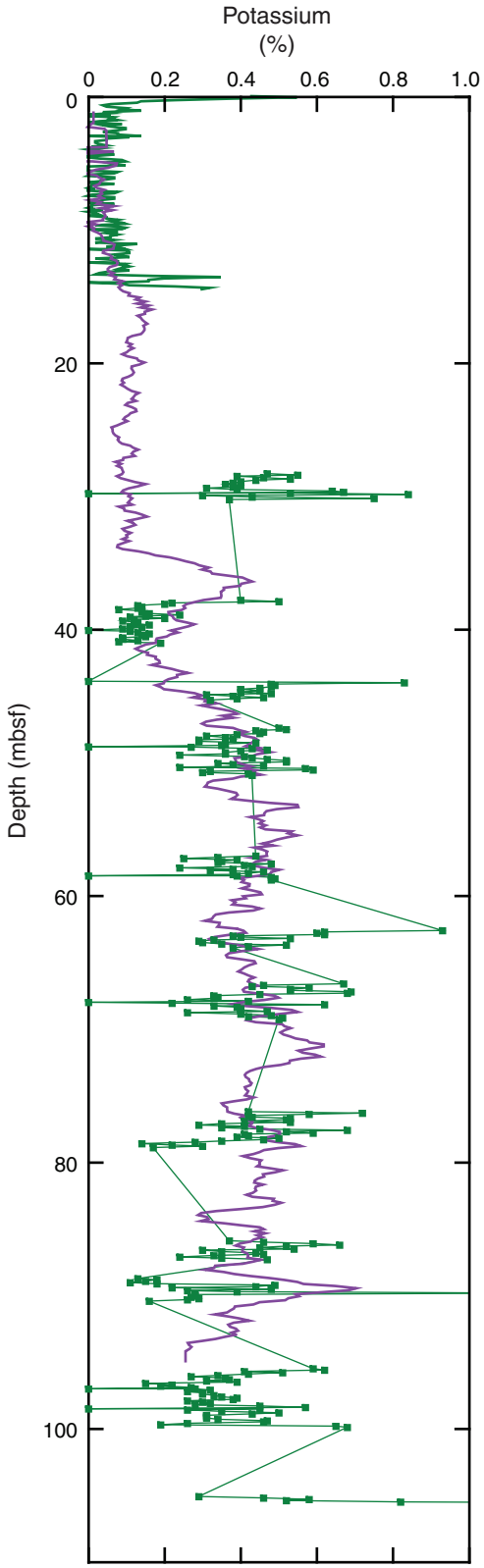

Figure F29. Summary of lithologic units and modal composition of minerals, Hole U1369B. RSO = red-brown to yellow-brown semiopaque oxide.

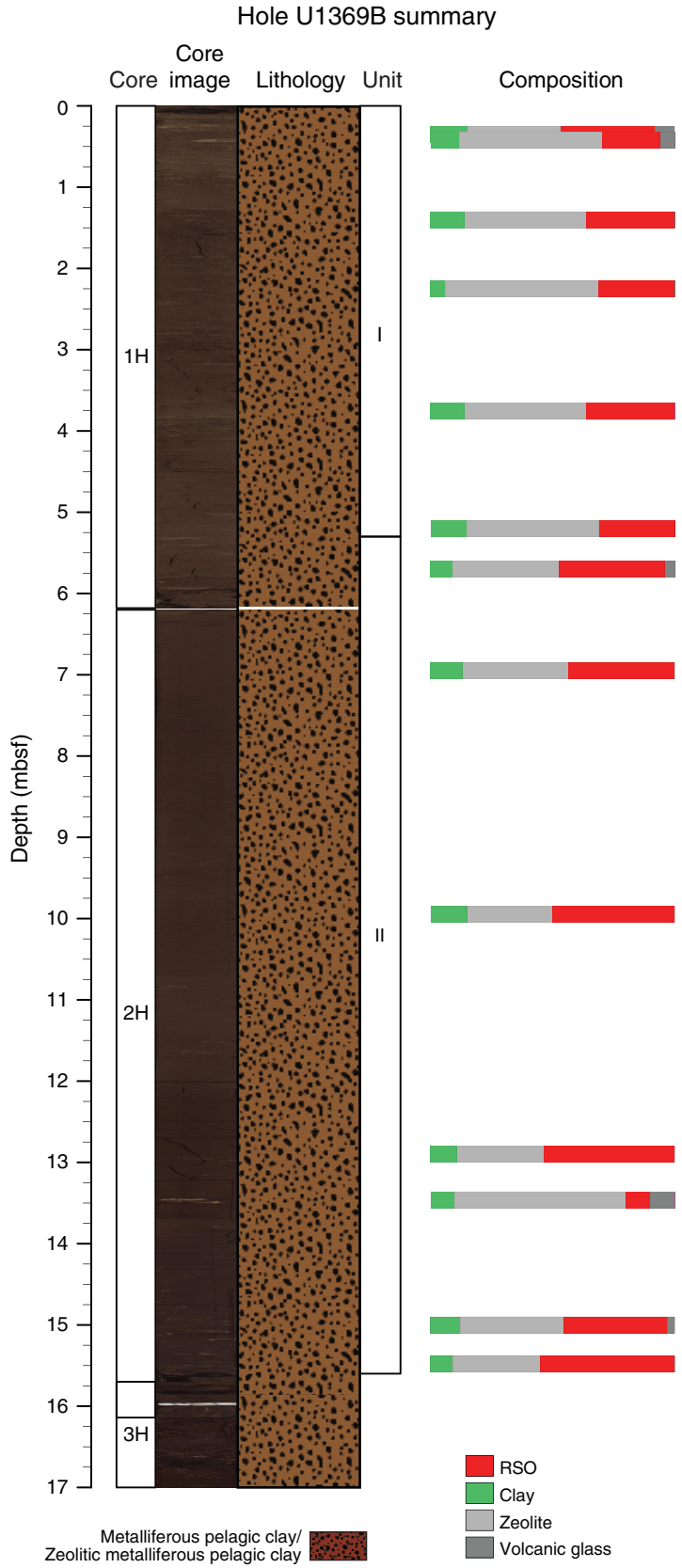

Figure F30. Plot of microbial cell counts, Site U1369. Solid circles = microbial cell abundances quantified by epifluorescence microscopy (direct counts), open circles = direct counts below minimum detection limit (red line). Cell counts below the blank are shown as 102 cells/cm^3 in order to present them in the graph.

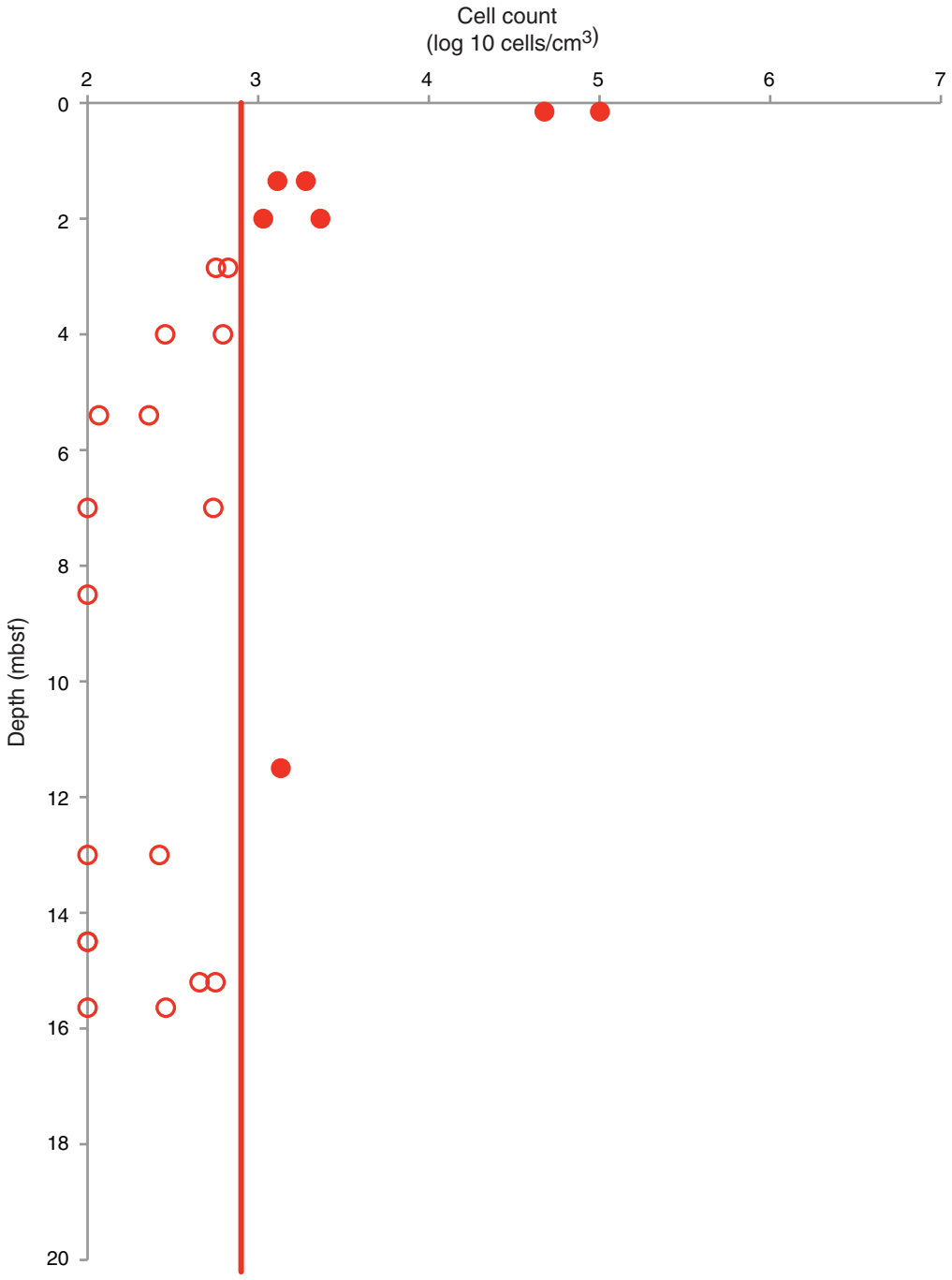

Figure F31. Profiles of (**A**) dissolved oxygen, (**B**) dissolved nitrate, (**C**) dissolved phosphate, and (**D**) dissolved inorganic carbon (DIC), Site U1369.

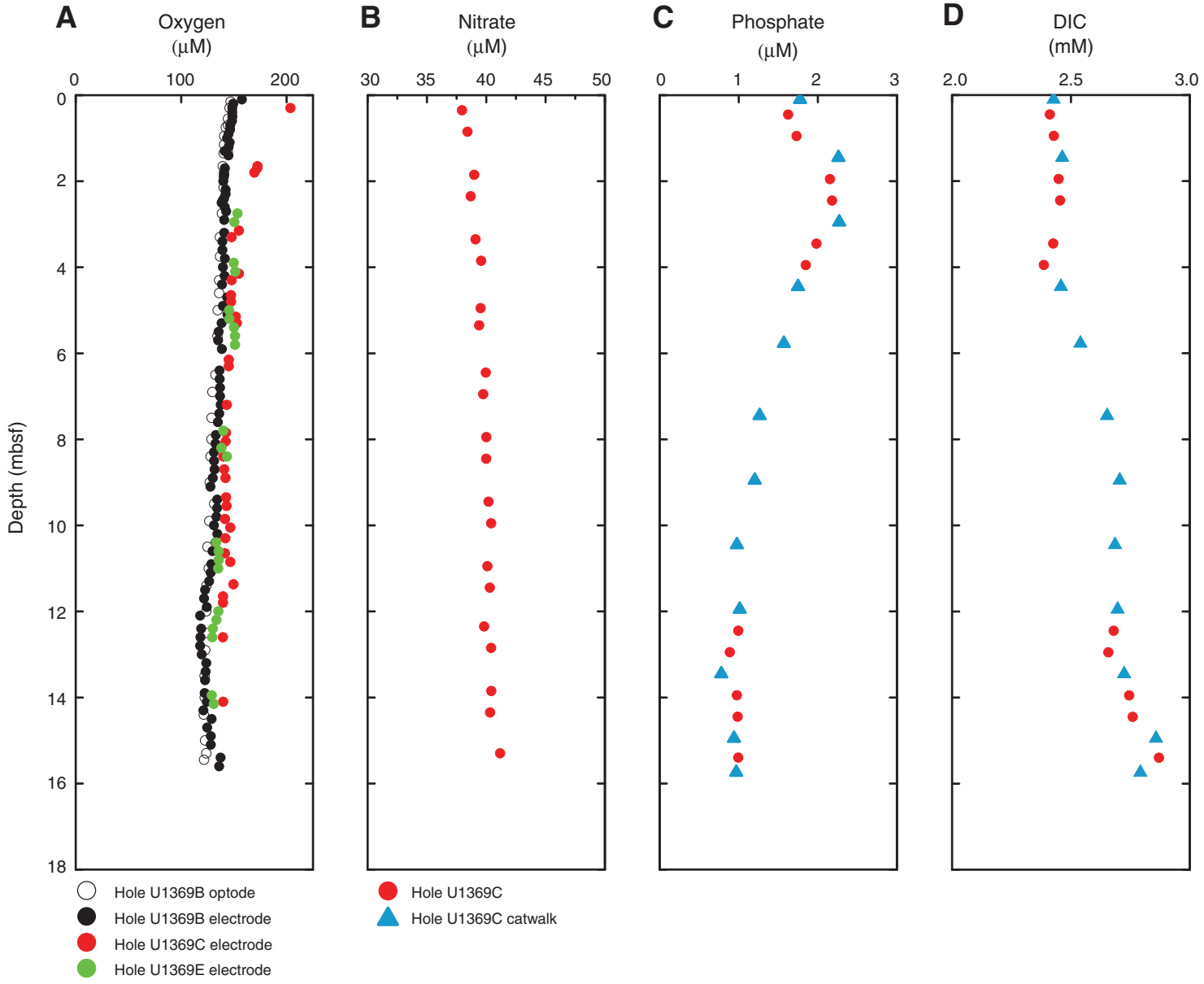

Figure F32. Summary of lithologic units and modal composition of minerals, Hole U1370D. RSO = red-brown to yellow-brown semiopaque oxide.

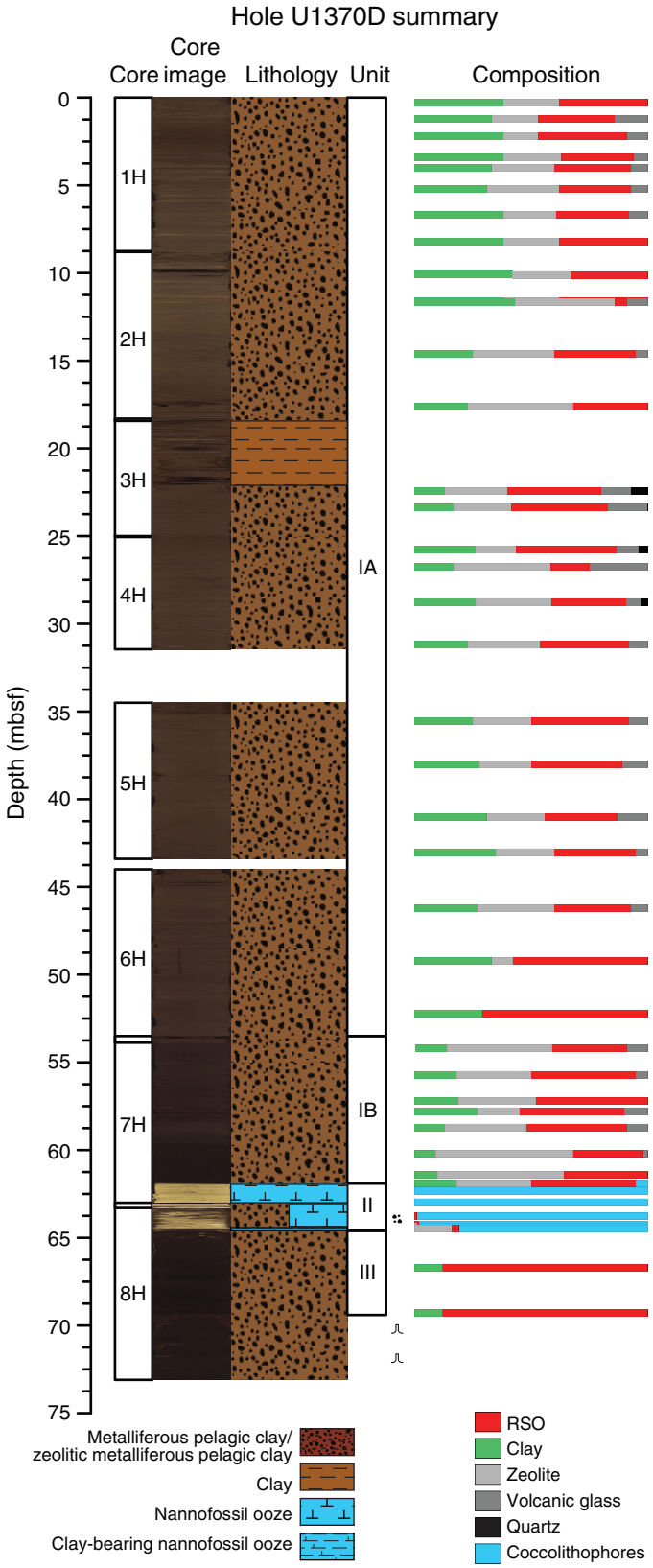

Figure F33. Profiles of (**A**, **B**) dissolved oxygen and (**C**) dissolved nitrate, Site U1370.

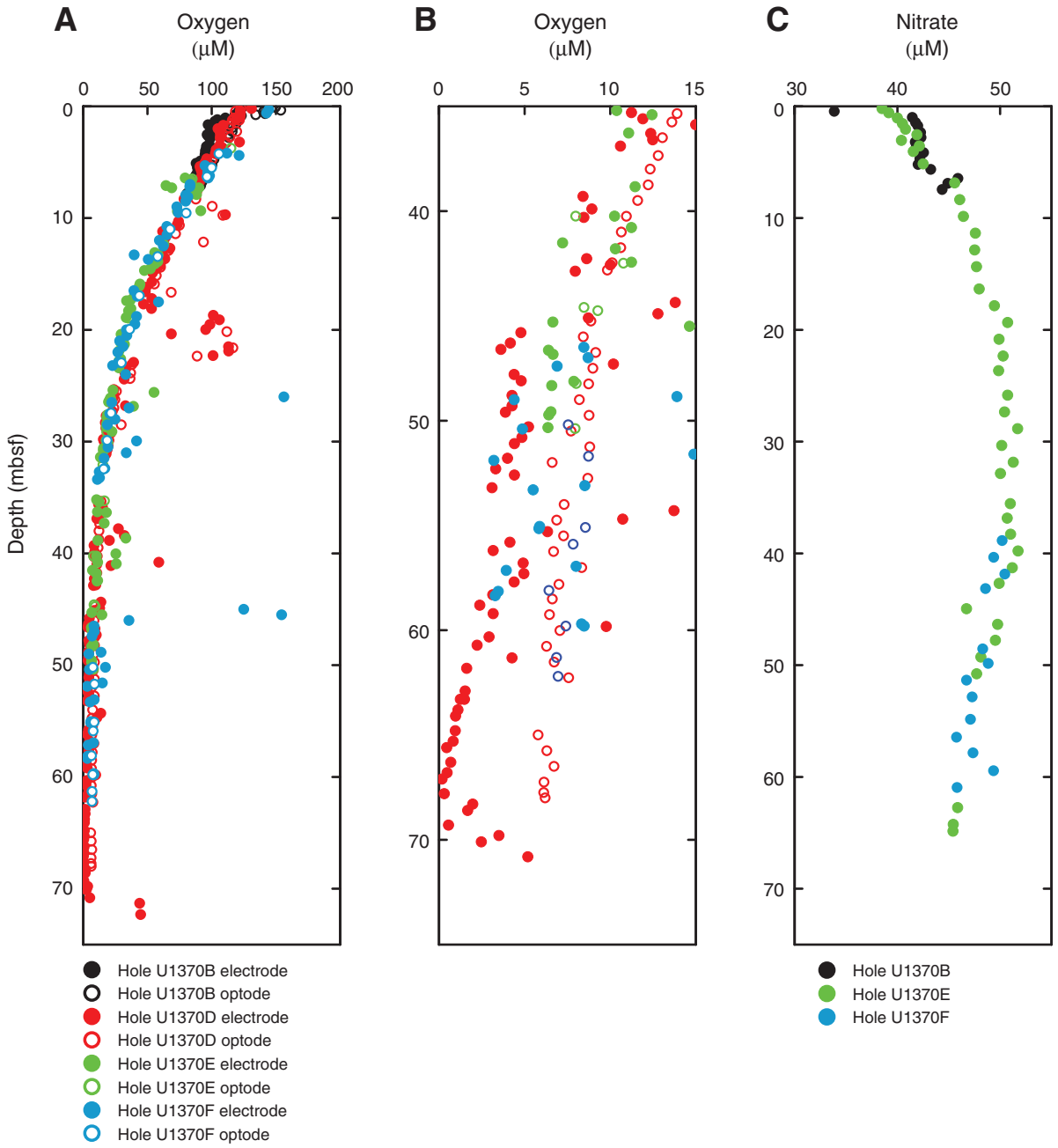

Figure F34. Profile of dissolved potassium, Site U1370. IC = ion chromatograph, ICP = inductively coupled plasma–atomic emission spectroscopy.

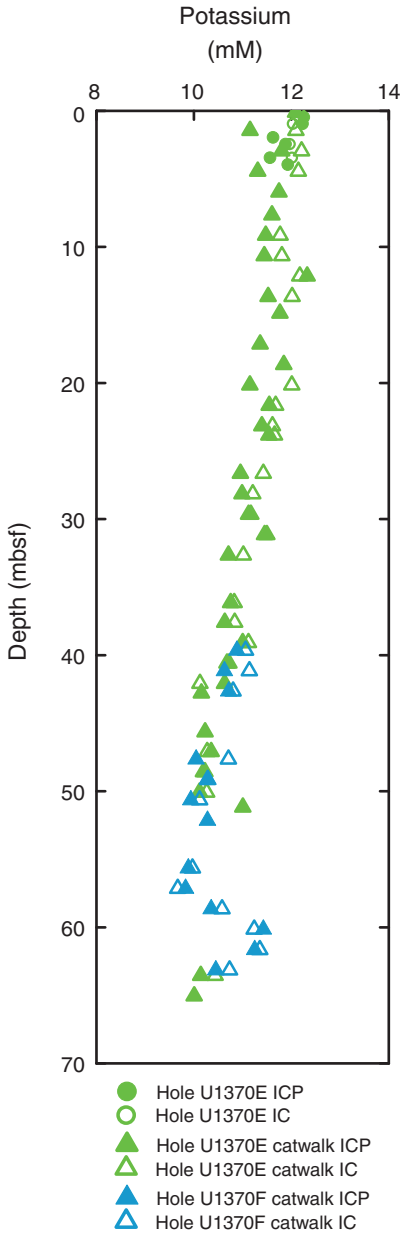

Figure F35. Summary of lithologic units and modal composition of minerals, Hole U1371D. RSO = red-brown to yellow-brown semiopaque oxide.

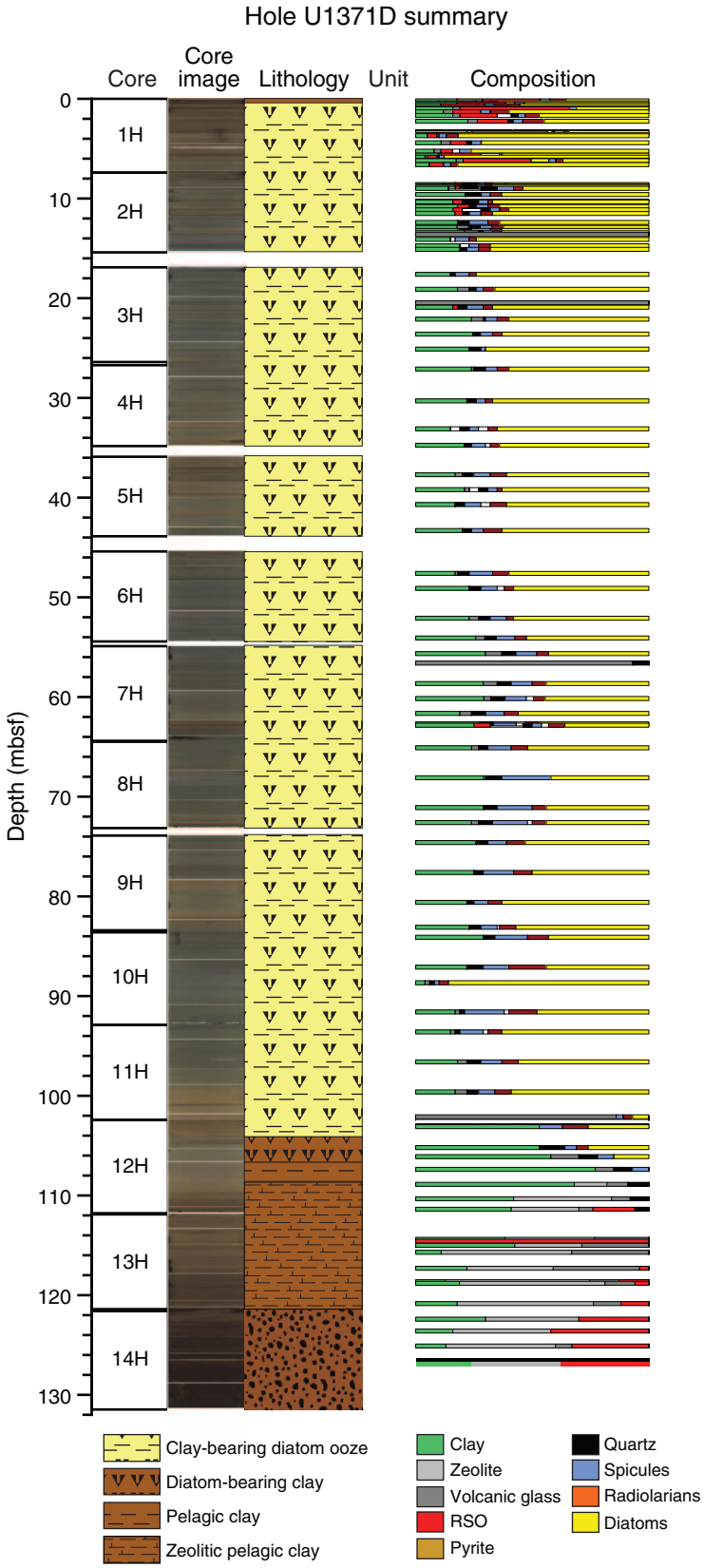

Figure F36. Profiles of dissolved chemicals, Site U1371. **A.** Oxygen. **B.** Nitrate. **C.** Ammonium. **D.** Manganese. **E.** Redox potential.